JOURNAL OF

THE ASIATIC SOCIETY OF BANGLADESH

SCIENCE

ISSN 1016-6947

Vol. 49 **No. 2** **December 2023**

THE ASIATIC SOCIETY OF BANGLADESH

THE ASIATIC SOCIETY OF BANGLADESH

Journal of the Asiatic Society of Bangladesh (Science)

Journal of the Asiatic Society of Bangladesh, Science is published twice a year (June and December comprising one volume) in English. Original research papers dealing with all branches of science with special reference to Asiatic studies by the members of the Society are published. Any non-member of the Society may publish a research paper if it is communicated by a member of the Society.

SUBSCRIPTION

Annual per volume:		Single issue:	
Inland :	Tk. 500.00	Inland :	Tk. 250.00
Foreign :	US$ 40.00	Foreign :	US$ 20.00

CORRESPONDENCE

All correspondence should be addressed to The General Secretary, The Asiatic Society of Bangladesh, 5 Old Secretariat Road (Nimtali), Ramna, Dhaka-1000, Bangladesh.
Phone : 9513783, E-mail : asbpublication@gmail.com, www.asiaticsociety.org.bd

PRINTED BY

SRL Printing Press
8/12 Babupura, Nilkhet, Dhaka-1205

JOURNAL OF THE ASIATIC SOCIETY OF BANGLADESH SCIENCE

Volume **49**, Issue 2, December 2023
ISSN **1016-6947** eISSN **2408-8676**
Available at: https://www.asiaticsociety.org.bd/journals
https://www.banglajol.info/index.php/JASBS

Journal of the Asiatic Society of Bangladesh, Science
is indexed in the following online scholarly database:

JOURNAL OF
THE ASIATIC SOCIETY OF BANGLADESH
SCIENCE

(J. Asiat. Soc. Bangladesh, Sci.)

Vol. 49 **No. 2** **December 2023**

CONTENTS

Guidelines to authors

The Journal of the Asiatic Society of Bangladesh publishes original research papers related to any field of sciences from anywhere in the world.

All manuscripts written in English and typed on one side of a good quality paper (A4) with one and a half space and 2.54 cm margins on all sides should be submitted in duplicate (one copy without identity of the authors) to the Editor. However, authors from overseas countries may submit soft copy of the paper. Regarding publication of the paper after review, the decision of the Editorial Board shall be final. All papers accepted by the Editorial Board are subjected to editorial modifications.

The manuscript of a full paper, preferably be limited within 12 typed pages (A4) including tables, figures, graphs, references, etc. For short communication it should not exceed five pages.

The manuscript should contain the following sub-titles in sequence: Title, Abstract, Key words, Introduction, Materials and Methods, Results and Discussion, Acknowledgements, if any, and References. In case of **'Short Communication'** no sub-titles are necessary.

Title: It should be brief and specific. The manuscript will have a separate title page giving name of the paper, authors name and address and a running head.

Abstract: It should not exceed 200 words containing the gist of results only.

Key words: Should not exceed 6 words and it should be after Abstract.

Text: The text of the article should be clear and precise. Introduction should be concise, precise and relevant to the study. Methods already published should be indicated by references. In case of modifications of a method give explicit descriptions. Results should be stated concisely and presented logically referring to tables and graphs. The same data should not be used both for the tables and for the graphs and/or figures. Simple data may be presented as a text instead of Tables and Figs. Each result should be followed by discussion or interpretation (in any case the Results and Discussion must not be separated) with appropriate reference(s). Discussion should deal with the obtained results and related results published nationally and internationally. Concluding remarks (without heading) must be given (that tally with the objective) in the last paragraph. The references in the text should be arranged chronologically.

Units: All measurements must be given in SI (International System) or SI-derived units.

Tables, Graphs and Figures: Number of tables, graphs and figures should be minimum. However, these should be typed separately. The graphs and figures should be drawn giving statistical analysis and properly labelled. The figures and graphs should be properly drawn with bold, solid lines so that these could be reduced up to half or less of the original. The photographs should be submitted on glossy papers or in JPEG format. Symbols in the graphs should be distinct and labels should be readable. Coloured photographs are also accepted.

References: In the text, references should be cited within brackets quoting author's surname and the year of publication in the appropriate place e.g. (Alva and Edwards, 1990; Kabir, 2005; Khan *et al*., 2008). References should be arranged alphabetically according to author's surname at the end of the paper. Names of journals and books should be in italics giving edition, year of publication and name of the publishers.

Examples:

Alva, A.K. and D.G. Edwards. 1990. Response of lupin cultivars to concentration of Ca and Al in dilute nutrient solutions. *J. Pl. Nutr.* **13**: 57-76.

Amin, F.B., Z.N. Tahmida Begum and R. Mandal, 2011. Impact of potassium and zinc on growth of cyanobacteria in seasonally flooded rice field of Meghna floodplain. *J. Asiat. Soc. Bangladesh, Sci*. **37**(2): 251-255

Helyar, K.R. and W.M. Porter. 1989. Soil acidification, its measurement and processes involved. In: *Soil acidity and plant growth*, A.D. Robson (ed.), Academic press, pp. 61-101.

Kabir, S.M. 2005. Acid sulfate ecosystem and their sustainable management. Unpublished Ph.D. thesis. Department of Soil, Water and Environment. Univ. of Dhaka, Bangladesh.

Khan, H.R., S.M. Kabir, M.M.A. Bhuiyan, F. Ahmed, S.M.A. Syeed and H.-P. Blume, 2008. Response of Mustard to Basic Slag and Aggregate Size Treatments under Modified-Plain-Ridge-Ditch Techniques Used for the Reclamation and Improvement of Cheringa Acid Sulfate Soil. *Soil and Environ*. **27**(1): 1-10.

Khoiyangbam, R.S. and N. Gupta. 2012. *Introduction to Environmental Science*. Publ. The Energy and Resources Institute, New Delhi.

The author(s) must submit one computer composed hard copy of the revised paper along with the CD in MS Word version 8.

Final galley proofs, if possible, will be sent to authors. No alternations or additions in the text are desirable at this stage.

Off-prints

A contributor of each paper is entitled to get 5 off-prints free of cost.

Declaration

While submitting a paper the individual authors are to sign a declaration to the effect that (i) the work reported has been carried out by them and they prepared the manuscript, (ii) they take public responsibility for the contents of the paper, (iii) the paper has not been published before in any referred scientific journal or has not been submitted to such journal for publication.

Review of books

Books for review should be sent to the Editor in duplicate.

J. Asiat. Soc. Bangladesh, Sci. **49**(2): 121-138, December 2023 DOI: https://doi.org/10.3329/jasbs.v49i2.70760

HEALTH RISKS ASSOCIATED WITH SOURCES OF WATER: AN EXPLORATORY STUDY FROM TURAG-TONGI RIPARIAN AREAS, BANGLADESH

SHAMIMA PRODHAN* AND MAHBUBA NASREEN
Institute of Disaster Management and Vulnerability Studies, University of Dhaka, Dhaka, Bangladesh

Abstract

The present study aims to investigate the available water sources for drinking and domestic purposes and their relationship with the occurrence of diseases in a given community. To accomplish this, 1826 households in the Turag River area of Tongi at twelve different locations were surveyed. Six focus group discussions (FGDs) and twelve key informant interviews (KIIs) were also conducted in six different Turag River locations. Data on water quality has been gathered from various government surveys (BNDWQS, 2011; BBS, 2017; SVRS, 2019, etc.), international reports (WHO, World Bank, etc.), individual studies, and other relevant sources. Of all the recorded (13) drinking water sources, motorized tubewells were the most common and were used by 73.8 percent of respondents. Other sources include pipe connections into the yard (16.7%) and dwelling (4.5%), deep and shallow tube wells (2.6%), public tap water (2.1%) etc. The study also revealed that a notable percentage (2.8%) of the survey population still depended on open sources such as rainwater, rivers, lakes, ponds, etc., for drinking and domestic purposes. The respondents also reported the presence of yellow crust (iron) and other unwanted components in their water sources, with foul odors and unpleasant tastes. It has also been documented that the communities have been suffering from various diseases, such as diarrhea, skin diseases, dysentery, malaria, jaundice, typhoid, tuberculosis, pneumonia, cholera, etc. diseases over the past year. The Spearman's rho (ρ's) test showed significant associations between these diseases and the water sources. The issues identified by the present study are likely to aid policymakers in including water and health concerns in national policy and ensuring access to sustainable water resources, aligning with SDGs 6.1, 6.3, and 6.4.

Keywords: Sources of water, disease incidence, water quality, river, drinking water.

Introduction

Access to safe and clean water is a fundamental human right, and its importance cannot be overstated when maintaining good health. Yet, for several decades, roughly a billion people in developing nations lacked access to reliable, safe water sources (Hunter *et al.*,

*Corresponding author: sp.idmvs@du.ac.bd

2010). It has been estimated that 2.1 billion people worldwide (29% of the world's population) have no access to safe drinking water and are responsible for 1.2 billion deaths yearly (Hannah and Max, 2021). Over 70 percent of the urban population in developing countries either lack adequate water supplies, or receive unsafe water, or both (Kamal, 2003). Safe drinking water availability in urban areas is a major challenge (Zuthi *et al.*, 2009) due to the steady population growth, declining groundwater availability, and river water pollution (Nahar *et al.*, 2014; Parvin *et al.*, 2022; Xu *et al.*, 2022).

Drinking water quality is essential to human health, as 80 percent of diseases worldwide are linked to poor drinking water quality (Lin *et al.*, 2022). While Bangladesh has made significant progress in providing universal access to improved water sources, access to safe drinking water remains 41 percent (1.8 million out of its 165 million people) in 2023 (Water.org, 2023). Bangladesh faces an enormous challenge in supplying safe water to the capital city's fast-growing population (ABD, 2013), resulting in many households heavily relying on a combination of safe sources such as shallow tube wells, piped water supplies, etc., and unsafe sources, such as rivers, canals, dug wells, rainwater, water vendors, etc., to meet their daily water needs (ABD, 2013; Roy and Dutta, 2017). Poor sanitation practices, industrial waste, and agricultural runoff put these water sources at risk of contamination. Due to the practice of discharging untreated domestic and industrial waste, rivers in urban areas have also been linked to water quality issues. This has increased the level of toxic metals (Rashid *et al.*, 2012; Zakir *et al.*, 2013; Hasan *et al.*, 2014; Islam *et al.*, 2015), fecal coliform, and other harmful bacteria (Zuthi *et al.*, 2009; Sarker *et al.*, 2019), which has a variety of adverse health effects (Schwarzenbach *et al.*, 2010; WHO, 2012; Alidadi *et al.*, 2019; Lin *et al.*, 2022; Sing *et al.*, 2022). Usage of contaminated water from both safe and unsafe sources causes various waterborne diseases like diarrhea, cholera, jaundice, typhoid, hepatitis, etc. (Rahman, 2016). It is responsible for approximately 3.5 million deaths annually (World Vision, 2021), making it one of the leading causes of global mortality (Berman, 2009). Additionally, according to estimates from WHO and UNICEF in 2000, as well as Rosegrant and Cai (2002), poor drinking water contributes to an estimated four billion instances of diarrhea each year, which results in two million fatalities. The lower income group suffers the most since they cannot afford safe drinking water for an active and healthy life (Rahman and Jahan, 2003).

The Seventh Five Year Plan (SFYP, 2016–2030) of the Government of Bangladesh calls for the availability and accessibility of safe drinking water to all rural and urban residents, synonymous with the goal (six) of the United Nations' Sustainable Development Goals (SDGs, 2016–2030). The current research, therefore, can benefit

policymakers by highlighting the significance of safe water for public health and suggesting strategies for the sustainable supply and management of water for those who lack access to it. However, the present study entails understanding **a)** available water sources for drinking and domestic usage and **b)** the differential impacts of water quality on the health of the dependent communities.

Methods

Selection of study area and population: The Turag is a prominent river in Bangladesh that is only 7.9 km away from Dhaka (Haque, 2018). This river is of paramount importance as the main drainage channel of Dhaka city (Salam and Alam, 2014) and is of great importance from an economic point of view (Ahmed and Bodrud-Doza, 2013). The Turag is also home to a substantial amount of human activity ranging from navigation (Rahman *et al*., 2013), fishing (Baki *et al*., 2015), agriculture (World Bank, 2007), and in many instances, as a source of water for domestic purposes (Bhuiyan *et al*., 2011). Considering the sources of drinking water and the proportion of households adjacent to the Turag River, twelve areas, namely Konabari, Kashimpur, Ichharkandi, Palasana, Gutia, Gusulia, Bhakral, Bhadam, Rashadia, Kathaldia, Abdullahpur, and Mausaid (Map 1) were selected for the survey. Before selecting these survey areas, several reconnaissance visits were made to familiarize the area with potential samples and identify the diverse water security challenges in different areas. The visits also enabled us to design the survey questionnaire and sampling strategy.

The study follows a probability sampling technique in drawing the sample households, the unit of analysis. The study population covered the households living within half a kilometer of the banks or canals of the Turag River with the samples from the newly growing industrial zones. Households living near a river within a given distance having the chance of being exposed to the river were treated as the target population. Similarly, the households residing a short distance from the river and less likely to be exposed to the river were treated as the control population.

Data collection and analysis: To capture the intra-household water resource usage, the survey focused on individual household data. A total of 1826 households were surveyed purposively from December 2017 to February 2018 across the selected twelve sites along the Turag River area. The data was collected using a mobile data collection software called "Organizational Network Analysis (ONA)." To do this, the questionnaires have been transformed into an online version and made suitable for ONA. The household head or his/her spouse was the target respondent. A standard semi-structured survey

questionnaire was developed and applied to collect data from the respondents. The questionnaire was pre-tested through eight interviews during scoping and revised following the pre-test. The questionnaire was in English, but interviews were conducted in the local language, Bangla.

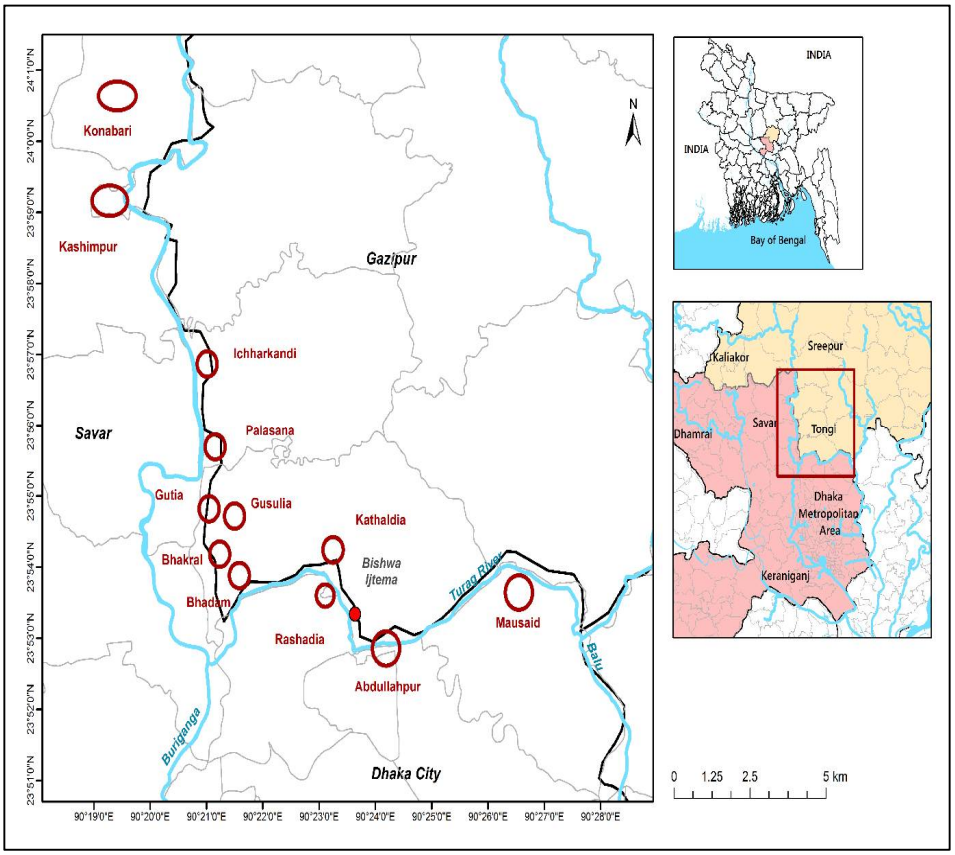

Map 1: Study sites along the Turag river area (Source: REACH, Oxford)

Likewise, six FGDs comprised 7 to 8 participants, and twelve KIIs were conducted concurrently at six selected study sites (Kashimpur, Konabari, Bhadam, Bhakral, Abdullahpur, Mausaid). A thematic checklist was developed to collect information through focus groups and key informant interviews. Locally knowledgeable persons, political leaders, doctors, local volunteers, members of civil societies, government officials, and non-government officials participated in the KII. Local medical institutes

were also visited to understand the extent of waterborne diseases in the survey areas. In addition, we carefully analyzed over seventy (70) scientific articles, conference and workshop proceedings, national and international reports, survey data published by the government and other respected organizations (BBS, DoE, BNDWQS, SVRS, HIES, etc.), books, online citations, and other relevant materials. This helped us understand the current state of groundwater and the Turag River, the quality of available water sources, and the sources of contamination.

The study employs statistical and descriptive techniques to analyze the survey data. Any errors in spelling, grammar, or punctuation have been corrected. The primary level of analysis was done using ONA, and further statistical analysis was done using the Statistical Package for Social Sciences (SPSS) version 25. Descriptive statistics were utilized to explore the general characteristics of the study population. Spearman's rho (ρ's) values were obtained to investigate the relationship between the dependent variable (disease incidence) and independent variables (water sources) of the study. The statistical significance level was set at 97.5% for both ends (equivalent to 95% significance level). Then again, to examine how communities become infected with diseases linked to water usage, disease ecology theory was used to understand the process.

Results

Respondents' characteristics: Among the 7134 population in 1826 households surveyed, 50.1 percent (n=3573) were male, and 49.9 percent (n=3561) were female. The average household size is 4.0, slightly smaller than the national average urban household size of 4.4 (BBS, 2011). Out of all households, 91.4 percent are headed by males (n=1669) and only 8.6 percent by females (n=157), which is 84.1 percent of male-headed and 15.9 percent of female-headed households in Dhaka according to Bangladesh Sample Vital Statistics (2020). The highest concentration of the population exists in the age group of 16-25, with male and female percentages of 20.6 and 25.2, respectively. Age group ranges from 26-35 and 6-15, securing 2nd and 3rd highest rank (20.1% and 19.4%, respectively). The percentage of the population aged 0-5 is 7.5 percent, and the population aged 66 and over is 2.3 percent. Of the surveyed respondents, 28.5 percent (n=928) were recorded as illiterate, 25.8 percent (n=923) completed primary school, and only 3.3 percent (n=160) had a bachelor's or higher degree. The surveyed household members were found to work in garment factories (10.8%), in business (7.5%), as skilled laborers (2.7%), in non-government services (1.5%), in farming (2.8%), in fishing (1.2%), etc. occupations.

Sources of water for drinking and domestic purposes: Fig. 1 shows that the motor tubewell (73.8%) was the primary source of water supply among the studied communities, followed by piped water into the dwelling (4.5%), piped water into the yard (16.7%), deep and shallow tubewell water (2.6%), and tap water (2.1%). Communities were also found to depend on vented water sources (bottled water/tanker trucks/cart tanks) (0.4%) when other alternative sources were unavailable. Other water sources (0.7%) include neighbors' water sources, compressor and submersible pumps, brickfields, etc. Also, a certain percentage (2.8%) had been recorded using open sources such as rivers, lakes, ponds, and rainwater for drinking purposes. As this group has no fixed sources, they alternatively collect drinking water from electric/motor tube wells owned by other households (2.2%), deep and shallow tube wells (0.3%), public standpoints (0.1%), ponds (0.1%,), etc. based on its availability and whenever they get accessed to it.

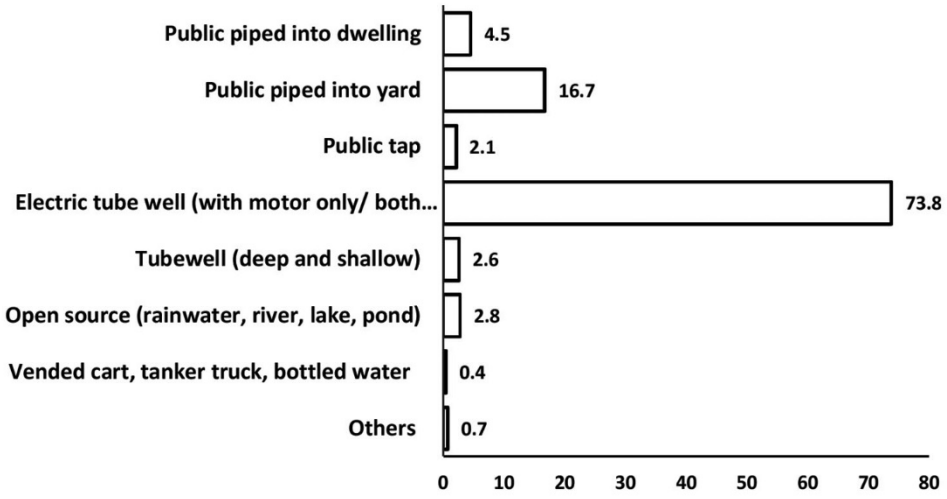

Fig. 1. Sources of drinking water (%) identified in the studied area.

The household survey also shows that communities' primary water sources for domestic uses come from motorized tubewell (69.1%), piped water (19.8%), tap water (2.1%), and deep and shallow tubewell water (2.3%). A noticeable percentage of people (21.1%) were also found to depend on unsafe sources like rivers, canals, ponds, lakes, and rainwater for cooking, washing (vegetables, clothes, dishes, etc.), bathing, and hygiene purposes.

Respondents also revealed that the water they drank is unsafe (4.2%); their primary justifications for this belief include the presence of yellow crust in the storage pot locally identified as iron (2.9%) and various unwanted components (1.3%), with terrible odor and taste (1.0%). Also, when asked about the condition of the water they use for domestic purposes, 6.9 percent (n=126) of respondents reported that the water they use is dirty. Interestingly, these people found supply or ground sources, especially motor tubewell water, much more polluted than the Turag River water they depend on for various domestic uses (FGDs).

Disease incidence among studied communities

Disease prevalence among the studied community over the past year: The surveyed community suffered (27.5%, n=1968; N=7134) from various diseases in the past year; gastric ulcers and stomach pain ranked the highest (36.6%). Diseases like skin problems (12.6%); dysentery, diarrhea (12.5%); chikungunya, and dengue (11.1%); jaundice (9.2%); typhoid (6.0%); tuberculosis, pneumonia (5.4%); cholera (0.8%), etc. (Fig. 2) were also well documented. Illnesses such as body pain, back pain, respiratory problems, gynecological problems, tonsils, and fever were most frequent under other categories and represented 30.1 percent of the total count. Gender-wise illness shows no significant variation, although the females were affected more (64.8%) than males (59.5%). Both males (16.6%) and females (20%) were documented to suffer from gastric ulcers at a higher percentage than other diseases recorded. They may stem from irregular eating habits and water consumption from unsafe sources. Overall, focus group discussions and key informant interviews revealed that women continue to have higher rates of cholera, dysentery, and skin issues than males due to their considerably higher engagement in water-related activities.

Area-wise (Table 1), the rate of unsafe water intake was the highest among the communities living in Ichharkandi (1.4%) and Palasana (1.1%). However, disease incidence in those areas remained lower than in other areas regarding the total population surveyed (13.1% in Ichharkandi and 15.8% in Palasana). Among other areas, the second-highest surveyed population was documented in Kathaldia (n=914; 12.8%), though disease occurrence remained the lowest (14.8%). Drinking water sources in this community were piped connections (7.2%) and motorized tube wells (4.9%), and no interaction with unsafe water was documented.

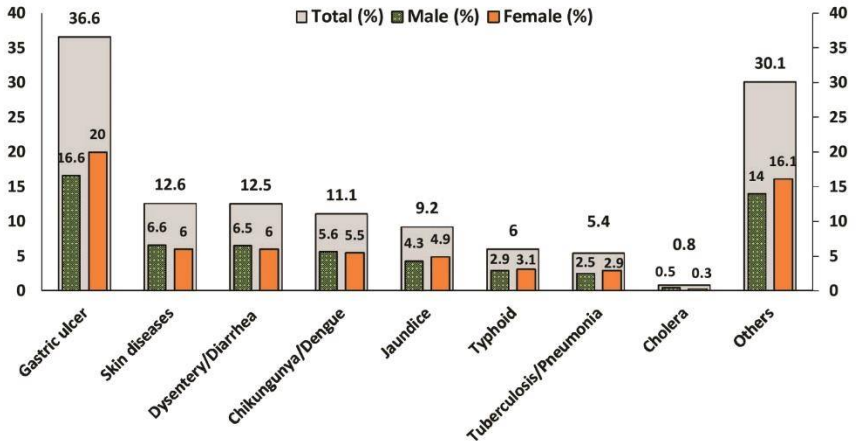

Fig. 2. Gendered variations (%) of disease occurrence.

Table 1. Area-wise disease occurrence and dependent sources of water.

Area	Population		Disease		Disease incidence (%)	Sources of drinking water			
						Supply/ groundwater		Open water sources	
	n	%	n	%		n	%	n	%
Konabari	1040	14.6	400	5.6	38.5	248	13.7	0	0.0
Kasimpur	786	11.0	306	4.3	38.9	204	11.3	1	0.1
Ichharkandi	582	8.2	76	1.1	***13.1***	163	9.0	***25***	***1.4***
Palasana	411	5.8	65	0.9	***15.8***	109	6.0	***21***	***1.1***
Gutia	435	6.1	78	1.1	17.9	104	5.8	0	0.0
Gusulia	279	3.9	60	0.8	21.5	65	3.6	1	0.1
Bhakral	362	5.1	132	1.9	36.5	85	4.7	0	0.0
Bhadam	590	8.3	171	2.4	29.0	197	10.8	0	0.0
Kathaldia	***914***	***12.8***	***135***	***1.9***	***14.8***	***222***	***12.1***	***0***	***0.0***
Rashadia	270	3.8	145	2.0	53.7	69	3.9	0	0.0
Abdullahpur	832	11.7	533	7.5	64.1	221	12.1	3	0.2
Mausaid	633	8.9	344	4.8	54.3	140	7.7	0	0.0
Total	**7134**	**100**	**2445***	**34.3**	**34.3**	**1827***	**100.2**	**51***	**2.8**

*M.R.; Source: H.H. Survey, 2017-18; Supply/groundwater: motorized tubewell, pipe water, tap water, deep and shallow tubewell, etc.; Open water sources: river, lake, pond, rainwater, etc.

The FGD participants identified skin diseases, dysentery, diarrhea, dengue, chikungunya, respiratory problems, typhoid, cholera, fever, jaundice, and gastric as their greatest health risks (Table 2). Women are more likely to engage in water-related activities and work with dirty Turag River water for domestic chores, making them more susceptible to developing skin problems (FGDs and KIIs). Itching in intimate parts was also an issue for women as they were contingent on polluted water for bathing and toileting (FGDs and KIIs).

Table 2: Health profile of studied communities based on FGDs and KIIs

The greatest health risk identified by the community	Score	Rank
Skin problem/itching	11	1
Stomach upset/dysentery/diarrhea	10	2
Respiratory problem/asthma	4	3
Dengue/chikungunya	4	3
Jaundice	3	4
Typhoid	2	5
Cholera	2	5
Fever	2	5
Gastric	1	6
Kidney problems	1	6
Body swelling	1	6

Source: FGDs and KIIs, 2018

Spearman's rho analysis (ρ's) results, as presented in Table 3, show that among all diseases, dysentery shows significant relation with piped water into the dwelling ($p<0.016$); cholera with pond water ($p<0.001$); typhoid with rainwater ($p<0.005$); jaundice with deep tubewell ($p<0.009$) and vended water ($p<0.017$); gastric, ulcers with piped water into the dwelling ($p<0.002$), piped water into the yard ($p<0.032$), river water ($p<0.002$) and pond water ($p<0.018$). Chikungunya, dengue, and malaria show significant relation with piped water into the dwelling ($p<0.001$), piped water into the yard ($p<0.001$), shallow tubewell ($p<0.001$), and motor tubewell water ($p<0.003$); diseases like tuberculosis, pneumonia found significantly linked with river and canal water ($p<0.001$).

Table 3. Spearman's rho (ρ's) test of association between disease incidence and water sources

Spearman's rho (ρ's) test of association	p-value
Dysentery/ Diarrhoea ~ Piped water into the dwelling	0.016**
Cholera ~ Pond	0.001*
Typhoid ~ Rainwater	0.005*
Jaundice ~ Deep tubewell	0.009*
Jaundice ~ Vended truck	0.017**
Gastric/ulcers ~ Piped water into the dwelling	0.002*
Gastric/ulcers ~ Piped water into the yard	0.032**
Gastric/ulcers ~ River/canal	0.002*
Gastric/ulcers ~ Pond	0.018**
Chikungunya/Dengue ~ Piped water into the dwelling	0.001*
Chikungunya/Dengue ~ Piped water into the yard	0.001*
Chikungunya/Dengue ~ Shallow tubewell	0.001*
Chikungunya/Dengue ~ Motor tubewell	0.003*
Tuberculosis/ Pneumonia ~ River/Canal	0.001*

(Each value on the table represents the test statistics value at a 95% significance level). **significant at 0.05, *significant at 0.01

Case of malnutrition among the studied communities: Collecting and analyzing malnutrition data is essential because it increases the susceptibility to disease occurrence. Of the total people surveyed (n=7134), 18.2 percent (n=1298) were documented malnourished, and more females (51.3%, n=666) were found malnourished than males (48.7%, n=632). It is also found that malnutrition remains highest among the most active age groups, i.e., 16-25 yr (20%), 6-15 yr (18.2%), 26-36 yr (16.1%), 36-45 yr (12.9%), and 46-55 yr (10.3%) while it was lowest among infant (>5 yr) and elderly (<66 yr) group.

Discussion

This section is further discussed under two main parts. The first part provides a general discussion of findings to support the objectives set. The second part attempts to fit the study findings on the adopted theory.

Linking disease occurrence with sources of water: Though in the present study, motorized tube wells, deep and shallow tube wells, and piped and tap water supplies were

documented as the primary water sources, communities were also found to depend on rivers, ponds, and other sources of doubtful water quality for household use (21.1%) as well as for drinking (2.8%) due to lack of sufficient and easily accessible water supply. According to the BBS (2017) and SVRS (2019) reports, tap water accounts for 23.7 and 27.5 percent of the primary drinking water sources in urban areas, respectively, while tube wells make up 60.2 and 67.1 percent. Additionally, the SVRS (2019) report found that 1.8 percent of Bangladesh's population (about four million people) depended on unsafe sources (ponds, rivers, streams, or unprotected wells, springs, etc.), which corresponds to 3 percent of the country's overall population according to the World Bank (2018) report. In a similar work, Jinnah's (2007) research shows that 3.8 percent of Bangladesh's slum dwellers use rivers, ponds, lakes, and canals as drinking water sources. As revealed in the current study (FGDs and KIIs), interacting with unprotected sources, in this case, the Turag River water for cooking, washing, bathing, and other domestic uses results in health issues like dysentery, skin problems, respiratory problems, etc. among the examined people (Table 2).

The presence of yellow crust or iron in supply water has been confirmed and labeled as unsafe to drink by the studied community (2.9%). According to BNDWQS (2011), the average concentration of iron (Fe) present in the shallow (2.65 mg/L) and deep tubewell (1.37 mg/L) water throughout the country exceeded DOE (1997) Bangladesh standards of 0.3 mg/L and 1.0 mg/L, respectively. Consuming excessive iron has the potential to cause multiple organ dysfunction such as liver fibrosis (Heming *et al.*, 2011), diabetes (Swaminathan *et al.*, 2007; Heming *et al.*, 2011), lung and heart disease (Milman *et al.*, 2001), etc. as reported in case of the studied population. Simultaneously, unpleasant tastes or odors pointed out by the studied communities (1.0%) in microbiologically safe water supplies may act as a deterrent to the use of safe sources, exposing them to unprotected water sources, in this case, the Turag River, and thereby increasing the people health risks (Hunter *et al.*, 2010). As reported by the World Bank (2018), *E. coli* is found in 80 percent of private piped water taps across the country, a number that is comparable to water taken from ponds. MICS (2019) report verified that 84.1 percent of households in Dhaka use water sources tainted with *E. coli*. Moreover, the work of More (2017) demonstrates that in Bangladesh, very high *E. coli* risk levels (p>100 CFU/100 mL) were found in 46.3 percent of piped water into dwellings and 3.6 percent of tube wells. The presence of microorganisms in the tubewell water of Bangladesh is also confirmed by the work of Hoque *et al.* (2006), Rahman *et al.* (2014), Kabir *et al*. (2016), Sarker *et al.* (2019), etc. Thus, disease incidence among the studied communities might

result from microbial components and other harmful contaminants in their relied water sources.

Although in the present study, most of the disease occurrence shows significant relations with safe water sources, diseases like cholera, typhoid, and tuberculosis depend entirely on open sources such as ponds (<0.001), rain (0.005), river water (< 0.001), etc. As shown in Table 3, diarrhea and dysentery are associated with piped water. Payment *et al.* (1997) also discovered tap water to be a pivotal contributor to these diseases. Worldwide, cholera continues to be a serious public health issue that can result in up to 4.0 million cases and 95,000 fatalities each year (Ali *et al.*, 2015). However, the prevalence of cholera in the current study is still low (0.8%; Fig. 2) but shows a strong association with pond water ($p>0.001$; Table 3), which is consistent with Sheppard's (1995) findings that cholera transmission is associated with surface water. Additionally, according to Hashizume *et al.* (2008), the chance of acquiring cholera is raised due to drinking tubewell water and visiting unhygienic toilets. Also, practices like bathing, washing utensils and clothes, washing mouth in pond water, and occasionally drinking are significantly associated with this type of illness (Mukherjee *et al.*, 2011). The work of Parvin *et al.* (2022) indicates that rain influences typhoid occurrence by increasing fecal contamination, supported by the present study findings where the occurrence of typhoid is found to be significantly linked with rainwater (Table 3). However, some studies (Corner *et al.,* 2013; Dewan *et al.,* 2013) show that communities living near large bodies of water (lakes and river networks) are particularly susceptible to typhoid outbreaks, which is true in the case of the present study. Jaundice, which was found to be significantly associated with tube wells ($p<0.009$) and carts water ($p<0.017$) in the studied communities, is brought in by a high concentration of coliforms and gram-negative bacteria. Jaundice is also believed to be associated with water deficits in all megacities (Kumar *et al.,* 2022), sewage water infiltration in the water supply, and improper water handling practices (Rathour *et al.,* 2022). The association of jaundice with cart water (vented truck) might be because it was in short supply from regular sources and handled unhygienically by seller groups. On the other hand, the possible explanation for the connection of jaundice with tubewell water in this study is likely due to its contamination with sewage lines or old, rusted pipelines lying close to sewer lines. According to HIES (2016), gastric ulcers among urban dwellers (20.3%) are most common; in the present study, gastric ulcers were found linked to both safe (piped water into dwelling and yard) and unsafe (river and pond) sources (Table 3). Nonetheless, the increased prevalence of stomach ulcers in surveyed communities might result from an irregular diet, drinking less water, and stress-related factors (Shamsuddeen *et al.,* 2009).

Dengue and chikungunya fever are rapidly spreading viral diseases that are very common among the studied population (Fig. 2). Stagnant water in urban areas and poor waste management create potential breeding grounds for mosquitoes and other disease-carrying vectors, increasing the risk of dengue and chikungunya fever. They spread because the vectors breed in water bodies close to where the surveyed people are living. Though not regarded as a water-related illness, respiratory problems (tuberculosis, pneumonia) in the surveyed communities are found in a percentage of 5.4, corresponding to 9.4 percent of the population in metropolitan areas (BBS, 2017). While skin problems are quite prevalent among the examined populations (12.6%), their prevalence is still lower (2.4% in the metropolitan area), according to the BBS report (2017). Many interviewees (FGDs) affirmed having skin issues because of their engagement in water-related household activities and regular exposure to river water, in line with similar findings from the works of Halder and Islam (2015), Hanif *et al.* (2020), etc. This type of skin problem occurs when hazardous substances accumulate in the body because of the disposal of textile dyes in the surrounding river (Ahmed *et al.*, 2005) and contaminated groundwater through infiltration (Nishat *et al*., 2001; Motlagh, 2013; Mohiuddin, 2019). Another prevalent condition in the populations under study is malnutrition (18.2%). Malnutrition can also aggravate the risks of other diseases caused by water pollution. Prüss-Üstün *et al*. (2008) claimed that consuming contaminated water and exercising poor hygiene might lead to persistent diarrhea and other infectious diseases, ultimately contributing to malnutrition.

Implications of adopted theory into study findings: The adopted theory, however, suggests that the interaction of three factors- habitat, population, and behavior, often affects disease prevalence (Meade and Emch, 2010). Hence, the study aims to comprehend how host-pathogen interactions in urban environments with various types of water sources affect the occurrence and spread of diseases.

The adopted disease ecology framework views the studied *communities* as the potential hosts of the disease, where the people's susceptibility or resistance to diseases is influenced by their age, sex, modalities of work, etc. Females are revealed to be more susceptible to some illnesses than males due to their differing roles in domestic tasks involving water. Alternatively, the most active age group (26-35 yr) of the studied communities, primarily in charge of water-related household activities, continues to have the highest rate (27.6%) of disease occurrence. The water resources (Fig. 1) on which the communities under study rely for their daily water needs and the quality, availability, and cost of these services are all considered *habitats.* The study communities' disease occurrence has remained relatively high and linked with supplied and surface water (Table 3). Water from these sources may contain harmful substances or microbes,

exposing the community to diseases like diarrhea, dysentery, cholera, jaundice, typhoid, etc. Disease ecology theory also recognizes the role of human *behavior* and water-related activities in disease transmission. Human *behavior*, which includes household-level hygiene practices, water collection, water storage, water handling practices, waste disposal practices, etc., can contaminate water and cause the spread of diseases that are transmitted through water. However, further research and analysis require a comprehensive understanding of disease ecology and its relationship with urban water sources.

Conclusion

Water and health are intricately interconnected, and this exploratory study from urban Bangladesh sheds light on the challenges communities face in accessing clean and safe water. Safe water supplies free from microbes, parasites, and chemical or physical contaminants are essential to sustainably growing cities and citizens' well-being, as ignorance of extending water services to millions of people plays a crucial role in underpinning health. By prioritizing easy accessibility and ensuring its quality, we can pave the way toward healthier and more sustainable urban communities in Bangladesh and beyond. An expanded water intervention program by the Government and NGOs to ensure a satisfactory level of safe water supply can effectively ensure good health. However, future studies are urged to focus on aspects other than water quality, such as household-level sanitation and hygiene practices, the quantity of water for drinking and household uses, water storage and treatment practices to acquire a greater knowledge of how diseases arise, like the issues addressed in Goal 6 of Agenda 2030 of drinking water, sanitation, and hygiene.

Acknowledgment

This document is an output from the REACH program funded by U.K. Aid from the U.K. Foreign, Commonwealth and Development Office (FCDO) to benefit developing countries (Programme Code 201880). However, the views expressed and information contained in it are not necessarily those of or endorsed by FCDO, which accepts no responsibility for such opinions, data, or any reliance on them.

References

Ahmed, S., K. Tapley, A. Clemett and M. Chadwick. 2005. *Health and safety in the textile dyeing industry*. Stockholm Environment Institute and Bangladesh Centre for Advanced Studies, Gulshan, Dhaka, Bangladesh. pp. 31.

Asian Development Bank (ADB). 2013. *Bangladesh-ADB: 40 years of development partnership.* Mandaluyong City, Philippines: Asian Development Bank. pp. 176.

Ahmed, T. and M. Bodrud-Doza. 2014. *State of Turag river*. Strengthen the Civil Society Capacity and Voice on Water Co-operation, Dhaka

Ali, M., A. R. Nelson, A. L. Lopez and D. A. Sack. 2015. Updated global burden of cholera in endemic countries. *PLoS Neglected Trop. Dis.* **9**(6): e0003832.

Alidadi, H., S. B. Tavakoly Sany, B. Zarif Garaati Oftadeh, T. Mohamad, H. Shamszade and M. Fakhari. 2019. Health risk assessments of arsenic and toxic heavy metal exposure in drinking water in northeast Iran. *Environ. Health Prevent. Med.* **24**(1): 59.

Berman, J. 2009. *WHO: Waterborne Disease is the World's Leading Killer*. VoA.

Bhuiyan, M., M. A. Rakib, S. B. Dampare and S. Y. Ganyaglo. 2011. Surface water quality assessment in the central part of Bangladesh using multivariate analysis. *KSCE J. Civil Engin.* **15**(6): 995-1003.

BNDWQS (Bangladesh National Drinking Water Quality Survey-2009). 2011. Bangladesh Bureau of Statistics, Planning Division, Ministry of Planning, Government of the People's Republic of Bangladesh, and UNICEF.

BBS (Bangladesh Bureau of Statistics) 2011. *Population and Housing Census 2011*. Urban area report, Statistics and Informatics Division, Ministry of Planning, Government of the People's Republic of Bangladesh.

Baki, M. A., M. R. Islam, M. M. Hossain and N. A. Bhuiyan. 2015. Livelihood assessment and assessment of fishing community in adjacent area of Turag-Buriganga River, Dhaka, Bangladesh. *Inter. J. Pure Appl. Zool.* **3**(4): 347-353.

BBS (Bangladesh Bureau of Statistics). 2017. *Preliminary Report on Household Income and Expenditure Survey 2016.* Statistics and Informatics Division, Ministry of Planning, Government of the People's Republic of Bangladesh.

BSVS (Bangladesh Sample Vital Statistics). 2019. Bangladesh Bureau of Statistics (BBS). Statistics and Informatics Division (SID), Ministry of Planning, Government of the People's Republic of Bangladesh.

Corner, R.J., A.M. Dewan and M. Hashizume. 2013. Modelling typhoid risk in Dhaka metropolitan area of Bangladesh: the role of socio-economic and environmental factors. *Inter. J. Health Geograph.* **12**(13): 1-15.

Department of Environment (DoE). 1997. *The Environment Conservation Rules*. Ministry of Environment and Forest, Government of the People's Republic of Bangladesh, Dhaka, Bangladesh. pp. 212-214.

Dewan, A. M., R. Corner, M. Hashizume and E. T. Ongee. 2013. Typhoid fever and its association with environmental factors in the Dhaka metropolitan area of Bangladesh: a spatial and time-series approach. *PLOS Neglect. Trop. Dis.* **7**(1): e1998.

Hoque, B. A., K. Hallman, J. Levy, H. Bouis, N. Ali, F. Khan, S. Khanam, M. Kabir, S. Hossain and M. Shah Alam. 2006. Rural drinking water at supply and household levels: quality and management. *Inter. J. Hygiene Environ. Health*, **209**(5): 451-460.

Hashizume, M., Y. Wagatsuma, A.S.G. Faruque, T. Hayashi, P.R. Hunter, B. Armstrong and D. Sack. 2008. Factors determining vulnerability to diarrhoea after floods in Bangladesh. *J. Water Health*, **6**(3): 323-332.

Hunter, P. R., A. M. MacDonald and R. C. Carter. 2010. Water Supply and Health. *PLoS Medicine*, **7**(11): 1-9.

Heming, N., P. Montravers and S. Lasocki. 2011. Iron deficiency in critically ill patients: highlighting the role of hepcidin. *Critical Care*, **15**: 210.

Hasan, K., R. Khan, K. Nesha and M. Happy. 2014. Analysis of water quality using chemical parameters and metal status of Balu river at Dhaka, Bangladesh. *Open J. Water Pollut. Treat.* **1**(2): 58-74.

Halder, J. N. and N. M. Islam. 2015. Water pollution and its impact on human health. *J. Environ. Human*, **2**(1): 36-46.

Haque, M. E. 2018. *Study on Surface Water Availability for Future Water Demand for Dhaka City*. Unpublished PhD Thesis submitted to the Department of Water Resources Engineering, Bangladesh University of Engineering and Technology (BUET), Dhaka.

HIES (Household Income and Expenditure Survey). 2019. *Report on the household income and expenditure survey 2016*, Bangladesh Bureau of Statistics (BBS).

Hanif, M., R. Miah, M. Islam and S. Marzia. 2020. Impact of Kapotaksha river water pollution on human health and environment. *Progress. Agricult.* **31**(1): 1-9.

Hannah, R. and R. Max. 2021. *Clean Water and Sanitation*. Published online at Our WorldIn Data.org.

Islam, M. S., M. K. Ahmed, M. Raknuzzaman, M. Habibullah-Al-Mamun and M. K. Islam. 2015. Heavy metal pollution in surface water and sediment: a preliminary assessment of an urban river in a developing country. *Ecol. Indicat.* **48**: 182-191.

Jinnah, A. I. S. 2007. *Rights of water connections for urban slum dwellers in Bangladesh: A study on DSK's experience in three slums of Mirpur, Dhaka*. Advancing Sustainable Environmental Health (ASEH). Water Aid, Bangladesh. pp. 1-8.

Kamal, A. M. 2003. Attitude and opinion of the profile regarding water supply: A case study of Slum dwellers. Water and Sanitation for Cities, World Habitat Day 2003 Souvenir, Bangladesh Institute of Planners (BIP).

Kabir, M. P., M. A. Islam, M. A. Akber and M. S. Ahsan. 2016. Bacteriological assessment of aquifer storage and recovery (ASR) water in southwest coastal Bangladesh. *J. Water, Sanita. Hygiene Develop.* **6**(2): 231-241.

Kumar, N., S. Sarkar, G. Mawari, M. K. Daga, S. Shree, U. Pathak, N. Garg, M. M. Singh and T. K. Joshi. 2022. Water quality and burden of jaundice with drinking water sources: a study from Haryana, India. *Intern. J. Commu. Med. Public Health*, **9**(12): 4566-4570.

Lin, L., H. Yang and X. Xu. 2022. Effects of water pollution on human health and disease heterogeneity: A review. *Front. Environ. Sci.* **10:** 880246.

MICS (Bangladesh Multiple Indicator Cluster Survey). 2019. Bangladesh Bureau of Statistics (BBS) and UNICEF Bangladesh. p. 333.

Milman N., P. Pedersen, T. Á Steig, K. E. Byg, N. Graudal and K. Fenger. 2001. Clinically overt hereditary hemochromatosis in Denmark 1948–1985: Epidemiology, factors of significance for long-term survival, and causes of death in 179 patients. *Ann. Hematol.* **80**(12): 737-744.

Meade, M. and M. Emch. 2010. *Medical Geography* (3rd Eds.). USA: Guilford Press and Publish.

Mukherjee, R., D. Halder, S. Saha, R. Shyamali, C. Subhranshu, R. Ramakrishnan, M. V. Murhekar and Y. J. Hutin. 2011. Five pond-centered outbreaks of cholera in villages of West Bengal, India: Evidence for focused interventions. *J. Health, Popul. and Nutrit.* **29**(5): 421-428.

Motlagh, J. 2013. *Hell for leather: Bangladesh's toxic tanneries ravage lives and environment*. Time Magazine: New York, USA.

More, V. 2017. Making safe drinking water commonplace in Bangladesh. *Bangladesh J. Sci. Indust. Res.* **52**: 12.

Mohiuddin, A. K. 2019. Chemical Contaminants and Pollutants in the Measurable Life of Dhaka City. *European J. Sustain. Develop. Res.* **3**(2): em0083.

Nishat, A., P. Shammin, I. Faisal and J. Junaid. 2001. Industrial Pollution. *In:* A. Nishat, M. Ullah and A. K. E. Haque (Eds.), *Bangladesh Environment Out Look 2001*. Centre for Sustainable Development (CSD): Dhaka, Bangladesh.

Nahar, M. S., J. Zhang, A. Ueda and F. Yoshihisa. 2014. Investigation of severe water problem in urban areas of a developing country: the case of Dhaka, Bangladesh. *Environ. Geochem. Health,* **36**(6): 1079-1094.

Payment, P., J. Siemiatycki, L. Richardson, G. Renaud, E. Franco and M. Prevost. 1997. A prospective epidemiological study of gastrointestinal health effects due to the consumption of drinking water. *Inter. J. Environ. Health Res.* **7**(1): 5-31.

Prüss-Üstün, A., R. Bos, F. Gore and J. Bartram. 2008. *Safer water, better health: Costs, benefits, and sustainability of interventions to protect and promote health*. World Health Organization, Geneva.

Parvin, F., M. M. Haque and S. M. Tareq. 2022. Recent status of water quality in Bangladesh: A systematic review, meta-analysis, and health risk assessment. *Environ. Challen.* **6**: 100416.

Rosegrant, M. W. and X. Cai. 2002. Global water demand and supply projections Part 2: Results and prospects to 2025. International Water Resources Association. *Water Inter.* **27**(2): 170–182.

Rahman, S. M. S. and S. Jahan. 2003. Planning for a viable water supply system for Barisal city, Water and sanitation for cities. World Habitat Day 2003 Souvenir, Bangladesh Institute of Planners (BIP) and Center for Urban Studies (CUS), Dhaka, Bangladesh.

Rashid, H., M. N. Hasan, R. P. Mohosena Begum Tanu, Z. P. Sukhan, M. S. Rahman and Y. Mahmud. 2012. Heavy metal pollution and chemical profile of Khiru river, Bangladesh. *Inter. J. Environ.* **2**(1): 57-63.

Rahman, M. T., S. H. Moly and A. Saadat. 2013. Environmental flow requirement and comparative study of the Turag river, Bangladesh. *Inter. J. Sci. Res. Enviro. Sci. (IJSRES),* **1**(10): 291-99.

Rahman, S. H., A. Fakhruddin, M. J. Uddin, M. S. Zaman, A. Talukder, T. M. Adyel and M. M. R. Sarker. 2014. Water quality of shallow tube wells is affected by sanitary latrines and groundwater flow. *J. Bangladesh Acad. Sci.* **37**(2): 231-243.

Rahman, M. R. 2016. *Water resources*. Bangladesh National Conservation Strategy.

Roy, S. and S. Dutta. 2017. Opportunities and challenges for promoting sustainable water services to the urban poor in Dhaka city. *J. Environ. Sci. Nat. Resour.* **10**(2): 1-10.

Rathour, R. K., D. Sakhuja, A. K. Bhatt and R. K. Bhatia. 2022. Municipal wastewater connection for water crisis and jaundice outbreaks in Shimla city: Present Findings and Future Solutions. *Inter. J. Environ. Res. Public Health,* **19**(18): 11266.

Sheppard, D. A. E. 1995. *John Snow: Anesthetist to a Queen and Epidemiologist to a Nation: A Bibliography*. Cornwell Edward Island, Canada: York Point.

Swaminathan, S., V. A. Fonseca, M. G. Alam and S. V. Shah. 2007. The role of iron in diabetes and its complications. *Diabet. Care.* **30**(7): 1926-1933.

Shamsuddeen, U., M. Yusha'u and I. A. Adamu. 2009. Helicobacter pylori: the causative agent of peptic ulcer. *Bayero J. Pure Appl. Sci.* **2**(2): 79-83.

Schwarzenbach, R. P., T. Egli, T. B. Hofstetter, U. Von Gunten and B. Wehrli. 2010. Global water pollution and human health. *Ann. Rev. Environ. Resour.* **35**(1): 109-136.

Salam, M. and M. S. Alam. 2014. Identification and Delineation of Turag river basin boundary using remote sensing techniques. *J. Environ. Sci. Nat. Resour.* **7**(1): 169-175.

Sarker, S., S. Mahmud, R. Sultana, R. Biswas, P. P. Sarkar, M. A. Munayem, R. Ali, M. Wasim, M. F. Ali, M. O. Faruque and F. Z. Evamoni. 2019. Quality assessment of surface and drinking water of Nakla Paurosova, Sherpur, Bangladesh. *Adv. Microbiol*. **9**(8): 703-727.

SVRS (Bangladesh Sample Vital Statistics). 2020. Bangladesh Bureau of Statistics (BBS). Statistics and Informatics Division (SID), Ministry of Planning, Government of the People's Republic of Bangladesh.

Singh, A., T. Trushna, M. Kalyanasundaram, J. Ashok, A. J. Tamhankar and V. Diwan. 2022. Microplastics in drinking water: a macro issue. *Water Supply*, **22**(5): 5650–5674.

World Health Organization (WHO) and the United Nations Children's Fund (UNICEF). 2000. *Global Water Supply and Sanitation Assessment 2000 Report.* WHO/UNICEF, Geneva/New York. pp. 47.

World Bank. 2007. *Dhaka: Improving living conditions for the urban poor*. Bangladesh Development Series; Paper no. 17 Washington, D.C.: World Bank Group.

World Health Organization (WHO). 2012. *Pharmaceuticals in drinking water*. Available online at https://apps.who.int/iris/handle/10665/44630

World Bank. 2018. *Promising Progress: A Diagnostic of Water Supply, Sanitation, Hygiene and Poverty in Bangladesh.* WASH Poverty Diagnostic, World Bank, Washington, DC.

World Vision. 2021. *Waterborne disease facts and how to help.* Available online at https://www.worldvision.ca/stories/clean-water/cholera-waterborne-disease-facts

Water.org. 2023. *Bangladesh's water and sanitation crisis*. Available online at https://water.org/our-impact/where-we-work/bangladesh/#:~:text=Out%20of%20its%20population%20of,less%20than%20%243.10%20a%20day.

Xu, X., H. Yang and C. Li. 2022. Theoretical Model and Actual Characteristics of Air Pollution Affecting Health Cost: A Review. *Ijerph*, **19**: 3532.

Zuthi, M. F. R., M. Biswas and M. N. Bahar. 2009. Assessment of supply water quality in the Chittagong city of Bangladesh. *J. Engin. Appl. Sci.* **4**(3): 73-80.

Zakir, H., M. M. Rahman, A. Rahman, I. Ahmed and M. Hossain. 2013. Heavy metals and major ionic pollution assessment in waters of midstream of the river Karatoa in Bangladesh. *J. Environ. Sci. Nat. Resour.* **5**(2): 149-160.

(Revised copy received on 20.11.2023)

J. Asiat. Soc. Bangladesh, Sci. **49**(2): 139-148, December 2023 DOI: https://doi.org/10.3329/jasbs.v49i2.70763

ANALYZING THE LANDUSE LAND COVER CHANGE OF SONADIA ISLAND FROM 1990 TO 2020

MUNIRA NUSRAT, MAISHA HOSSAIN MIM AND MD. HUMAYUN KABIR*
Department of Geography and Environment, University of Dhaka, Dhaka, Bangladesh

Abstract

Remote sensing and Geographic Information Systems (GIS) are essential tools in determining the spatiotemporal extent of Landuse, and Land Cover (LULC) changes, as well as a variety of individual concerns, such as annual and seasonal changes in LULC caused by human interferences and interactions between the physical environment, cultural context, and anthropogenic factors. This study focuses on the LULC change of Sonadia Island, and it uses multi-temporal Landsat imagery from 1990 through 2020. The output analysis revealed four sub-features: mudflats, vegetation, open space, and water bodies. Vegetation cover decreased from 1486.71 hectares in 1990 to 986.13 hectares in 2000, and in 2020, the total area covered by vegetation increased significantly, reaching 1186.47 hectares, up from 497.97 hectares in 2010. Open space increased from 317.16 hectares in 1990 to 510.75 hectares in 2000. The net area expanded to 631.98 hectares in 2010 and then lost to 421.29 hectares in 2020. There was a consistent increase in the mudflats section from 1990 to 2010, when the amounts were 491.4 and 1179 hectares, respectively. By 2020, the area extent decreased to 796.41 hectares. From 1990 to 2000, the waterbody declined from 305.46 to 262.17 hectares, then slightly increased to 291.78 hectares in 2010, and then shrank again to 196.56 hectares in 2020. Therefore, this study could help policymakers decide on future landscape planning and evaluate Sonadia Island's current condition for long-term coastal management.

Keywords: LULC change, Remote sensing, GIS, Landsat, Coastal management.

Introduction

Land use denotes any anthropogenic activities or economic purpose linked with a specific piece of land. In contrast, land cover pertains to the features on the earth's surface (Lillesand and Kiefer, 2000). Land use and land cover are the most widely used techniques in geospatial analysis. Dynamic processes, land change matrices, and facts have all been identified using this change-based research. Land cover refers to the biophysical state of the earth's surface, which comprises soil, vegetation cover, water

*Corresponding author: mhk.geoenv@du.ac.bd

bodies, and other physical features (Liping *et al*., 2018). Land use is a method by which we can get maximum advantages in multiple types of activities, such as agriculture, habitations, industries, forestation, etc., through systematic land-use planning. This process is imperative for such development works strongly associated with a particular region's socio-economical outgrowth and to protect that region from environmental and ecological degradation (Islam *et al*., 2011).

Sonadia Island at Moheshkhali of Cox's Bazar district is located in the southeastern coastal region of Bangladesh with partial regular inundations by saline water. The island includes coastal and mangrove plantations, salt production fields, shrimp culture farms, plain agriculture lands, human settlements, etc. The ecosystem of this island was affected due to the accelerating rate of anthropogenic interceptions. To protect the ecosystem of this island, it was declared an Ecologically Critical Area (ECA) in 1999 under a section of the Bangladesh Environment Conservation Act, 1995 (MoEF, 2015). ECAs are ecologically designated areas or ecosystems influenced by human activities (Arefin *et al*., 2017). Bangladesh's coastal regions are a well-known cyclonic path subjected to strong cyclonic winds, storm surges, and tidal waves for many years, originating in the Bay of Bengal. Since 1820, cyclones have killed an estimated one million people in Bangladesh (Talukder *et al*., 1992), and the after-effects of these natural hazards include loss of human life, crops, and houses, pollution of the drinking water due to the inundation of land and ponds by saline water (Islam *et al*., 2011). Sonadia Island has gone through profound changes because the Government required to make it a digital island with seventeen projects, which include three power plants, four gas pipelines, two LNG terminals, five economic zones, one regional highway, and one eco-tourism park along with IT park (Mollah *et al*., 2021). Remote sensing and GIS techniques are becoming some of the most useful and prominent analytical tools for resource planners and managers (FAO, 1988), as they interlink spatial and attribute data for outputs in the form of maps, tables, and figures (Hossain *et al*., 2007). Therefore, the study focuses on detailed land cover and land-use transformations in Sonadia Island to find information about pre-existing land-use patterns and spatio-temporal land-use changes in land use over 30 years utilizing GIS and RS techniques.

Sonadia Island is located at 21°N and 91°E in Bangladesh's far southeastern edge, a few kilometers north of Teknaf Peninsula, north-west of Cox's Bazar town, and is delimited on the west and east by the Bay of Bengal (Fig. 1) (Arefin *et al*., 2017). The Moheshkhali Channel separates Sonadia Island from the mainland, while the Bara Channel separates it from Moheshkhali Island. The soil in this area is made up of various proportions of sand and clay. The soil in the north is clayey, and it is flooded by the sea. The land in the

southern half of the island is almost entirely sandy (DoE, 1999). The island as a whole has a mild climate with significant humidity. Summer starts in March and lasts until the beginning of June. Sonadia Island is a low-lying barrier island with a gently sloping altitude range of 0-4 meters (DoE, 1999).

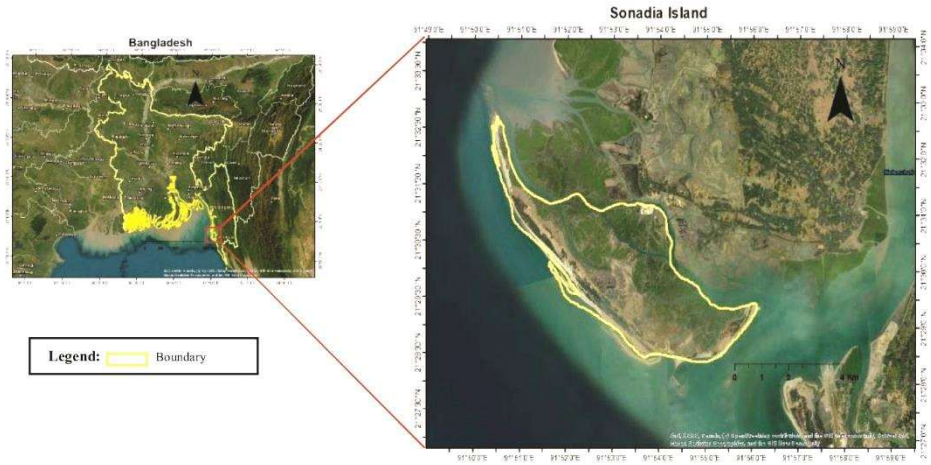

Fig. 1. Sonadia Island in Moheshkhali upazila of Cox's Bazar district, Bangladesh.

Materials and Methods

Data Acquisition and Image Processing: Table 1 shows the type of data collected from which sources and the key information needed to understand the data acquisition clearly. After data collection, the images were processed in ArcMap 10.8, which included layer stacking and research area clipping through the shape file.

Development of Classification Scheme (Supervised Classification)**:** The maximum likelihood classification mechanism was implemented for image interpretation. In supervised classification, sample pixels from images that are characteristics of specific classes are picked. Then, image processing software (ArcMap 10.8) is used to classify all other pixels in the image using these training sites as references.

Production of Initial Land Cover Map (Post-processing): After completing all the required steps, the acquired maps have been produced by ArcMap 10.8. The statistical analysis and graphs of different land classes of the images have been prepared with the help of Microsoft Excel.

Table 1. Landsat data acquisition details were used in the study.

Satellite ID	Path/Row	Acquisition date	Spatial resolution
Landsat 5	136/45	16-1-1990	30 m
Landsat 5	136/45	28-1-2000	30 m
Landsat 5	136/45	23-1-2010	30 m
Landsat 8	136/45	19-1-2020	30 m

Source: (earthexplorer.usgs.gov)

Accuracy Assessment: For image accuracy, the Kappa coefficient and overall accuracy, including individual user and producer accuracy of each class, have been assessed (Table 2 and Table 3).

Table 2. Image accuracy assessment.

Category	Formula
Overall Accuracy	(Total number of correctly classified pixels/ Total Number of reference pixels) *100%
User Accuracy	{Number of correctly classified pixels in each category/ Total Number of reference pixels in that category (The Row Total)} * 100%
Producer Accuracy	{Number of correctly classified pixels in each category/ Total Number of reference pixels in that category (The Column Total)} * 100%
Kappa Coefficient (T)	{(TS *TCS) −Σ (Column Total * Row Total)} / {TS^2- Σ (Column Total * Row Total)} *100%

Table 3. Image accuracy assessment results for LULC classification of the Sonadia Island.

Feature classes	User (%)				Producer (%)				Overall accuracy (%)	Kappa coefficient (T) (%)
	1990	2000	2010	2020	1990	2000	2010	2020		
Mixed vegetation	80	100	87.5	100	80	85.7	100	100	92	89.2
Open space	100	87.5	100	100	83.3	100	100	100	92.3	89.7
Water body	100	100	100	100	100	100	87.5	91.8	96.2	98.3
Mudflats	88.8	83.3	88.8	88.8	100	83.3	100	100	96.9	95.8

Area Calculation and Spatio-Temporal Change Detection: Following the creation of the initial land cover map, the area was measured using ArcMap10.8 to detect spatio-temporal changes.

Results and Discussion

The land use land cover distribution maps, acquired from the Landsat images analysis, are described below. Four different land classes have been identified from the images, and each color symbolizes the distribution of the area of each classified LULC, which is for four distinct periods (1990, 2000, 2010, 2020) outlined in the subsequent segment in a regulated way.

Landuse/ Land cover classification

Land class (1): Mixed vegetation: Sonadia Island is mostly covered with mangroves and coastal forest, which contains diverse vegetation, Jhau trees, and hilly forests. Sonadia Island's natural safeguard against cyclonic wind and storm surges is the mangrove forest, which is largely found in the southwestern half of the island. This class is critical for the coastal ecology and, more importantly, for protecting people and property in the area from cyclones and tidal surges. Again, the hilly forest, Jhau trees, and mixed vegetation are essential for the local communities, as they protect the topsoil from the impact of raindrops and add organic matter to the soil. Besides, they rely on the forest for many of their daily needs, e.g., fuel, wood, fodder, etc.

Land class (2): Open space: The sections of vacant segments not used for any purpose are called open spaces, including sand beaches, dunes, and salt fields.

Land class (3): Mudflats: Mud flats constitute the upper zone of tidal flats, depositional processes being dominated by the fallout of suspended sediment comprising sortable silts, flocs, and aggregates (Chang *et al.,* 2007; Flemming, 2012). Mudflats*,* or tidal flats, are coastal wetlands formed on sheltered shores where the rivers or tides can deposit greater sediments (silt, clay, and detritus). These form in areas where tides or rivers have deposited sediments. As rivers and numerous streams are present in Sonadia and bounded by the Bay of Bengal in the west, east, and south, this island has its fair share of mudflats.

Land Class (4): Water Body: Small wetlands, ponds, and lagoons are examples of intertidal zones delineated by water bodies. This stretch's northwestern and northeastern parts, which are mostly exposed to storm surges, include intertidal flat deposits.

Fig. 2 depicts the distribution of land cover for the study area in 1990. The map clearly shows that there was a significant amount of vegetation present throughout the area. The most prevalent land cover types then were vegetation cover and mudflats. The distribution of the study area's land cover in 2000 is shown in Fig. 3. The map showed that the area's substantial amount of vegetation, which was present throughout 1990, had

decreased, and the number of mudflats emerged in the vicinity with the decline of vegetation cover. Mudflats and open spaces were the two predominant land cover types at the time. Figure 4 illustrates how the study area's land cover was distributed in 2010. The map reflects that between 1990 and 2000, the area's substantial extent of vegetation cover had declined. Around that area where the vegetation decreased, the number of mudflats also expanded. The two most prominent land cover types at that time were mudflats and open spaces. The distribution of land cover for the study area in 2020 is represented in Fig. 5.

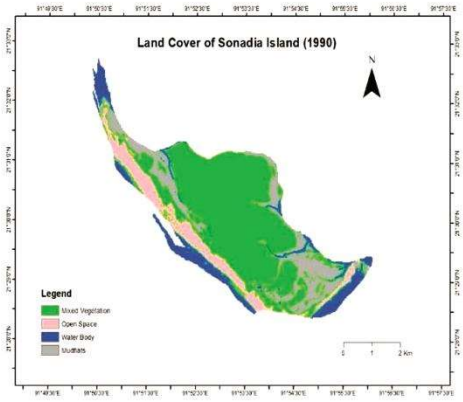

Fig. 2. Land Cover Map of Sonadia Island, 1990.

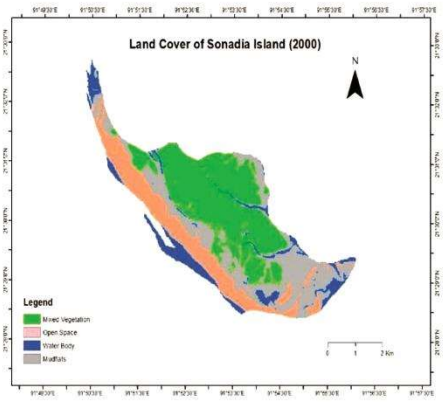

Fig. 3. Land Cover Map of Sonadia Island, 2000.

The map made it apparent that the significant decrease in vegetation cover that had been observed in previous years had dramatically reversed. Along with increased vegetation volume, there was obvious evidence of a decline in mudflats and water bodies. At that time, vegetation and mudflats were the most prevalent land cover types.

Changes in areal extent of LULC: The distribution of LULC extent of Sonadia Island from 1990 to 2020 is represented as a data table in acres so that we can study the pattern of changes in the LULC over time (Table 4). According to the analysis, the total quantity of land on Sonadia Island was estimated to be above 6000 acres.

The total area covered by vegetation decreased from 1486.71 hectares in 1990 to 986.13 hectares in 2000. Compared to 2020, the entire area covered by vegetation increased significantly, reaching 1186.47 hectares, from 2010, when it was substantially reduced to 497.97 hectares. 2000, there were 510.75 hectares of open space, up from 317.16 hectares

in 1990. The size increased to 631.98 hectares in 2010 and then declined to 421.29 hectares in 2020. In the mudflats section, there was a consistent increase from 1990 to 2000 and 2010, when the extents were 491.4, 841.68, and 1179 hectares, respectively; by 2020, the extent reduced to 796.41 hectares. From 1990 to 2000, the waterbody declined again, from 305.46 to 262.17 hectares, then somewhat increased to 291.78 hectares, and then again reduced to 196.56 hectares.

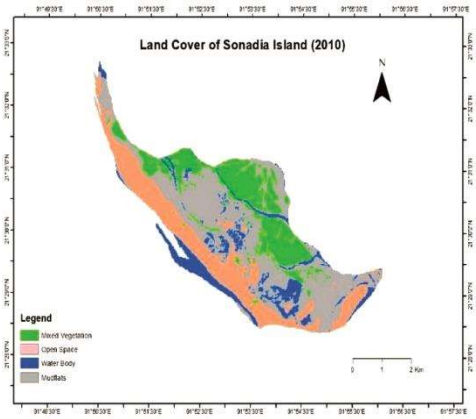

Fig 4. Land Cover Map of Sonadia Island, 2010.

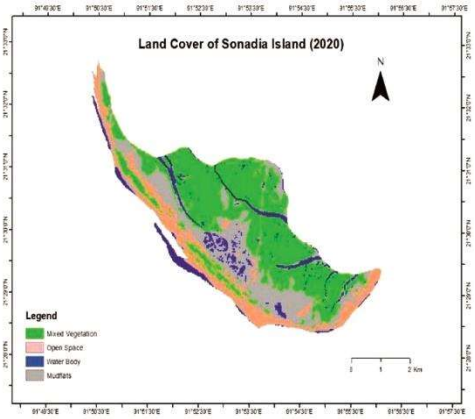

Fig 5. Land Cover Map of Sonadia Island, 2020.

Table 4. Spatio-temporal variations in areal extent of LULC Change of Sonadia Island between 1990 and 2020.

Year	Mixed vegetation (ha)	Open space (ha)	Mudflats (ha)	Water body (ha)	Grand total (ha)
1990	1486.71	317.16	491.4	305.46	2600.73
2000	986.13	510.75	841.68	262.17	2600.73
2010	497.97	631.98	1179	291.78	2600.73
2020	1186.47	421.29	796.41	196.56	2600.73

The hypothesis of the analyzed LULC change of Sonadia island: Driving forces influencing the changes

Vegetation Vs. Mudflats: It can be seen from the trend analysis graph of vegetation and mudflats that there is an inverse relationship between mudflats and vegetation coverage

of Sonadia Island from 1990 to 2020 (Table 4). There was a significant increase in mudflat coverage from 1990 to 2010 but a significant decrease in mixed vegetation coverage from 1999 to 2010.

The island area has lost its natural complexity due to human intervention, such as extensive and illegal deforestation and slope modification, unplanned settlement development, and crop cultivation on adjacent lands (Islam *et al.,* 2011). On the other hand, Sonadia Island's mangrove forest has been infringed upon, primarily for shrimp aquaculture. Mangroves, which generally inhabit mudflats during their early stages of formation, live in the emerging tidal mudflats. It can be hypothesized from the analysis that, even though locals have come to rely on the forest for many household necessities like firewood, housing materials, and boat-building materials, as well as herbal plants for traditional remedies and other minor items, mixed vegetation coverage has decreased between 2000 and 2010. The extent of vegetation in 2010 was at its lowest level, as shown in the trend analysis graph. Extremely Severe Cyclonic Storm Sidr, struck Sonadia Island in 2007, causing damage to the island's infrastructure. From 1990 to 2010, the expansion of mudflats may be due to increased local economic activities like shrimp cultivation, salt farming, and watermelon farming. The overall percentage of mangroves in the Sonadia Island region has been rising recently as a result of newly developed mangrove forests along the eastern and western coasts, as well as the plantation of mangrove trees by the Forest Department and locals as they become aware of the significance of protecting their property (Hossain *et al.,* 2023). The expansion of vegetation cover in certain areas is a time-consuming process. After 2010, the Forest Department and the Ministry of Environment and Forest (MoEF) launched an afforestation program, resulting in a substantial increase in vegetation coverage in 2020, and at the same time, mudflat coverage dropped substantially. As a result, the vegetation and the mudflats have an asymmetric connection. Mudflat coverage expanded significantly as vegetation coverage fell. Again, mixed vegetation coverage rose disproportionately as mudflats coverage decreased. Thus, it is apparent from the trend analysis of the hypothesis mentioned above that changes in open space and an increase in mudflats resulted from a drastic decline in vegetation and water bodies.

Open Space: The open space segment consistently increased from 1990 to 2010, with 317.16, 570.15, and 631.98 hectares, respectively. Then it reduced to 421.29 hectares in 2020. However, effective coastal afforestation initiatives, particularly from 2000 to 2017 (Abdullah *et al.,* 2019), led to a gradual increase in vegetation, impacting the extent of the island's open spaces in 2020. The significant change in the open space segment (Table 4) is attributable to Sonadia Island's limited land use diversity. The soil texture in this

area contains a sizable amount of sand (DoE, 1999). Since there is a lot of saltwater intrusion, this land is unsuitable for farming.

Water Body: This section of the trend analysis graph (Table 4) depicts that water body coverage continues to shrink. Due to anthropogenic activity and excessive use of freshwater body features such as small wetlands, ponds, and lagoons, the volume of water bodies has reduced. Anthropogenic interferences also contribute to the pollution of certain freshwater bodies.

Conclusions

The current study uses remote sensing and GIS methods to depict spatio-temporal changes in land use and land cover over a thirty-year period. Four sub-features, including vegetation, open spaces, mudflats, and water bodies, were identified on Sonadia Island. The key land classes that have significantly altered during the last thirty years include vegetation, open space, mudflats, and water bodies. Knowing the island's various land cover classes is necessary to assess and carry out effective land-use planning for any development or improvement project on Sonadia Island.

References

Abdullah, A. Y. M., A. Masrur, M. S. G. Adnan, M. A. A. Baky, Q. K. Hassan, and A. Dewan. 2019. Spatio-temporal patterns of land use/land cover change in the heterogeneous coastal region of Bangladesh between 1990 and 2017. *Remote Sens.* **11**(7): 790.

Arefin, M.S., M.K. Hossain, and M.A. Hossain, 2017. Plant diversity of Sonadia Island – An ecologically critical area of south-east Bangladesh, *Bangladesh J. Plant Taxon.* **24**(1): 107-116.

Chang, T.S., B.W. Flemming and A. Bartholoma, 2007. Distinction between sortable silts and aggregates in muddy intertidal sediments of the East Frisian Wadden Sea, Southern North Sea. *Sediment. Geol.* **202**: 453-463.

DoE 1999. GIS and Cartographic Services – Final Report, Pre-Investment Facility Study: Coastal and Wetland Biodiversity Management Project (Project BGD/94/G41), Dhaka, Bangladesh.

FAO 1988. Aspects of FAO's Policies, Programmes, Budget and Activities Aimed at Contributing to Sustainable Development. Document to the 94th session of FAO council, Rome: Food and Agriculture Organization of the United Nations.

Flemming, B.W. 2012. Siliciclastic back-barrier tidal flats. In: *Principles of Tidal Sedimentology,* R.A. Davis Jr. and R.W. Dalrymple (eds.), *Springer, Dordrecht,* pp. 231-267

Hossain, M.S., S.R. Chowdhury and M.A.T. Chowdhury, 2007. Integration of remote sensing, GIS and participatory approach for coastal island resource use zoning in Bangladesh, Songklanakarin, *J. Social Sci. and Hum.* **13**(3): 413-433.

Hossain, M. S., M. Yasir, M. S. Shahriar, M. Jahan, S. Liu and A. J. Niang, 2023. Morphological change assessment of a coastal island in SE Bangladesh reveals high accumulation rates. *Region. Stud. Marine Sci.* p. 62.

Islam, M.A., M.K. Maitra, A.B.K. Majlis, S. Murshed and S. Rahman, 2011. Spatial Changes of Landuse/Land Cover of Moheshkhali Island, Bangladesh: A Fact Finding Approach by Remote Sensing Analysis, *Dhaka Univ. J. Earth Environ. Sci.* **2**: 43-54.

Lillesand, T.M. and R.W. Kiefer, 2000. *Remote sensing and image interpretation*, New York: John Wiley and Sons.

Liping, C., S. Yujun and S. Saeed, 2018. Monitoring and predicting land use and land cover changes using remote sensing and GIS techniques: a case study of a hilly area, Jiangle, China. *PLoS ONE*, **13**(7): 1-23.

Mollah, T.H., M. Tahsin, N. Mohammad, M.R. Hasan and N. Mollah, 2021. Predicating Landuse/Land Cover Changes for 2050 Using CA-Markov Model and LCM: A Case for Maheshkhali Island, Bangladesh, *J. Faculty Social Sci. Jahangirnagar Univ.* **44**: 220-232.

MoEF 2015. Fifth National Report to the Convention on Biological Diversity, Ministry of Environment and Forest, Government of the People's Republic of Bangladesh, Dhaka, pp.164

Talukder, J., G.D. Roy and M. Ahmed (eds.). 1992. *Living with cyclone: Study on storm surge prediction and disaster preparedness*, Dhaka: Community development library. pp. 124

(Revised copy received on 04.10.2023)

J. Asiat. Soc. Bangladesh, Sci. **49**(2): 149-164, December 2023 DOI: https://doi.org/10.3329/jasbs.v49i2.70764

MEANDERS OF THE KABODAK RIVER, BANGLADESH

MUNIA TAHSIN[1] AND MOHD. SHAMSUL ALAM[*2]
[1]*International Centre for Climate Change and Development (ICCCAD), IUB, Dhaka*
[2]*Department of Geography and Environment, Jahangirnagar University, Savar, Dhaka, Bangladesh*

Abstract

The study explores the meandering patterns of the Kabodak River and investigates the relationship among geometric aspects like sinuosity, width, amplitude, radius of curvature, and wavelength. The variables like basin area, river length, and longitudinal profile were measured, and the geometric aspects such as sinuosity, radius of curvature, meander wavelength, and meander amplitude were interpreted and calculated using Google Earth Pro and ArcGIS 10.5. With the aid of the software SPSS and unscrambler X, the relationship among the geometrical aspects was examined. Besides, different meander patterns have been identified by analyzing the meander form. The result reveals that the upper and lower parts of Kabodak appear more sinuous than the middle. Nodal patterns in river sections vary, with the upper and lower sections experiencing increased sinuosity due to lower gradients, reduced flow, and blockage. In contrast, the middle section exhibits less sinuous characteristics because of neotectonics upliftment. Among the variables, meander wavelength, amplitude, and radius of curvature have weak positive correlations between and among them, except for the wavelength-amplitude relation. The relationship between wavelength and amplitude is inversely proportional. The variable width appears non-responsive with other variables, which makes sense as the river's width is already structuralized due to human interference. Theoretically, the Kabodak River's meandering pattern deviated from other meandering river studies due to human interference. Similar types of work on other meander rivers of the delta may be explored to see if the result corroborates. Besides, the effect of human intervention on meandering patterns and morphological processes needs further study.

*Keywords***:** Meander, Kabodak river, Sinuosity, Longitudinal profile, Geometric aspects.

Introduction

Though a common sight in a deltaic environment, Meander rivers may also occur in other parts of Bangladesh (Bagchi, 1944; Chowdhury, 1959). Because of its winding nature, it appears sinuous when seen from the sky. Such a unique plan-view is deeply connected

[*] Corresponding author: m.s.alam.ju@gmail.com

with a wide range of human activities like economic, ecological, environmental, and cultural activities (Alam *et al.,* 2022). In densely populated parts of the world, humans use river courses for habitation and livelihood (Kusratmoko, 2017; Kusratmoko *et al.,* 2019). Therefore, managing the functions of the rivers is essentially linked with the welfare of the population living along the river. In nature, the river bends due to numerous independent factors, like geology, climate, gradient, and time. (Montgomery, 1999; Schumm, 1967; Hogan and Luzi, 2010). These factors, again, are linked with the dependent variables, like river discharge, vegetation, hydraulic characteristics, and sediment transport (Buffington *et al.,* 2003; Montgomery and Buffington, 1993). The meandering rivers constantly change their banking because of this interaction between independent and dependent variables. In the short term, the gradient, energy (water discharge), and matter (sediment transport) affect the shape of a meander river channel. However, Church and Ferguson (2015) note that these variables' interactions typically serve as their guides.

The formation and persistence of river meanders have intrigued multiple scientific disciplines, including geomorphology, fluid dynamics, sedimentology, mathematics, and engineering. As a result, several theoretical frameworks have been put forward in the extended scholarly literature to provide a comprehensive understanding of the phenomenon of meandering (Morisawa, 1968; Leopold *et al.,* 1964). While disagreements persist regarding the classification and identification of meanders, some commonalities shed light on the mechanisms driving meander development. Early attempts to quantify meander processes identified consistent geometric ratios, such as the relationship between radius of curvature, meander length, and channel width (Thorne *et al.,* 1997). The relationships between meander length, channel width, and curvature radius are independent of bed and bank materials and connected to an unspecified mechanical principle (Knighton, 1977). The ratio of curvature to channel width is crucial for understanding flow resistance and offers insights into why channels of different sizes exhibit similar geometric patterns (Leopold and Wolman, 1960; Dury, 1970). Scientists developed statistical models rooted in heuristic reasoning, treating meanders as a type of random walk aimed at minimizing changes in flow direction through in-depth, velocity, and slope adjustments. However, while valuable for understanding large-scale meander patterns, these models do not fully predict the intricate details of meander evolution (Komatsu and Baker, 1994; Schumm and Khan, 1972).

Despite the abundance of scholarly literature on the subject matter, several academics have agreed that a comprehensive and satisfactory explanation for meandering remains elusive (Leopold *et al.*, 1964; King, 1966; Morisawa, 1968). The Gulf Stream and other streams characterized by straight sections with meandering thalwegs, sediment-free streams situated on glacial ice, and sediment-free streams located on solid rock formations much above base level all show meander patterns. This observation implies that natural streams have an inherent tendency to meander (Knighton, 1972; Zhang *et al.*, 2008). Therefore, sediment's role in erosion, transportation, and deposition during the creation and migration of meanders is mostly secondary (Leopold *et al.*, 1964; Davis, 1913). In Bangladesh, meandering rivers are common regarding availability, followed by braided rivers and linear channels (Chowdhury, 1959). In his 1959 work 'Morphological Analysis of the Bengal Basin,' Chowdhury covers both parts of Bengal, encompassing a wide range of studies that delve into the erosional, depositional, and transportation activities of the Bengal rivers (Rob, 1989). The greater floodplains and the Ganges deltaic plains are low-lying, and valley gradients are low; thus, channel meanders occur quickly (Banglapedia, 2015). Furthermore, a second arc on the perimeter of the simple loop gradually forms to create compound loops (Brice, 1974). Over time, each meander slowly grows to greater and greater size, increasing in arc and radius, until the neck of a valley-side spur or a floodplain lobe is narrowed and worn through (Schumm, 1963).

Knowledge about meandering rivers is essential, as many economic activities are associated with these rivers. Learning about the nature and behavioral pattern of the meandering river will help in river management. The researchers chose the Kabodak River as a case study because of its unique characteristics. The river flows through a moribund delta, a mature delta, and terminates near a tidally active deltaic region. This makes it an ideal river for investigating the process of meander formation (Fig. 1). The Kabodak River originated from the Mathabhanga River and disconnected from its source in the Chuadanga district (Banglapedia, 2021). The river flows through the Jhenaidah, Jessore, Satkhira, and Khulna districts and finally meets the Shibsha River at Paikgacha upazila in the Khulna district. Along the whole length of the Kabodak River, it exhibits different subsurface lithologic conditions and hydrogeomorphologic settings. The objective is to identify the meandering patterns of the different parts of the Kabodak River and investigate the relationship among geometric aspects like sinuosity, width, amplitude, radius of curvature, and wavelength.

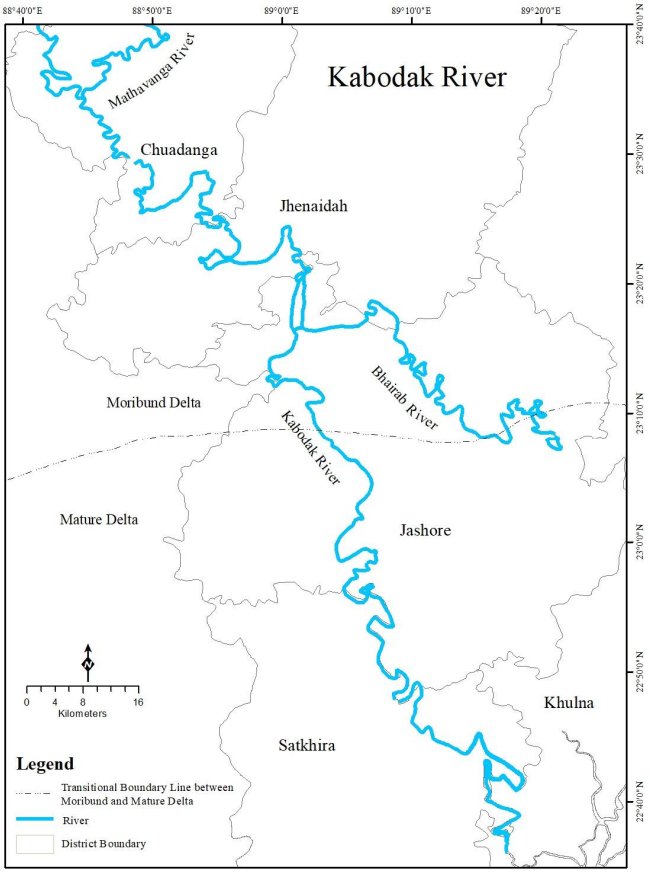

Fig. 1. The Kabodak river.
Complied by the authors, 2023.

Methodology

In this study, the Kabodak River of Bangladesh is selected to measure the types and number of meander patterns developed by the river and the relationship among the geometric aspects like width, amplitude, radius of curvature, and wavelength. The specific activities carried out as a part of this study are summarized below:

Identification and delineation of the Basin area of the Kabodak River: The study uses high-resolution DEM data downloaded from USGS (2019) to identify and delineate the river basin. Then, the study computes the flow direction with the Flow Direction tool. To find the contributing area, we used a flow accumulation threshold. The output is a raster displaying the delineated watersheds for the Kabodak River.

Measurement of the River Length: The Kabodak River's length was determined using Landsat OLI images. To pinpoint the precise initiation and termination points of the Kabodak River, a reference was made to Banglapedia 2021. Subsequently, a transect was drawn across the middle section of the Kabodak River, and the river length was measured accordingly.

Drawing the longitudinal profile: The river's geometric attributes were extracted from the Digital Elevation Model (DEM) dataset. This involved identifying and delineating the thalweg line, which corresponds to the river's lowest point. To obtain the longitudinal profile of the Kabodak River, the elevation profile tool was utilized. This tool facilitated the generation of a comprehensive representation of the river's elevation changes along its entire course. (Fig. 2).

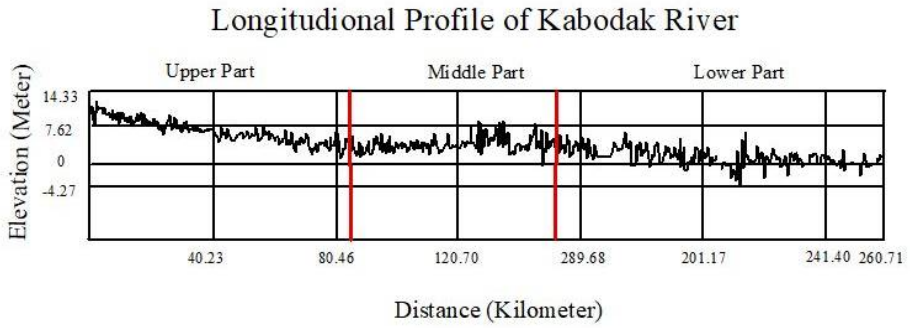

Fig. 2. Longitudinal profile of the Kabodak river, 2023.
Source: Compiled by the authors, 2023)

Measuring geometric aspects of the meander: Sinuosity, width, amplitude, radius of curvature, and wavelength are quantified as geometric aspects (Fig. 3). sinuosity was calculated as the along-channel distance divided by the Euclidian distance per bend and meander. Using the ruler tool in Google Earth Pro, the channel length is measured from the centerlines. In the wet season, meander width is measured in Google Earth Pro by measuring from bank to bank. The meander amplitude was calculated as the highest normal distance of the channel position from the meander belt centerline as defined by the inflection points. The radius of curvature was determined from the meander belt centerlines using Google Earth Pro's ruler "circle" tool, and the meander wavelength was estimated using the centerlines of two sequential meander bends. Finally, the relationship among geometric aspects is measured using the SPSS and unscrambler X software.

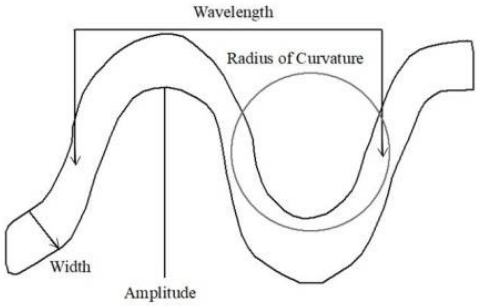

Fig. 3. Geometric Aspects of a River.
Source: Complied by the Authors, 2023.

Assessing meander pattern: Based on the meander node and complexity, the authors of this paper divided the shapes into four major groups (Fig. 4).

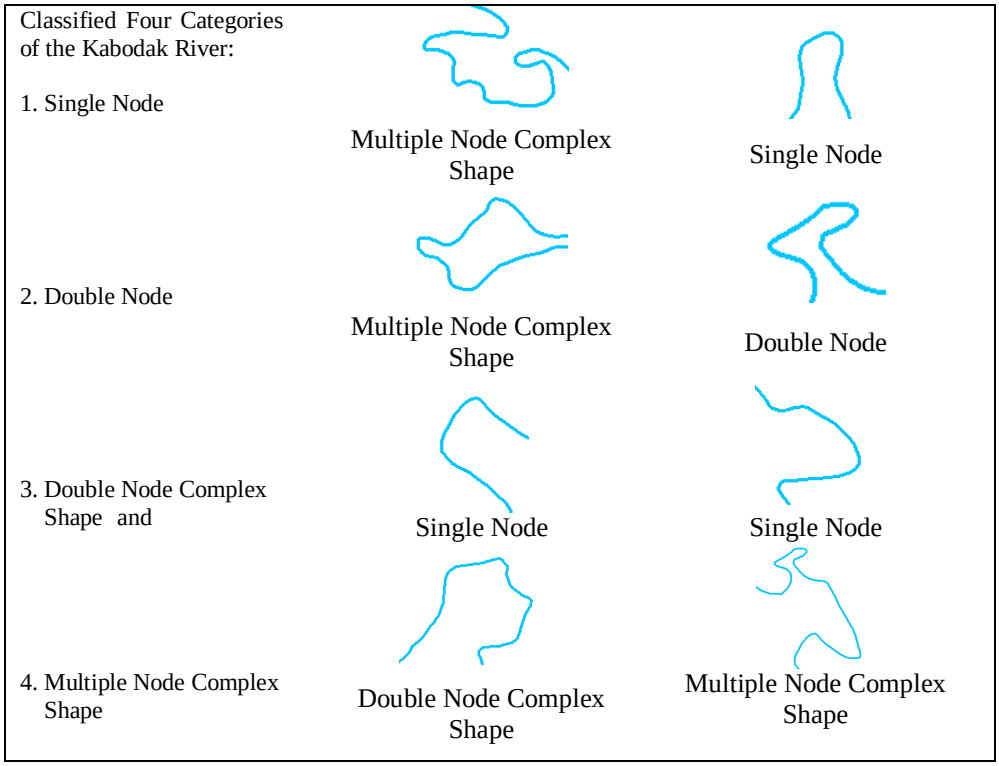

Fig. 4. Complex Shape of Meander Bend of Kabodak River.
Compiled by the authors, 2023.

Results

Basin area and length of the Kabodak River: The orientation of the river is north-south directed. The current measurement of the river's entire length is around 262.5 km, while the basin area of the Kabodak River is roughly 2,918.67 square kilometers.

The Kabodak River now relies mainly on channeling its tributaries for its flow. The first-order stream within the Kabodak river basin (Fig. 5) has accounted for the highest proportion of contribution, namely 50.24%. The subsequent notable contribution is derived from the 2nd Order stream, which accounts for 24.88% of the total. The third-order stream accounts for 10.14% of the total contribution, while the fourth-order stream exhibits the lowest contribution at 6.28%. The contribution exhibits a reduction of 8.45% in the fifth-order stream. This implies that this river's primary water source is derived mainly from smaller tributaries. Fig. 5 demonstrates that the middle part has the greatest quantity of order streams.

On the contrary, the upper part exhibits a shortage of primary and secondary streams, leading to an exceedingly sinuous configuration due to diminished energy levels. In addition, a substantial quantity of first-order streams in the middle part of the river contributes to its heightened flow rate relative to other segments. The lower part of the river is situated inside a region characterized by tidal activity, resulting in partial flow from backwash water that aids in the river's continuation.

Longitudinal Profile of the Kabodak River

The sinuosity of a river is contingent upon its gradient. The longitudinal profile of the Kabodak River provides an overview of the gradient decline pattern seen along the whole river. The depiction of the upper, middle, and lower sections of the Kabodak River (Fig. 2) is based on the observed gradient decline. Upon analysis of the comprehensive profile of the Kabodak River, it is evident that the river exhibits a consistent downward trend, except for a notable deviation in the middle part. The upper part of the graph depicts a state of equilibrium, but notably, the central part exhibits erratic fluctuations, suggesting an unstable state inside this interval. This fluctuating state reaches a peak elevation of around 7.6 meters above sea level and then descends towards sea level. The data exhibits significant fluctuations. The underlying cause of this precarious state may be attributed to indistinct refraction close to Jhikargacha. Also, near the midpoint of the lower part, it eroded below sea level (-4.27 meters) because of extensive bed scouring during high flood incidence in 2000 and 2011.

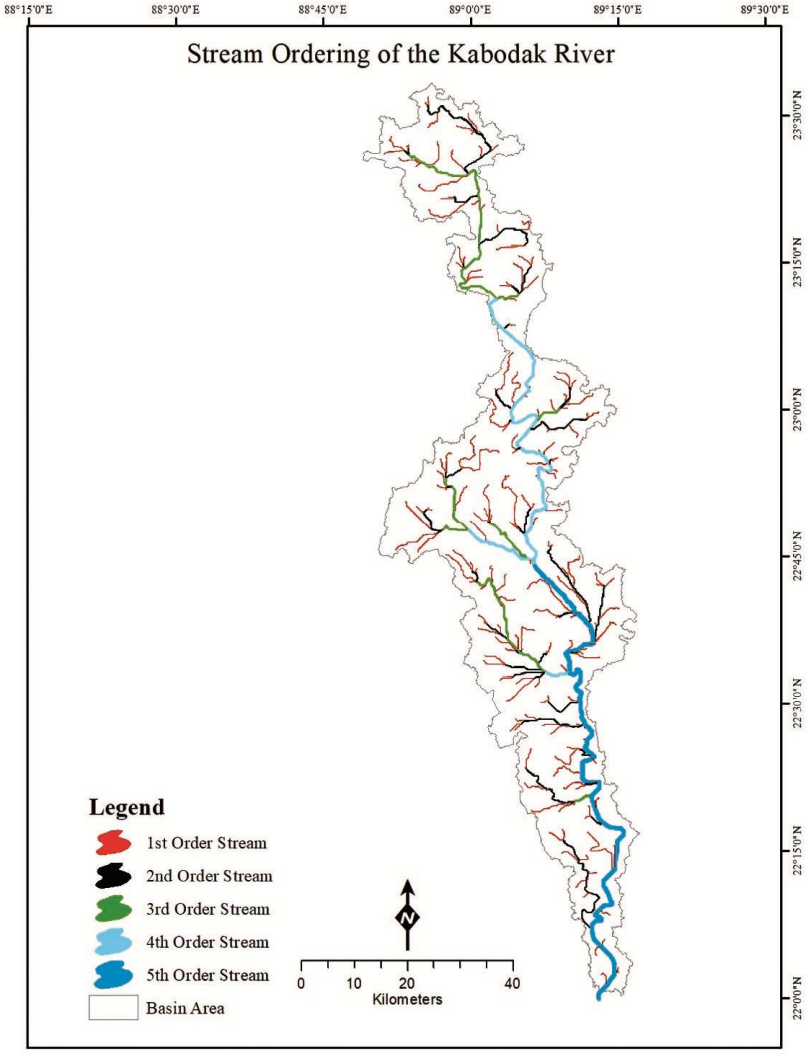

Fig. 5. Stream order map in Kabodak river basin, 2023.
Compiled by the authors, 2023.

This river's lower reach is tidal and exposed to heavy siltation, thus covering lower gradients and a high sinuosity ratio. On the other hand, the lower part has a sinuosity of 2.34, whereas the sinuosity of the whole river is 2.32. The central part would follow the same sinuosity trend if the middle part didn't face the fault line.

- Sinuosity Ratio of Kabodak River: 2.32;
- Sinuosity Ratio of the Upper part: 3.18;
- Sinuosity Ratio of Middle part: 1.66;
- The Sinuosity Ratio of the Lower part is 2.34.

The complex shape of the meander bend of the Kabodak River

The present categorization scheme classifies several forms of meander bends based on the number of nodes and the level of shaping complexity. The intricate formations of the Kabodak River can be classified into four primary categories (Fig. 4).

This research examines and analyzes 31 meander nodes within the Kabodak River. The complexity of the structure is attributed to the significant decrease in sedimentation and water flow originating from the top source. On the other hand, the lower portion is subject to elevated sedimentation and retrograde discharge due to tidal impacts. The energy diminishes, forming a lower gradient that gives rise to a complex meander in the upper section. Likewise, a significant sedimentation process leads to a complicated meander in the bottom section. Classifying a meander's form involves shape matching, sinuosity, radius-of-curvature, breadth, amplitude, and wavelength. The meander forms have been classified into four distinct groups. Thirty-one different shapes and planform photographs were analyzed to characterize each particular meander. This analysis was conducted to identify the specific shape type used in the present research, as shown in Table 1.

Table 1. Different shapes of the meander bend of the Kabodak river.

Node types	Upper part	Middle part	Lower part
1. Single Node	8	3	4
2. Double Node	2	0	1
3. Double Node Complex Shape	1	2	0
4. Multiple Node Complex Shape	4	0	6

Source: Compiled by the Authors, 2023.

Table 1 reflects a visual representation of the variation in meander form along different river sections. The upper portion of the river exhibits the most complexity in meander shape (48.39%). In contrast, the middle section displays the lowest diversity (16.13%),

which may be attributed to the inflow of several tributary streams and a relatively steep gradient compared to other parts of the river. The complicated structure of the bottom section is mostly attributed to its low gradient and the backwash effect resulting from the tidal activity in the area (35.48%).

Relationship among the Geometric Aspects of the Meander Pattern

It's important to know how the four geometric properties (width, radius of curve, wavelength, and amplitude) relate because any change in one affects the other three differently. Primary concerns in studying geometric aspects of meandering rivers include point bar development and concave bank erosion (Harvey, 1988). For example, the water-holding capacity will decrease as the river's width decreases, just as accretion will rise in the point bar. In some areas, such as along riverbanks, erosion will accelerate, and the amplitude is expected to increase. This can be understood better from the chronological changes of the Kabodak River (Fig. 6). In 1780, the higher river width exhibited lower sinuosity and amplitude; in contrast, during 2019, with decreasing width, sinuosity increased, and amplitude widened along the whole length of the river.

For assessing the relationship among the geometric aspects of the Kabodak River, 54 meander bends are counted and analyzed. The relation among and between width-radius of curvature (A), width-wavelength (B), and width-amplitude (C) are almost non-responsive as the width of the river has been partly regulated because of human interferences (Fig. 7). The link between wavelength and radius of curvature (D) demonstrates a responsive correlation. A positive correlation exists between the wavelength and the radius of curvature of a river. The research posits that an increase in the wavelength of the river corresponds to an increase in the radius of curvature. The result corroborates a similar study undertaken by Dury in 1970. However, as the values of these two particular meander factors increase, it becomes challenging to forecast the characteristics of the wavelength accurately.

The correlation between the radius of curvature and amplitude (E) implies a similar outcome for the relationship between wavelength and radius of curvature (D). An inverse-proportional connection exists between the wavelength and amplitude (F). An increase in wavelength results in a reduction in amplitude. Conversely, a decrease in wavelength will increase amplitude. This relationship applies to all meandering rivers.

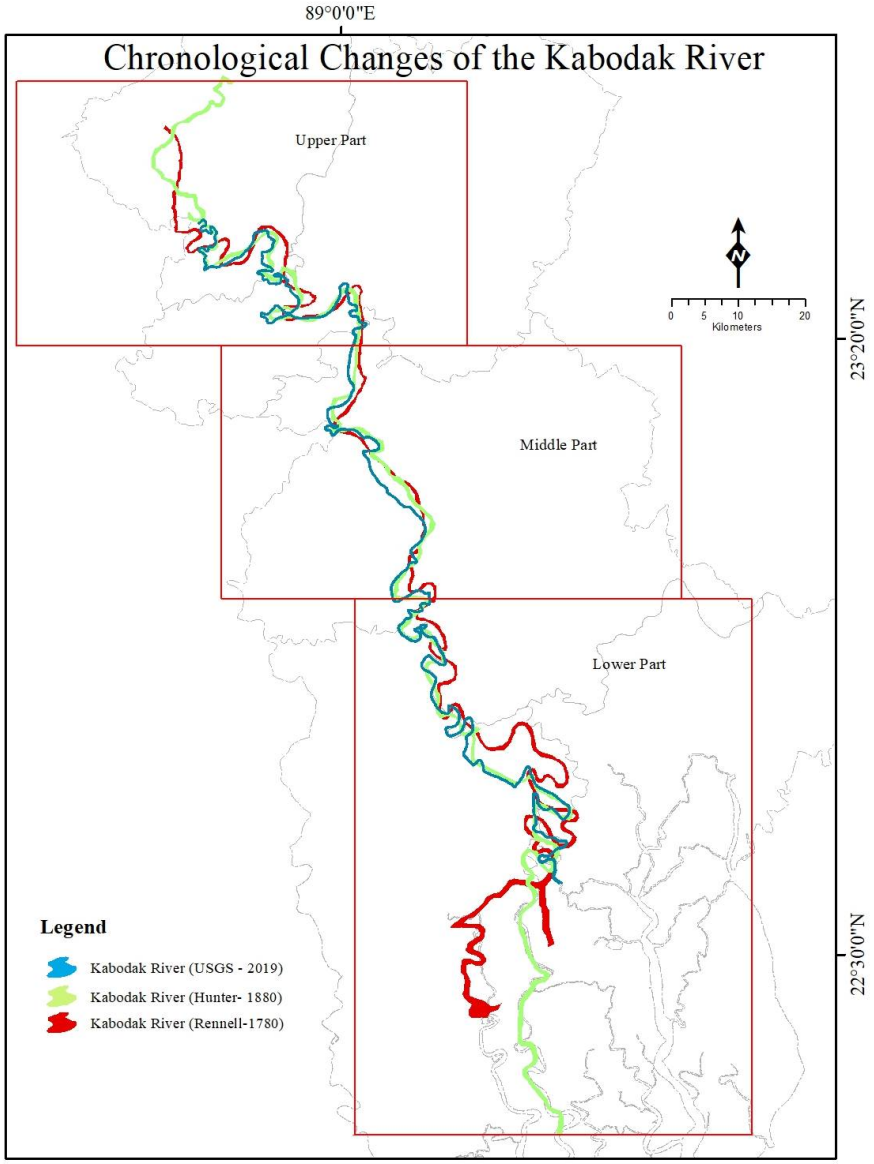

Fig. 6. Variations in channel shifting tendency at different parts of the Kabodak River between 1777 and 2019
Source: Compiled by authors, 2023

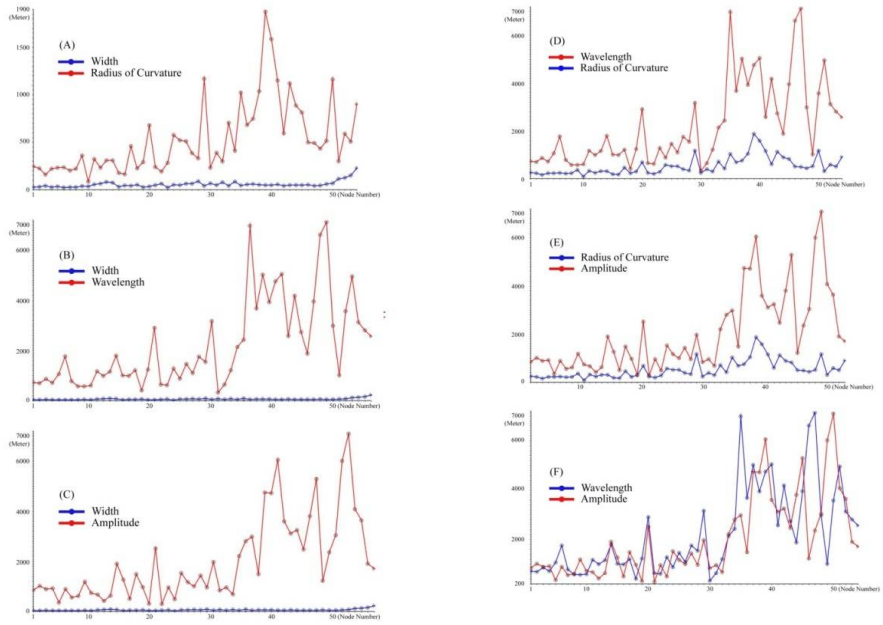

Fig. 7. Relationship among the meander patterns of the Kobodak river.
Source: Compiled by the authors, 2023

Discussion

The Kabodak River has a meandering pattern with a relatively high sinuosity ratio. The upper part exhibits the most sinuosity compared to the other two segments. The upper part of the channel has been disconnected from its main channel, resulting in a lack of water flow (energy) from the upstream and subsequently causing an increase in the sinuosity ratio. In contrast, it can be seen that the middle part of the river has the least sinuosity, having a nearly linear alignment possibly in part due to neotectonics uplift, but the lowest portion has a meandering pattern resulting from exposure to tidal siltation.

The Kabodak River has a consistent, progressive decrease in its gradient, resulting in a concave form. The perfect longitudinal profile of a river has a concave contour. The downstream section of the river is situated close to sea level. The lowest portion of the area experienced significant erosion below sea level (-4.27 meters) due to considerable bed scouring caused by heavy flood events in 2000 and 2011 (Tareq, 2016). The factors contributing to the formation of various meander characteristics include width, radius of curvature, amplitude, and wavelength. The process of altering the form of the radius of

curvature, amplitude, and wavelength takes a long time. However, the width of a river may be rapidly altered due to fluctuations in discharge volume or variations in the severity of human interference. Significantly, in the case of the Kabodak River, which has been subjected to human-induced structural interruptions, there is a lack of significant correlation between its width and the radius of curvature, amplitude, and wavelength. Types of human interferences responsible for narrowing the valley width are listed in Table 2.

Table 2. Types of human interferences on river course and their effects in different aspects.

<table>
<tr><th>Aspects</th><th>Human Interferences</th><th>Effects</th></tr>
<tr><td rowspan="2">Geomorphological</td><td>• Constructions of cross-roads
  </td><td rowspan="4">• Narrowing the river width to save cost hampers rapid downstream movement.
• Increased upstream siltation
• Decreased water holding capacity
• Flooding in streams due to ponding effects
• Expedite oxbow lake formations
• Narrowing width and
• Altered the natural river systems as well as the ecosystem</td></tr>
<tr><td>• Encroachment of the river through building and bridges construction along and across the river length
  </td></tr>
<tr><td>Agricultural</td><td>• Extension of agricultural practices along the river length by landfilling
 
  </td></tr>
<tr><td>Biological</td><td>• Water withdrwal for irrigation purposes</td></tr>
</table>

Source: Compiled by the Authors, 2023

The relationship between amplitude and wavelength is inversely proportional. The inverse relationship between wavelength and amplitude holds for all meandering rivers worldwide. There exists a positive correlation between the radius of curvature in terms of wavelength and the radius of curvature in terms of amplitude, mainly when the values of both parameters are low. As values rise, it becomes challenging to ascertain the precise nature of the link between them. The relationship in question pertains specifically to the Kabodak River, where the lower section of the river is subject to tidal influence and the backwater effect. Predicting this relationship for the lower portion of the Kabodak River presents a challenge.

Based on empirical observations and quantitative measurements, it is evident that the occurrence of nodal patterns and their intricacy is mainly seen in the upper (48.39%) and lower sections (35.48%) of the river. However, it is essential to note that the underlying causes and processes contributing to these phenomena exhibit notable variations. Various factors influenced the sinuosity of the river in different sections. The river showed increased sinuosity in the upper and lower parts due to a lower gradient, reduced flow, and blockage from the source. Conversely, the middle section (16.13%) displayed distinct characteristics resulting from tectonic upliftment, the influx of energy from numerous streams of different orders, and the discharge from the Bhairab River located in the Jessore district.

Conclusion

The Kabodak River, located in the deltaic part, is a deceptively complicated meandering river. Hydro-geomorphological conditions, along with human interference and overexploitation of its resources, distinctly shape the river from other meandering rivers. The relationship among and between geometric characteristics such as width, amplitude, radius of curvature, wavelength, and patterns is more complicated than in any other meandering rivers of Bangladesh. Therefore, the management strategy of the Kabodak River might need a different approach from that of Bangladesh's other meandering rivers. The true nature and behavioral pattern of three distinct meandering sections are entirely different, thus necessitating different sets of measures for each section of the river.

Acknowledgment

The authors would like to express their gratitude for the technical assistance provided by Dr. Tanjinul Hoque Mollah, Associate Professor in the Department of Geography and

Environment at Jahangirnagar University. Besides, the authors acknowledge the anonymous reviewer for helpful suggestions on the paper.

References

Alam, M. S., Kamrunnahar and M. Tahsin. 2022. Baors of the Kabodak River Types: Formation and Evolving Nature. *Jahangirnagar Bishwavidyalay Bhugol O Poribesh Samikkhan.* **38**: 1-13.

Bagchi, K. G. 1944. *The Ganges Delta.* Calcutta University Press, Calcutta. pp. 3-23.

Banglapedia. 2015. Bengal Delta. National Encyclopedia of Bangladesh

Banglapedia. 2021. Kabodak River. National Encyclopedia of Bangladesh

Brice, C. J. 1974. Evolution of Meander Loops. *Geol. Soc. Amer. Bull.* **85**: 581-586.

Buffington, J.M., R.D. Woodsmith, D.B. Booth, and D.R. Montgomery 2003. Fluvial processes in Puget Sound Rivers and the Pacific Northwest. In: *Restoration of Puget Sound rivers.* Univ. Wash. Press, Seattle. pp. 46-78.

Chowdhury, M.I. 1959. Morphology of the Bengal Basin. Unpublished Master's thesis. Univ. Cambridge, UK.

Church, M. and R. I. Ferguson. 2015. Morphodynamics: Rivers beyond steady state. *Water Resou. Res.* **51**(4): 1883-1897.

Davis, W. M. 1913. Meandering valleys and underfit rivers. *Ann. Assoc. Amer. Geograph.* **3**(1): 3-28.

Dury G. H. 1970. General theory of meandering valleys and underfit streams. *Rivers and River Terraces.* pp 264–275

Harvey, D. M. 1988. Meanderbelt dynamics of the Sacramento River, California. The California riparian systems conference. California.

Hogan, D. L. and D. S. Luzi. 2010. Channel geomorphology: Fluvial forms, processes, and forest management effects. Compendium of forest hydrology and geomorphology in British Columbia. BC Ministry of Forests and Range, Forest Science Program, Victoria, BC, and FORREX Forum for Research and Extension in Natural Resources, Kamloops, BC Land Management Handbook No **66**: 331-371.

King, C. A. M. 1966. Techniques in geomorphology. In: *Geological Megazine*, Edward Arnold, Ltd., London, **103**(5): 1-342.

Knighton, A. D. 1972. Meandering habit of supraglacial streams. *Geol. Soc. Amer. Bull.* Vol. **83**: pp. 201-204.

Knighton, A. D. 1977. The meander problem. *Geography* **62**(2): 106-111.

Komatsu, G. and V.R. Baker. 1994. Meander properties of Venusian Channels. *Geology* **22**: 67-70.

Kusratmoko, E. 2017. Modeling Landuse/Landcover Changes with Markov-Cellular Automata in Comering Watershed, South Sumatera. In: IOP Conference, *Earth Environ. Sci*. **54**.

Kusratmoko, E., A. Wibowo and A. A. Kurnia. 2019. Changes in the value of sinuosity index in Komering River channel, province south Sumatera, years 1990 - 2016. IOP Conference Series. *Earth Environ. Sci.* **338**:1-8.

Leopold, L.B. and M.G. Wolman. 1960. River meanders. *Geol. Soc. Amer. Bull.* **71**: 76-794.

Leopold, L.B., M.G. Wolman and J.P. Miller. 1964. Fluvial Processes in Geomorphology. Freeman, San Francisco. pp. 522.

Montgomery, D.R. 1999. Process domains and the river continuum. *J. Amer. Water Resou. Assoc.* **35**(2): 397-409.

Montgomery, D.R. and J.M. Buffington. 1993. Channel classification, prediction of channel response, and assessment of channel condition. Report: TFW-SHlO-93-002, Prepared for the SHAMW committee of the Washington State Timber/Fish/Wildlife Agreement. pp. 110.

Morisawa, M. 1968. *Streams, their dynamics, and morphology*. New York, McGraw-Hill. pp. 175.

Rob, A. M. 1989. Fluvial morphology of the Gangetic delta. Unpublished Ph.D thesis. Department of Geography. Aligarh Muslim University, India.

Schumm, S. A. 1963. Sinuosity of alluvial rivers on the great plains. *Geol. Soc. Amer. Bull.* **74**(9): 1089.

Schumm, S. A. 1967. Meander wavelength of alluvial rivers. *Science*. **157**(3796): 1549-1550.

Schumm, S. A. and H. R. Khan. 1972. Experimental study of channel patterns. *Geol. Soc. Amer. Bull.* **83**: 1755-1770.

Tareq, M. S. 2016. Environmental management of the waterlogging problem in south-west coastal region of Bangladesh. Unpublished M.Sc Thesis. Bangladesh University of Engineering and Technology.

Thorne, C. R., R. D. Hey and M. D. Newson. 1997. *Applied fluvial geomorphology for river engineering and management*. Chichester, UK. John Wiley and Sons. pp. 111-180

USGS (United States Geological Survey). 2019. Landsat TM 8. (Accessed November 14, 2021).

Zhang, B., N. S. Ai, Z. W. Huang, C. B. Yi and F. C. Qin. 2008. Meanders of the Jialing River in China: morphology and formation. *Chinese Sci. Bull.* **53**(2): 267-281.

(Revised copy received on 02.11.2023)

J. Asiat. Soc. Bangladesh, Sci. **49**(2): 165-177, December 2023 DOI: https://doi.org/10.3329/jasbs.v49i2.70766

ABUNDANCE AND CONTROL OF RUGOSE SPIRALING WHITEFLY, *ALEURODICUS RUGIOPERCULATUS* MARTIN, INFESTING COCONUT IN SEVEN COASTAL DISTRICTS OF BANGLADESH

MD. MOHASIN HUSSAIN KHAN*
Department of Entomology, Patuakhali Science and Technology University, Dumki, Patuakhali, Bangladesh

Abstract

A survey was conducted in the farmers' orchards of 7 coastal districts, namely Patuakhali, Barguna, Barishal, Khulna, Bhola, Laxmipur, and Noakhali of Bangladesh to know the abundance of rugose spiraling whitefly on coconut and an experiment consisting of 5 treatments and an untreated control following RCBD with 3 replications was also carried out for controlling rugose spiraling whitefly at Patuakhlai Science and Technology University (PSTU) campus during January to May, 2022. Results revealed that the highest abundance (23 egg spirals, 34 nymphs, 31 adults per leaflet, respectively) of rugose spiraling whitefly was found at Khulna, followed by Noakhali (19 egg spirals, 31 nymphs, 27 adults per leaflet, respectively) while the lowest (9 egg spirals, 13 nymphs, 11 adults per leaflet, respectively) was in Patuakhali among 7 coastal districts. Although all insecticidal treatments (T_1 = Tyfos 48 EC (Chlorpyrifos) @ 1 ml/L of water, T_2= Caught 10 EC (Cypermethrin) @ 1 ml/L of water, T_3 = Nitro 505 EC (Chlorpyrifos + Cypermethrin) @ 1 ml/L of water, T_4= Fyfanon 57 EC (Malathion) @ 1 ml/L of water, T_5= Bioclean @ 1 ml/L of water) effectively reduced the different stages of rugose spiraling whiteflies compared to untreated control, the lowest mean number of egg spirals (0.00), nymphs (0.11) and adults (0.11) per leaflet were obtained by the application of Nitro 505EC @ 1 ml/L of water followed by Bioclean @ 1 ml/L of water at 3 DAS. The highest percent reduction of egg spirals (100%), nymph (98.82%), and adult (98.79%) of whitefly population over control were also obtained by the application of Nitro 505EC @ 1 ml/L of water followed by Bioclean @ 1 ml/l of water at 3 DAS. These two chemicals were found to be very effective for controlling rugose spiraling whiteflies. Considering environmental safety, Bioclean @ 1 ml/L of water is recommended to use against this pest as an eco-friendly approach for safe food production.

Keywords: Abundance, coconut, control, rugose spiraling whitefly, *Aleurodicus rugioperculatus*

Introduction

Coconut palm, *Cocos nucifera* L. (Arecales: Arecaceae), is now widely grown throughout tropical regions of the world, including Brazil (Omena *et al.*, 2012), coastal areas of Bangladesh, and is recognized as an essential source of income for coconut growers.

* Corresponding author: mohasin1965@pstu.ac.bd

Coconut is a fruit of high economic value due to its diversified utilization, which covers 0.65% of Bangladesh's total cultivated lands for fruit crops. About 80% of the country's total production of coconut is contributed by the country's southern areas (BBS, 2011). The national yield of coconut has been estimated at an average of 51 kg/fruit-bearing tree/year with a total production of 3,83,833 MT/year from an area of 9,152 acres (BBS, 2016). But coconut production is enormously hindered by the ravages of various insect and mite pests from seedling to their maturity. Bangladesh is a humid and subtropical country favoring the luxuriant growth of different insect species with rich diversity. Recently, coconut palms have been seen to be seriously affected due to the severe infestation of an alien invasive crop pest known as the Rugose Spiralling Whitefly, *Aleurodicus rugioperculatus* Martin (Hemiptera: Stemorrhyncha: Aleyrodidae) in Bangladesh. Martin described this species from Belize in Central America in 2004 based on puparia collected from the undersurface of coconut leaves (Martin, 2004). These whitefly species were newly added to the species list of whiteflies in Florida as *A. rugioperculatus* Martin, known initially as the gumbo limbo spiraling whitefly. Still, it is presently named the rugose spiraling whitefly. Foreign species can attain invasive pest status when they are accidentally introduced to new areas where they are isolated from their natural enemies and if indigenous beneficial species like predators and /or parasitoids cannot suppress pest populations (Duan *et al.*, 2015). It is a very destructive pest that mainly threatens coconut plantations. It causes damage to coconut palms and other broad-leaved host plants in its native range (Mayer *et al.*, 2010). The pest was first noticed in Tamil Nadu, Kerala, Karnataka, and Andhra Pradesh in July 2016 (Sundararaj and Selvaraj, 2017; Karthick *et al.*, 2018). The species caused damage to coconut trees across vast areas on a large scale and infested other host plants. It cannot kill the host plant by its infestation. Still, it may hamper the average growth of its host by excreting a sticky glistering liquid substance called honeydew on which sooty mold grows which retards photosynthesis. They can cause stress to the host plant by removing nutrients and water and accelerating the growth of black sooty molds. Ants and wasps are also attracted to honeydew and protect the whiteflies from their natural enemies (Stocks and Hodges, 2012). There are numerous available insecticides to manage whiteflies, but the technique of spraying application and site to use the product vary by label (Mannion, 2010). Sanitation and synthetic chemical control costs can substantially affect homeowners and businesses (Kumar *et al.*, 2013). Considering the above facts, the present experiment was

undertaken to determine the abundance of invasive rugose spiraling whiteflies on coconuts and their control in seven selected southern coastal districts of Bangladesh.

Materials and Methods

Survey on the abundance of rugose spiraling whitefly on coconut in seven southern coastal districts of Bangladesh

Systematic surveys were carried out in the farmers' orchards of 7 locations, namely Patuakhali, Barishal, Barguna, Khulna, Bhola, Laxmipur, and Noakhali districts of Bangladesh, to know the abundance of rugose spiraling whitefly on coconut during January to May 2022. Fourteen upazilas, two from each district, were selected as study areas of the survey. Seven hundred plants were selected randomly for data collection by taking fifty coconut trees from each upazila. Out of 50, five trees were selected randomly to observe the abundance of whiteflies (number of egg spirals, nymphs, and adults per 5 leaflets) per frond of a coconut tree.

Evaluation of insecticides for controlling rugose spiraling whitefly on coconut

The experiment was carried out on coconut trees grown in the Patuakhali Science and Technology University campus, Dumki, Patuakhali, from January to May 2022. The experiment was laid out in an RCB design with three replications. One tree was treated as a treatment replication. Five treatments viz., T_1 = Tyfos 48 EC (Chlorpyrifos) @ 1 ml/L of water, T_2= Caught 10 EC (Cypermethrin) @ 1 ml/L of water, T_3 = Nitro 505 EC (Chlorpyrifos + Cypermethrin) @ 1 ml/L of water, T_4= Fyfanon 57 EC (Malathion) @ 1 ml/L of water, T_5= Bioclean @ 1 ml/L of water and T_6 = Control were applied. The spraying was done with the help of a hand sprayer. The spraying was done on all frond leaflets by calculating the solution volume required for each treatment. Data on the number of egg spirals/leaflets, nymphs/leaflets, adults/leaflets, and the presence of sooty mold encrustation in fronds were recorded at 3, 6, and 9 days after spraying.

Statistical analyses: The data obtained were statistically analyzed to determine the incidence and control of coconut whiteflies. The mean values of all the characters were calculated, and analysis of variance was performed using WASP 1.0 (Web Agri Stat Package) software, and means were separated by CD values.

Plate 1. Photographs of different treatments applied for controlling rugose spiraling whitefly

Results and Discussion

Abundance of rugose spiraling whitefly

Number of egg spirals per leaflet: Live egg spirals/leaflet ranged between 9.36 and 23.41 in most of the surveyed locations of coastal districts, while the live egg spirals/leaflet was less than 10 in Patuakhali district. The highest number of egg spirals per leaflet was found in the Khulna district (23.41 egg spirals/leaflet), followed by Noakhali (19.31 egg spirals/leaflet) and Bhola (17.18 egg spirals/leaflet). But the lowest number was in Patuakhali (9.36 egg spirals/leaflet), followed by Laxmipur (11.23 egg spirals/leaflet), Barishal (13.24 egg spirals/leaflet) and Barguna (15.16 egg spirals/leaflet) (Fig. 1).

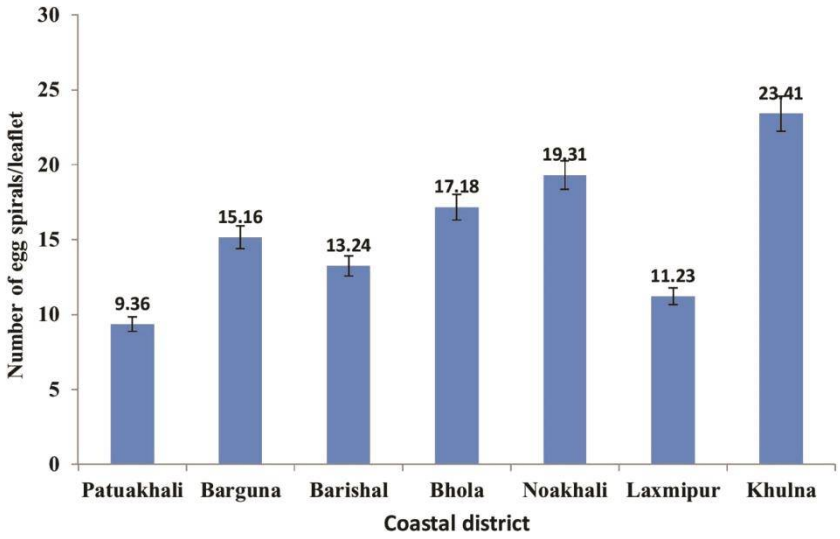

Fig. 1. Number of rugoses spiraling whitefly egg spirals/leaflets of the coconut tree

Number of nymphs per leaflet: Nymphs/leaflets ranged between 13.41 and 34.17 nymphs in the surveyed locations of coastal districts, whereas the population was less than 15 in Patuakhali district. The highest number of nymphs/leaflet was recorded in the Khulna district (34.17 nymphs/leaflet), followed by Noakhali (31.25 nymphs/leaflet), Bhola (27.34 nymphs/leaflet) and Barguna (23.28 nymphs/leaflet). In contrast, the lowest number was in Patuakhali (13.41 nymphs/leaflet), followed by Laxmipur (15.47 nymphs/leaflet) and Barishal (19.16 nymphs/leaflet). (Fig. 2).

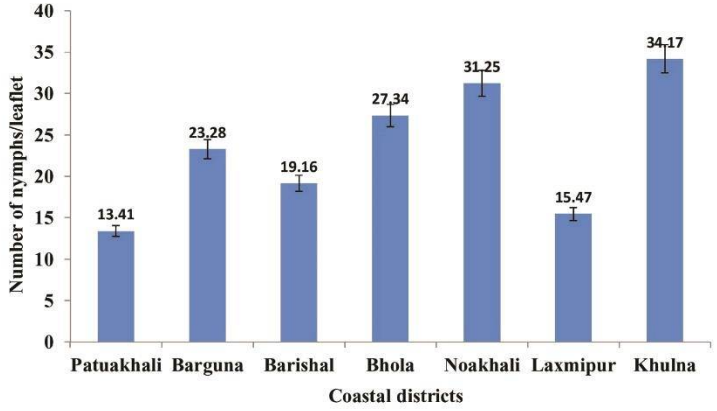

Fig. 2. Number of rugose spiraling whitefly nymphs/leaflet of coconut tree

Number of adults per leaflet:

Number of adults per leaflet: Adults/leaflets ranged between 11.13 and 31.36 in the surveyed locations of coastal districts, whereas the adult population of the pest was less than 15 in Patuakhali and Laxmipur districts. The highest number of adults/leaflet was observed in Khulna district (31.36 adults/leaflet), followed by Noakhali (27.17 adults/leaflet), Bhola (24.29 adults/leaflet) and Barguna (21.34 adults/leaflet) while the lowest number was in Patuakhali (11.13 adults/leaflet) followed by Laxmipur (14.22 adults/leaflet) and Barishal (16.41 adults/leaflet). (Fig. 3).

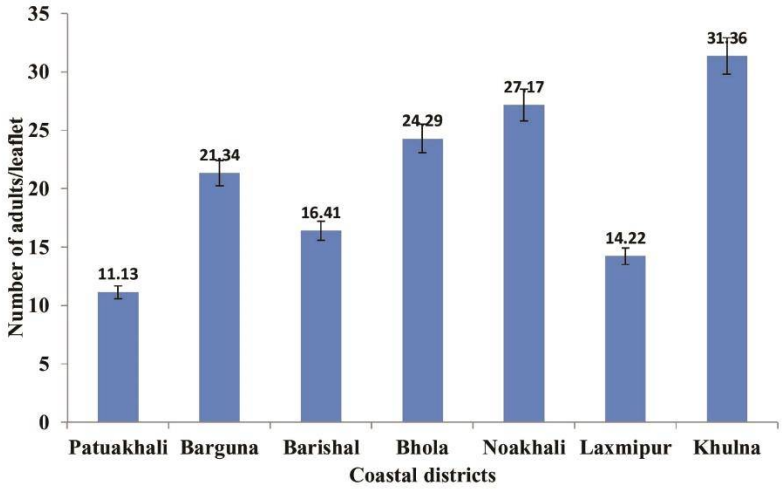

Fig. 3. Several rugose spiraling whitefly adults/leaflets of the coconut tree.

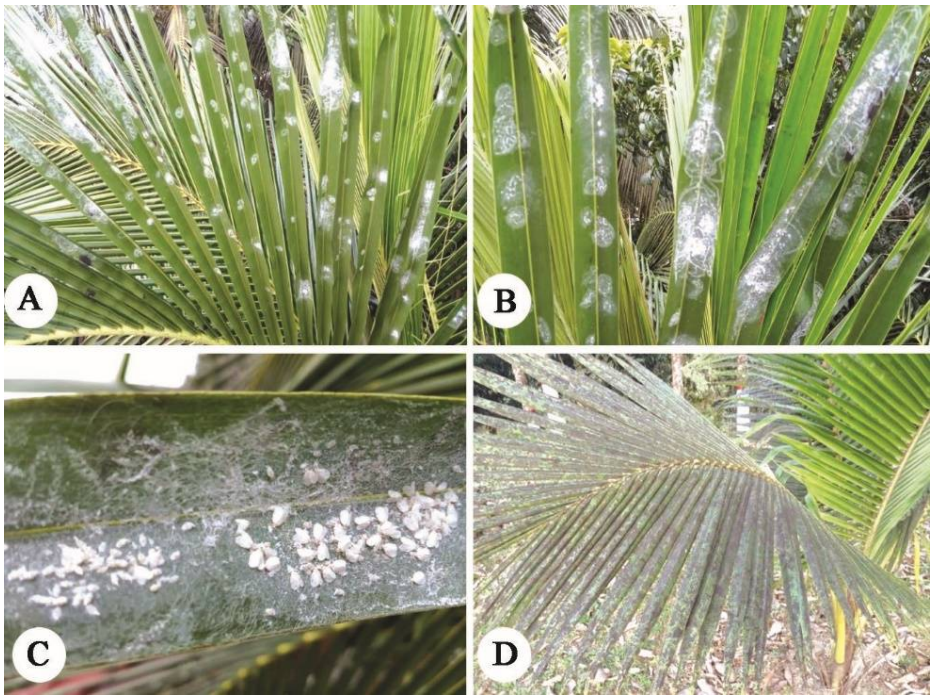

Plate 2. Photographs of the abundance of rugose spiraling whiteflies as egg spirals (A&B), nymphs (A&B), adults (C), and sooty mold symptoms (D).

Control of rugose spiraling whitefly

Efficacy of insecticides on egg spirals of rugose spiraling whiteflies: The effect of insecticides on the egg spirals of rugose spiraling whiteflies on different days after spraying is presented in Table 1. At 3 DAS, no egg spirals were recorded in T_3 (0.00) treated leaflets, but the lowest number of egg spirals was found in T_5 (0.33) treated leaflets, which was statistically similar to T_1 (0.67) and T_2 (1.00) and T_4 (1.33) treated leaflets. The number of egg spirals/leaflets on all insecticidal-treated leaflets differed significantly from untreated control (T_6) leaflets, with the highest number (13.33) of egg spirals/leaflets recorded.

At 6 DAS, no egg spirals were observed in T_3 (0.00) treated leaflets, which was identical to T_5 (0.00), but the lowest number of egg spirals was found in T_1 (0.33), which was statistically similar to T_2 (0.67) and T_4 (0.33) treated leaflets. The number of egg spirals/leaflets on all insecticidal-treated leaflets differed significantly from untreated control (T_6) leaflets, where the highest number (13.97) of egg spirals/leaflets was recorded.

At 9 DAS, no egg spirals were found in all treated leaflets, and no significant differences existed among treatments. However, the number of egg spirals/leaflets on all insecticidal-treated leaflets differed significantly from untreated control (T_6) leaflets, where the highest number (15.39) of egg spirals/leaflets was observed.

The highest percent reduction of egg spirals/leaflets was obtained from T_3 (100%), followed by T_5 (99.23%) and T_1 (97.68%) treated leaflets, and the lowest was in T_2 (95.99%) treated leaflets, followed by T_4 (96.13%).

Table 1. Efficacy of insecticides on egg spirals of rugose spiraling whiteflies at 3, 6, and 9 days after spraying

Treatments	Mean number of egg spirals/leaflets at			Mean	% reduction over control
	3 DAS	6 DAS	9DAS		
T_1	0.67b (1.05)	0.33b (0.88)	0.00b (0.70)	0.33	97.68
T_2	1.00b (1.18)	0.67b (1.05)	0.00b (0.70)	0.57	95.99
T_3	0.00b (0.70)	0.00b (0.70)	0.00b (0.70)	0.00	100.00
T_4	1.33b (1.29)	0.33b (0.88)	0.00b (0.70)	0.55	96.13
T_5	0.33b (0.88)	0.00b (0.70)	0.00b (0.70)	0.11	99.23
T_6	13.33a (3.76)	13.97a (3.79)	15.39a (3.94)	14.23	-
CV (%)	**18.91**	**19.74**	**21.36**		
CD (at 1%)	**1.934**	**2.150**	**2.575**		

DAS = Days after spraying; CD= Critical difference value. Figures in parentheses are transformed values based on square root transformation, values are averages of 3 replications.

T_1 = Tyfos 48 EC (Chlorpyrifos) @ 1ml/L of water, T_2= Caught 10 EC (Cypermethrin) @ 1 ml/L of water, T_3 = Nitro 505 EC (Chlorpyrifos + Cypermethrin) @ 1 ml/L of water, T_4= Fyfanon 57 EC (Malathion) @ 1 ml/L of water, T_5= Bioclean @ 1 ml/L of water and T_6 = Control.

Efficacy of insecticides on nymphs of rugose spiraling whiteflies: The effect of insecticides on the nymphs of rugose spiraling whiteflies on different days after spraying is given in Table 2. At 3 DAS, the lowest number of nymphs/leaflets was observed in T_3 (0.33) treated leaflets, which was identical to T_5 (0.33) treated leaflets, followed by T_1

(0.67) and T_2 (0.67) and T_4 (1.00) treated leaflets. The number of nymphs/leaflets on all insecticidal treated leaflets differed significantly from untreated control (T_6) leaflets, with the highest number (12.00) of nymphs/leaflets recorded.

At 6 DAS, no nymph was observed in T_3 (0.00) treated leaflets, but the lowest number of nymph was found in T_5 (0.33), which was statistically similar to T_1 (0.33), T_2 (0.33) and T_4 (0.33) treated leaflets. The number of nymphs/leaflets on all insecticidal treated leaflets differed significantly from untreated control (T_6) leaflets, with the highest number (9.64) of nymphs/leaflets recorded.

At 9 DAS, no nymph was found in all treated leaflets, with no significant difference among treatments. However, the number of nymphs on all insecticidal treated leaflets differed significantly from untreated control (T_6) leaflets, where the highest number (6.23) of nymphs/leaflets was observed.

The highest percent reduction of nymphs/leaflet was obtained from T_3 (98.82%) treated leaflets, followed by T_5 (97.36%) and T_1 (96.45%), which was identical to T_2 (96.45%), but the lowest was in T_4 (95.26%) treated leaflets.

Table 2. Efficacy of insecticides on nymph of rugose spiraling whiteflies at 3, 6, and 9 days after spraying

Treatments	Mean number of nymph/leaflets at			Mean	% reduction over control
	3 DAS	6 DAS	9DAS		
T_1	0.67b (1.05)	0.33b (0.88)	0.00b (0.70)	0.33	96.45
T_2	0.67b (0.99)	0.33b (0.88)	0.00b (0.70)	0.33	96.45
T_3	0.33b (0.88)	0.00b (0.70)	0.00b (0.70)	0.11	98.82
T_4	1.00b (1.18)	0.33b (0.88)	0.00b (0.70)	0.44	95.26
T_5	0.33b (0.88)	0.33b (0.88)	0.00b (0.70)	0.22	97.36
T_6	12.00a (3.60)	9.64a (3.15)	6.23a (2.58)	9.29	-
CV (%)	**21.62**	**21.38**	**23.21**		
CD (at 1%)	**0.886**	**0.723**	**0.670**		

DAS = Days after spraying; CD= Critical difference value. Figures in parentheses are transformed values based on square root transformation, values are averages of three replications.

T_1 = Tyfos 48 EC (Chlorpyrifos) @ 1 ml/L of water, T_2= Caught 10 EC (Cypermethrin) @ 1 ml/L of water, T_3 = Nitro 505 EC (Chlorpyrifos + Cypermethrin) @ 1 ml/L of water, T_4= Fyfanon 57 EC (Malathion) @ 1 ml/L of water, T_5= Bioclean @ 1 ml/L of water and T_6 = Control.

Efficacy of insecticides on adult rugose spiraling whiteflies: The effect of insecticides on the adults of rugose spiraling whiteflies on different days after spraying is presented in Table 3. At 3 DAS, the lowest number of adults was observed in T_3 (0.33) treated leaflets, which was identical to T_1 (0.33) and T_5 (0.33) treated leaflets, followed by T_2 (0.67), which was also similar to T_4 (0.67) treated leaflets. The number of adult/leaflets on all insecticidal treated leaflets differed significantly from untreated control (T_6) leaflets, where the highest number (10.00) of adult/leaflets was recorded.

At 6 DAS, no adult was observed in T_3 (0.00) treated leaflets, but the lowest number of egg spiral was found in T_5 (0.33), which was statistically identical and similar to T_1 (0.33), T_2 (0.33), and T_4 (0.33) treated leaflets. The number of adult/leaflets on all insecticidal treated leaflets differed significantly from untreated control (T_6) leaflets, where the highest number (9.24) of adult/leaflets was recorded.

At 9 DAS, no adult was found in all treated leaflets except T_4 (0.33) treated leaflets, and there was no significant difference among treatments. However, the number of adult/leaflets on all insecticidal treated leaflets differed significantly from untreated control (T_6) leaflets, where the highest number (8.00) of adult/leaflets was observed.

Table 3. Efficacy of insecticides on adult rugose spiraling whiteflies at 3, 6, and 9 days after spraying

Treatments	Mean number of adult/leaflets at			Mean	% reduction over control
	3 DAS	6 DAS	9 DAS		
T_1	0.33b (0.88)	0.33b (0.88)	0.00b (0.70)	0.22	97.58
T_2	0.67b (0.99)	0.33b (0.88)	0.00b (0.70)	0.33	96.37
T_3	0.33b (0.88)	0.00b (0.70)	0.00b (0.70)	0.11	98.79
T_4	0.67b (0.99)	0.33b (0.88)	0.33b (0.88)	0.44	95.15
T_5	0.33b (0.88)	0.33b (0.88)	0.00b (0.70)	0.22	97.58
T_6	10.00a (3.23)	9.24a (3.08)	8.00a (2.91)	9.08	-
CV (%)	**24.19**	**27.79**	**18.04**		
CD (at 1%)	**1.151**	**1.260**	**0.682**		

DAS = Days after spraying; CD= Critical difference value. Figures in parenthesis are transformed values after square root transformation, values are means of 3 replications.

T_1 = Tyfos 48 EC (Chlorpyrifos) @ 1 ml/L of water, T_2= Caught 10 EC (Cypermethrin) @ 1 ml/L of water, T_3 = Nitro 505 EC (Chlorpyrifos + Cypermethrin) @ 1 ml/L of water, T_4= Fyfanon 57 EC (Malathion) @ 1 ml/L of water, T_5= Bioclean @ 1 ml/L of water and T_6 = Control.

The highest percent reduction of adult/leaflet was obtained from T_3 (98.79%) treated leaflets, followed by T_5 (97.58%), which was identical to T_1 (97.58%), but the lowest was in T_4 (95.15%) treated leaflets followed by T_2 (96.37%).

There is no available research report on the chemical control of rugose spiraling whiteflies due to a new invasive coconut pest. Effective control can be achieved using systemic insecticides in the soil as granular formulations, drenching, burying pellets, or injection, to the trunk as trunk injection and as basal bark spray, or to the leaf; however, soil and trunk applications receive the advantage of the systemic properties of these products and give longer-term control (Mannion, 2010). Quick knockdown of the whiteflies occurred by spraying contact insecticides on the leaves but will provide only a few weeks of control. Elango et al. (2021) stated that the population dynamics of a new invasive whitefly species, *A. rugioperculatus*, was found throughout the year on coconut palms. Observations recorded at weekly intervals showed that the whitefly population accelerated from the first week of July (130.8 nymph/leaf/frond), reaching the maximum during the first week of October (161.0 nymph/leaf/frond), which gradually declined to a minimum during April. The agro-climatic conditions of different regions varied, for which arthropods showed changing trends in their natural incidence and extent of damage to the crop. Weather parameters did not influence the incidence of rugose spiraling whiteflies despite its requirement for developing management strategies. In the case of large trees, there may be some barriers that need to be taken into consideration before concluding.

First, getting sufficient insecticidal active ingredients or volume to large trees can sometimes take much work. Second, it is challenging to design a sampling program to get an accurate representation of the entire infestation of the tree. Third, seasonal leaf shedding reduces the availability of leaves to the whitefly population, and therefore, it is impossible to easily link the density of the whitefly population with insecticidal treatment. Consequently, the efficacy of synthetic chemical insecticides in such a case demands further investigation. These findings are also supported by Taravati et al. (2013). Many reported plant species are expected to be incidental hosts that cannot sustain long-term rugose spiraling whitefly populations and, therefore, need minimal or no management practices. The prevalence of higher temperature increases metabolic activities at a faster rate in insects, resulting in a rapid build-up of pest population density in a shorter period. Likewise, the prevailing of high relative humidity influences the building up of the insect population. The population of both pests and natural enemies is reduced due to increasing rainfall, as heavy rains wash out the different life stages of the pests and natural enemies.

Conclusion

The abundance of rugose spiraling whitefly was the highest and most severe in Khulna and Noakhali districts, while the lowest was in Patuakhali among 7 coastal districts. The application of Nitro 505EC @ 1 ml/L of water and Bioclean @ 1 ml/L of water was found to be very effective for controlling rugose spiraling whiteflies.

Acknowledgments

The author is grateful to the UGC-PSTU authority for providing support and financial assistance to conduct the research.

References

BBS (Bangladesh Bureau of Statistics). 2016. Yearbook of agricultural statistics 2015 (27th Series). Statistics and Information Division, Ministry of Planning, Government of Bangladesh, Dhaka. pp. 557

BBS (Bangladesh Bureau of Statistics). 2011. Statistical Year Book of Agriculture. Ministry of Planning and Evaluation, Government of Bangladesh. pp .680

Duan, J.J., S.B. Leah, J.A. Kristopher, D.U. Michael and G.V.D. Roy. 2015. Population dynamics of invasive forest insect and associated natural enemies in the aftermath of invasion: implications for biological control. *J. Appl. Ecol.* **52**:1246–1254.

Elango, K., S.J. Nelson and P. Dineshkumar, 2021. Incidence forecasting of new invasive pest of coconut rugose spiraling whitefly (*Aleurodicus rugioperculatus*) in India using ARIMAX analysis. *J. Agrometeorol.* **23**(2): 194-199.

Karthick, K.S., C. Chinniah, P. Parthiban and A. Ravikumar, 2018. Newer report of Rugose Spiraling Whitefly, Aleurodicus rugioperculatus Martin (Hemiptera: Aleyrodidae) in India. *Inter.J. Res. Stud. Zool.* **4**(2): 12-16.

Kumar, V., C.L. McKenzie, C. Mannion, I. Stocks, T. Smith and L. S. Osborne, 2013. Rugose spiraling whitefly, *Aleurodicus rugioperculatus* Martin (Hemiptera: Aleyrodidae). EENY578. University of Florida, IFAS Extension, http://entnemdept.ufl. edu/creatures/orn/Aleurodicus_ rugioperculatus.htm (last accessed 15 July 2023).

Mannion, C. 2010. Rugose spiraling whitefly, a new whitefly in South Florida. Tropical Research and Education Center, University of Florida. p. 5.

Martin, J.H. 2004. The whiteflies of Belize (Hemiptera: Aleyrodidae) Part 1 - Introduction and account of the subfamily Aleurodicinae Quaintance and Baker. *Zootaxa.* **681**: 1-119.

Mayer, H., J. McLaunghlin, A. Hunsberger, L. Vasquez, T. Clcyzk and C. Mannion, 2010. Common questions about the gumbo limbo spiraling whitefly (Aleurodicus rugioperculatus). The Mami-Dade Cooperative Extension. pp. 1-4.

Omena, R.P.M., E.C. Guzzo, J.M.S. Ferreira, F.A.C. de Mendonça, A.F. de Lima, F. Racca-Filho and X. Ni, 2012 First report on the whitefly, *Aleurodicus pseudugesii* on the coconut palm, Cocos nucifera in Brazil. *J. Insect Sci.* **12**: 26.

Stocks, I.C. and G. Hodges, 2012. The rugose spiraling whitefly, *Aleurodicus rugioperculatus* Martin, a new exotic whitefly in south Florida (Hemiptera: Aleyrodidae). Florida Department of Agriculture and Consumer Services, Division of Plant Industry.

Sundararaj, R. and K. Selvaraj, 2017. Invasion of rugose spiraling whitefly, Aleurodicus rugioperculatus Martin (Hemiptera: Aleyrodidae): A potential threat to coconut in India. *Phytoparasitica.* **45**(1):71-74.

Taravati, S., C. Mannion and L.S. Osborne, 2013. Management of Rugose Spiraling Whitefly (*Aleurodicus rugioperculatus*) in the South Florida Landscape. *Proc. Fla. State Hort. Soc.* **126**: 276-278.

(Revised copy received on 20.11.2023)

J. Asiat. Soc. Bangladesh, Sci. **49**(2): 179-191, December 2023 DOI: https://doi.org/10.3329/jasbs.v49i2.70767

LIVELIHOOD IMPACT DUE TO RIVERBANK EROSION AMONG THE AFFECTED HOUSEHOLDS ALONG THE RIVER JAMUNA OF BANGLADESH

MD. FARUK HOSSAIN* AND SHAKIB AL FAHAD
Department of Geography and Environment, University of Dhaka, Dhaka, Bangladesh

Abstract

The present study examines the impacts of riverbank erosion on locals' lives and livelihoods in a particular area of the Jamuna River floodplain of Bangladesh. Riverbank erosion causes thousands of people to be affected, resulting in damage and loss of crops, cattle, housing structures, and farmland. It also erodes public infrastructures and communication networks significantly. This study undertakes empirical methods (including the open-ended questionnaire with a total of 155 households) to demonstrate the study's findings. The lack of adequate measures is the major factor associated with riverbank erosion in the study area. Land property loss becomes one of the major threats among the surveyed families. Some mitigation measures, such as using Geo bags and concrete blocks to protect the banks and operation of dredging machines to divert the water flow, are observed in the study area to reduce erosion. However, these measures are not bringing any effective solution to the local people's livelihoods due to the slow ongoing work processes.

Keywords: Riverbank erosion, livelihood, River Jamuna, Bangladesh

Introduction

Bangladesh is one of the world's disaster-prone countries located downstream of the Ganges-Brahmaputra-Meghna (GBM) catchment area (Islam *et al.*, 2021). Due to the flat and low-lying deltaic topographic position, people's lives and livelihoods are susceptible to various natural hazardous conditions (Mojid, 2020). Bangladesh ranked 9th most disaster-risk-prone country among 193 countries (Atwii *et al.*, 2022), 27th among the 191 multi-hazard-prone countries in 2022 (IASC and EC 2022), and 7th among the 180 long-term disaster-affected countries of the world from 2000 to 2019 (Eckstein *et al.* 2021). Riverbank erosion is a natural phenomenon that is common to fluvial and coastal environments in many countries of the world (Das *et al.*, 2007; Pati *et al.*, 2008), having a wide range of effects on socio-economy depending on the level and capacity of disaster

*Corresponding author: faruk.geoenv@du.ac.bd

preparedness, emergency response and recovery (Mamun 1996). Among the major rivers of Bangladesh, the river Jamuna is a braided river most susceptible to bank erosion due to its sand-dominant bank material composition. In recent years, human interventions in the Jamuna River floodplain area have increased due to undertaking various projects relating to river management. The construction of the Bangabandhu Jamuna Bridge and bank protection structures at Sirajganj, Sariakandi, and Bahadurabad have influenced the changes in the river's width. These types of structures obstruct the normal flow of the water and enhance the riverbank erosion (Chowdhury 2015).

Riverbank erosion has become a significant threat to about 20 riverine districts out of 64 Bangladesh districts, destroying approximately 8700 ha of land yearly. This erosion affects around 200000 people by destroying their houses and/or agricultural land (Alam, 2017). Consequently, bank erosion causes enormous impacts on the socio-economic condition of the people of affected areas (Freihardt and Frey, 2023). Due to erosion, the displaced people become disconnected from their birthplaces, lose land income sources, and are forced to engage in new livelihood activities (Barua *et al.*, 2019). Moreover, it becomes responsible for erasing public infrastructures and communication networks. The unregulated behavior of the rivers and encroachment pattern not only interrupt the life of the floodplain population but also put pressure on the urban growth centers and surrounding environment. Thus, it is essential to reduce the vulnerability of riverbank erosion at the local level by adopting various structural measures (Shahriar, 2021; Hutton and Haque, 2003). This study investigates how riverbank erosion affects people in a particular part of the Jamuna floodplain of Bangladesh.

This study aims to examine the salient factors associated with riverbank erosion and evaluate the livelihood effect resulting from riverbank erosion among the vulnerable households in the study area.

Materials and Methods

The present study was conducted by using both primary and secondary data. The relevant literature was reviewed mainly from online sources and published documents. Secondary sources of data and information were published, as well as unpublished research pertinent to the study topic. These included books, journal articles, research reports, government reports, NGO reports, conference proceedings, locally published reports, maps, and official websites.

The primary data and information were collected from selected households using semi-structured open-ended questionnaires. The respondents were selected based on a random sampling method. Face-to-face personal interviews provided the opportunity to gain in-depth information from respondents. These interviews provided information regarding the factors associated with riverbank erosion, impacts due to riverbank erosion, and the probable solution to this disaster.

Sample Size Determination for Household Survey: Sampling involves the selection of a subset of individuals from a larger group or population. The sampling process aims to select a proper population and gain participation to obtain accurate field-level data (Blair 2017). The respondents of the households were randomly selected from the population of the selected village of Shahzadpur Upazila in the Sirajganj district of Bangladesh. The sample size was calculated using the following formula (Yamane 1967), based on the number of households in the study villages, with a precision level of seven percent.

$$n = N/ (1 + N \times e^2)$$

In the case of this study, n = sample size (number of households chosen to interview); N = total households in the study areas; e = level of error. To minimize the risk of presenting a required sample size determination, a 95 percent confidence level and a precision level of seven percent were used. Based on the population of the selected villages, the proposed sample size was 155.

Data analysis

Weighted Average Index: The weighted average index (WAI) was the main statistical tool used, following the scaling technique (Khongsatjaviwat and Routray, 2015). The WAI identified the degree of importance of each indicator; it is considered a quick technique to assess the differences in respondent perceptions (Pakzad *et al.,* 2016). The WAI for each indicator was calculated by adding the response numbers, multiplying them by a weighted value between 0 and 1, and dividing the sum by the number of total responses (Pakzad *et al.,* 2016). This gave an overall weighted average score for each particular indicator. The formula for the calculation of WAI is as follows (Ha and Thang, 2017):

$$WAI = \Sigma S_i F_i / N$$

Where, WAI is the weighted average index ($0 \leq WAI \leq 1$), S_i is the scale value assigned at its priority, F_i is the frequency of household respondents, and N is the total number of observations. These indices were designed based on social scale; the value of each index was kept from 0 to 1. The type of each index is described as follows.

Perception Index

A perception index was applied to evaluate the level of heads of household perceptions of climate change governance practices in the study sites. It includes five levels (Table 1).

Table 1: Perception index levels.

Categories	Very good	Good	Medium	Poor	Very poor
Scale	1	0.75	0.5	0.25	0

Satisfaction Index

The formula for calculating the satisfaction index is as follows:

$$WAI = (1.00 \cdot f_1 + 0.75 \cdot f_2 + 0.50 \cdot f_3 + 0.25 \cdot f_4 + 0 \cdot f_5) / N$$

WAI is the weighted average index ($0 \leq WAI \leq 1$); f_1 is the frequency of the first scale choice; f_2 is the frequency of second scale choice; f_3 is the frequency of third scale choice; f_4 is the frequency of fourth scale choice; f_5 is the frequency of fifth scale choice. The overall assessment (OA) is calculated from the average WAI value (Nooriafshar *et al*., 2004).

Quantitative Data Analysis: IBM SPSS Statistics 24 software was used to analyze the quantitative data collected through household surveys to evaluate riverbank erosion issues in the study area. Moreover, ArcGis 10.8 Software was used to develop the study area map, and Landsat 8 image Source USGS Earth Explorer was applied to get the result.

The present study was conducted in Hat Panchil village (Fig. 1) of Koijuri Union of Shahjadpur Upazila under the Sirajganj district of Bangladesh. The study village has a history of facing bank erosion, and the process is still unabated, as appears on the map.

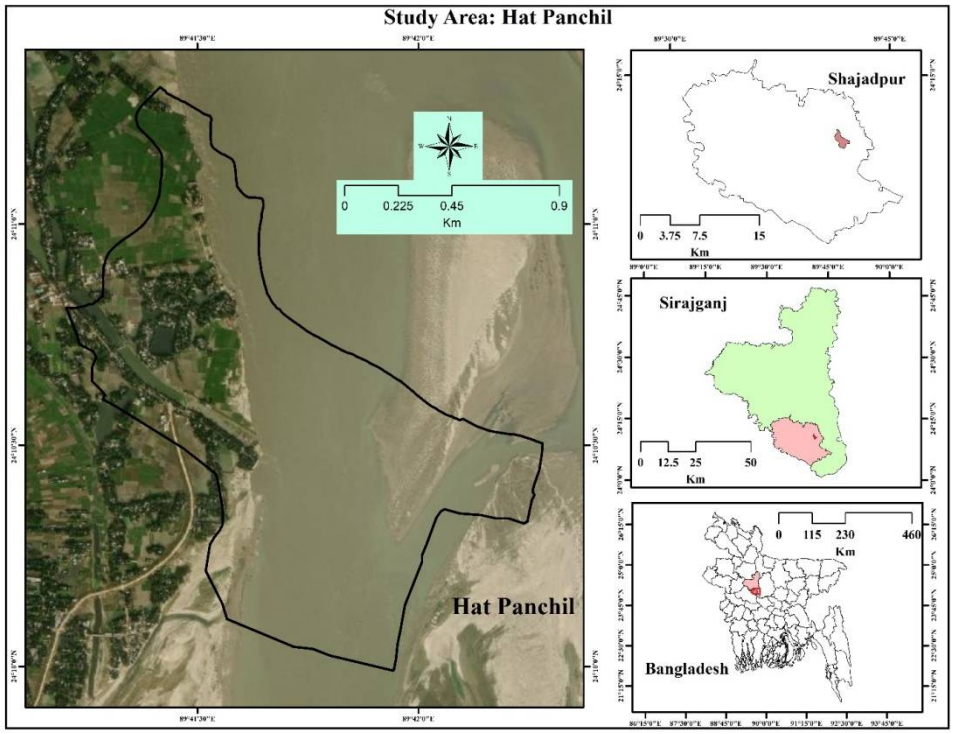

Fig. 1. The location of Hat Panchil and the surrounding landscape. Note that the river Jamuna has devoured a large chunk of the village.

Results and Discussion

The people of the present study area have suffered a lot due to riverbank erosion for the last few years. The present study identified the factors associated with riverbank erosion and inventoried the effect of erosion on local people's livelihood based on the field survey conducted in 2023. The details of the surveyed respondents are placed in Table 2.

Factors Associate with the Riverbank Erosion

Sirajganj district is considered one of the most erosion-prone areas in Bangladesh. According to the Center for Environmental and Geographic Information Services (CEGIS), 2009, the land loss was reported to be 622.2 ha/year. The location of the study village is close to the Jamuna River. When the riverbank erosion begins, this study area

becomes vulnerable to erosion. It has been observed that a large portion of the village eroded in the last 10 years between 2013 and 2023. In 2013, only a portion of the town was eroded; later, a large portion disappeared by 2023 (Fig. 2). The rest of the village might go to 'Nadi Shikhasti' (river erosion) unless adequate measures are taken immediately.

Table 2. Demographic Characteristics of the Surveyed Households at the study village, Hat Panchil.

Factors	Classes	Percentage
Gender	Male	87
	Female	13
Age range	18-24	2
	25-34	25
	35-44	31
	45-54	20
	55-64	14
	65+	8
Level of education	Illiterate	10
	Primary	55
	Secondary	30
	Technical/vocational	1
	College/university	4
Occupation	Farming	55
	Fishing	8
	Business	17
	Services	7
	Housekeeping	13
House type	Pucca	2
	Semi-pucca	16
	Kutcha	82

Source: Field Survey, 2023

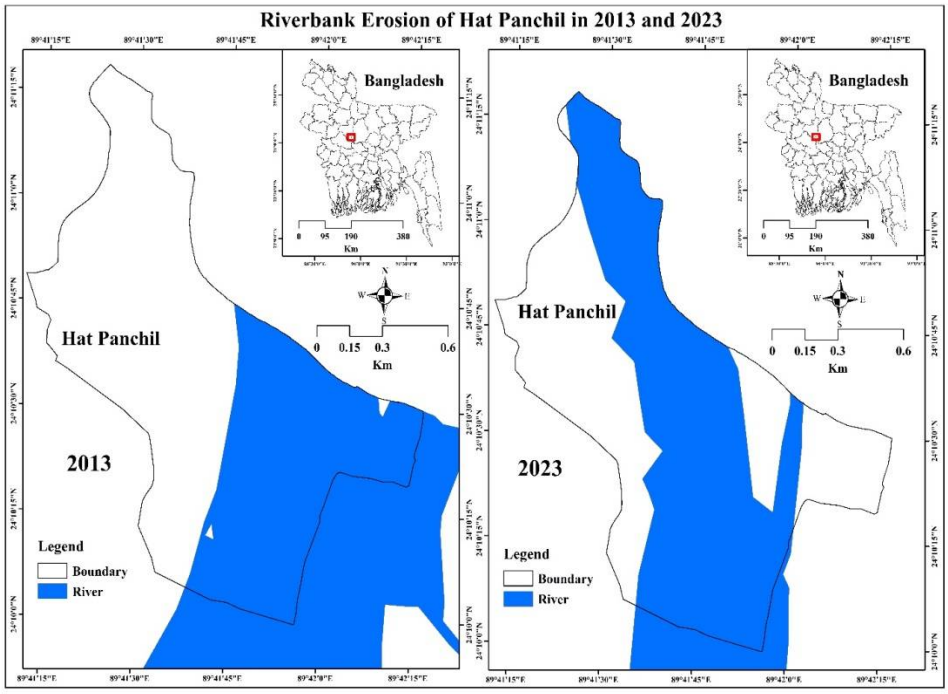

Fig. 2. Riverbank erosion of Hat Panchil village in 2013 and 2023. Note, a large part of the land has gone under 'Nadi Shikhasti' along the north-south axis, and two newly accreted land masses emerged as 'Nadi Payasti'- char land between 2013 and 2023.

The Jamuna River exhibits intense bank erosion of the char land, its bank composition with sandy materials, impart due to the braided nature, heavy monsoonal rainfall in upstream areas, causes variable water flow with characteristics seasonality in water levels in the river.

The river flow decreases downstream when the water level declines in the dry season. As a result, the upstream part of the river becomes dry quickly, and erosion occurs more during that time. The riverbank erosion issue of the present study area has appeared in different leading newspapers and television channels in the past (ACAPS and Start Network 2019).

Table 3. Factors associated with riverbank erosion in the study area.

Factors	Strongly disagree	Disagree	Neutral	Agree	Strongly agree	N = 155 WAI	OA
High water flow	26	20	18	25	11	0.55	M
Channel shape change	5	10	28	30	27	0.73	M
Climate change	30	28	22	8	12	0.49	M
Development of char lands	12	17	14	15	42	0.72	M
Lack of effective measures	0	6	10	32	52	0.86	H

Note: Strongly disagree (SD): 0.01–0.2; Disagree (D): 0.21–0.4; Neutral (N): 0.41–0.6; Agree (A): 0.61–0.8; Strongly agree (SA):0.81–1; WAI: weighted average index; OA: overall assessment, M=Medium, H=High.

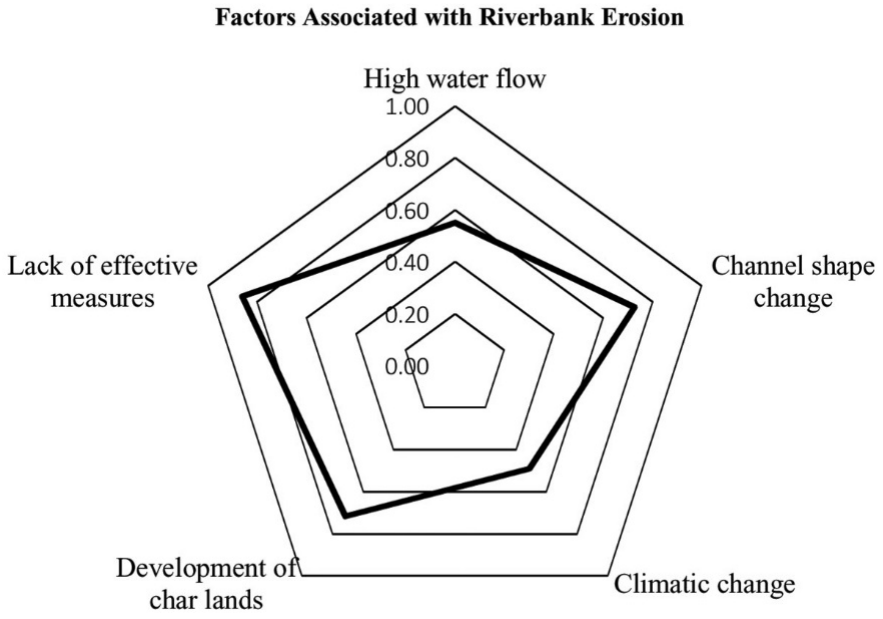

Source: Field Survey, 2023

Fig. 3. Factors associated with riverbank erosion in the study village.

Riverbank erosion became a common scenario in the study area. People are suffering a lot due to the unpredictable nature of bank erosion. Most respondents (WAI=0.86) mentioned that inadequate measures are causing substantial riverbank erosion in this area (Fig. 3). Channel shape and development of chars within the river channel were also responsible for erosion in the study area, and the WAI values were 0.73 and 0.72, respectively. Few respondents focused on the climatic change issue linked to riverbank erosion, and the WAI value was 0.49 (Table 3).

Impacts of Riverbank Erosion

The study village's people have been suffering from riverbank erosion for a long time. The population's economic loss and social vulnerability due to bank erosion have consistently increased in recent years. The effect of land loss involves the loss of homestead land, housing structures, crops, cattle, trees, and household utensils (Table 4). Loss of homesteads forces people to move to new places without any alternative options and puts them in disastrous situations.

Table 4. Relative Grading of Impacts of Riverbank Erosion by Respondents as Reflected in Survey.

Factors	Strongly agree	Agree	Neutral	Disagree	Strongly disagree	N = 155	OA
						WAI	
Loss of land property	82	10	4	2	2	0.92	VH
Become homeless	69	18	5	3	5	0.86	VH
Increase poverty	52	20	6	4	6	0.71	H
Loss of jobs	55	23	5	5	12	0.76	H
Disruption of children's education	32	27	10	24	7	0.86	VH
Decline family bonding	55	14	9	10	12	0.73	H
Displace from the birthplace	45	14	19	12	10	0.68	M

Note: Strongly disagree (SD): 0.01–0.2; Disagree (D): 0.21–0.4; Neutral (N): 0.41–0.6; Agree (A): 0.61–0.8; Strongly agree (SA):0.81–1; WAI: weighted average index; OA: overall assessment, VH=Very High, H=High, M=Medium.

From the field survey, it has been observed that the respondents focused more on land property loss (WAI=0.92). People in the surveyed area reported becoming homeless due to riverbank erosion (WAI=0.86). The WAI values for loss of job, disruption of children's education, and decline in family bonding were 0.76, 0.63, and 0.73, respectively (Fig. 4). The effect of riverbank erosion increased the poverty of the affected families, and the WAI value was 0.71. Many people were displaced from their birthplace due to riverbank erosion in the study area, and the WAI value was 0.63. So, riverbank erosion threatens the surveyed households' lives and livelihoods in the study area.

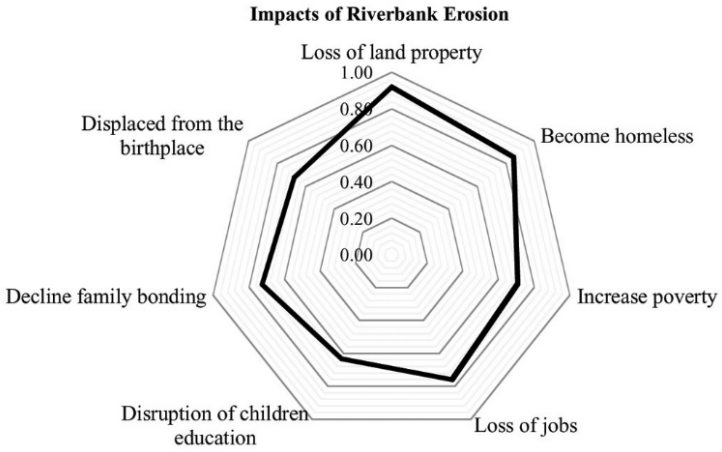

Source: Field Survey, 2023

Fig. 4. Impacts of riverbank erosion in the study village

Measures Undertaken to Reduce the Riverbank Erosion

To cope with the bank erosion process, various mitigation measures have been undertaken in the study area partly by the Water Development Board (BWDB). Geo bags covered some portions of the embankment in the study area to protect the area from erosion. However, in many bank sections, such measures have collapsed and are yet to be repaired. One of the structural measures to protect the river's shoreline is making concrete blocks. Many workers are engaged in making the blocks that will be placed on the vulnerable river bank to protect the area from erosion. The local people expect a long-lasting measure to cope effectively with the erosion problem. BWDB is dredging at the opposite side of the study village to develop a secondary channel that would support draining out extra water differently and save the area from erosion. Moreover, the

dredged sands are thrown into the riverbank erosion-prone areas for sedimentation or accretion of sands in the vulnerable portions.

The erosion-affected people of the area try to return to everyday life later, but it is a difficult task for them. The affected people did not receive the expected support from the government departments or others, so they suffered. Local print and social media provide good coverage of the situation. The relevant government departments have taken initiatives to protect the area from riverbank erosion. To supplement the government effort, the following points to be under consideration:

- Timely completion of the project: The ongoing projects to control the riverbank erosion of the study area should be finished on time so that vulnerable people can be saved from the erosion problem. The local people expect these projects to be completed with due diligence.
- Provision of financial support: The affected people need some financial support to restart their livelihood-related activities, and they can cultivate the available lands.
- Rehabilitation support for housing: Many people already lost their lands and homesteads due to erosion. These homeless people took shelter on the government embankment or other rented lands. So, they need to get land to rebuild their homes.
- Enlisting vulnerable families: The vulnerable families should be enlisted and provided the required support to improve their living conditions.
- Coordination with local NGOs: Various government departments and NGOs work in this area to support the people. Coordination among these organizations is essential to make their efforts more effective.

Conclusion

Riverbank erosion is one of the major natural events in Bangladesh, as it is responsible for thousands of people becoming homeless and landless every year. Jamuna River plays a significant role in affecting people's lives and livelihoods. The present study area is one of the worst-hit areas of riverbank erosion, and erosion is affecting the overall condition of the surveyed area significantly. The study revealed that factors such as high water flow, lack of effective measures, development of char lands, and channel shape change are the main reasons for river erosion in the study area. Government departments are undertaking various measures to reduce the erosion of the study area, and these measures are underway. However, people are passing difficult times due to the enormous effects on their lives and livelihoods. Effective measures relating to erosion can bring significant changes in people’s livelihoods and will support rehabilitating the affected communities.

Acknowledgment

The author is grateful to the Disaster Research Training and Management Center (DRTMC), Department of Geography and Environment, University of Dhaka, Dhaka, Bangladesh, for funding this research.

References

Alam, G.M.M. 2017. Livelihood cycle and vulnerability of rural households to climate change and hazards in Bangladesh. *Environ. Manage*. **59**: 777–791.

Atwii, F., Sandvik, D.K., Kirch, L., Paragi, D.B., Radtke, D.K., Schneider, S. and Weller, D. 2022. *World Risk Report 2022.* Institute for International Law of Peace and Armed Conflict (IFHV).

Barua, P., S.H. Rahman and M.H. Molla. 2019. Impact of river erosion on livelihood and coping strategies of displaced people in South-Eastern Bangladesh, *Int. J. Migration and Residential Mobility.* **2** (1): 34-55.

Blair, A.A.C. 2017. Climate change threats and adaptation responses in small island developing states: A comparative analysis of Antigua, Barbuda and Vanuatu. (Unpublished doctoral thesis), University of Newcastle, Australia.

Chowdhury, S.K. 2015. Riverbank erosion. In: *Banglapedia*: National Encyclopedia of Bangladesh, S. Islam and S. Miah (Eds.), Dhaka: Asiatic Society of Bangladesh. Retrieved from https://en.banglapedia.org/index.php/Riverbank_Erosion

Das J.D., T. Dutta, and A.K. Saraf. 2007. Remote sensing and GIS application in change detection of the Barak River channel, N.E. India. *J. Indian Soc. Remote Sens.* **35**(4): 301-312.

Eckstein, D., V. Kunzel and L. Schafer, 2021. *Global Climate Risk Index 2021.* Berlin: Germanwatch e.V. Retrieved: January 2021, from www.germanwatch.org/en/cri

Freihardt, J. and O. Frey. 2023.Assessing riverbank erosion in Bangladesh using time series of Sentinel-1 radar imagery in the Google Earth Engine. *Nat. Hazards Earth Syst. Sci*. **23**: 751-770.

Ha, H.D., and T.N. Thang. 2017. Fishery communities' perception of climate change effects on local livelihoods in Tam Giang Lagoon, Vietnam. In: *Redefining diversity and dynamics of natural resources management in Asia*, Shivakoti, G.T. Thang, N. Dung, D. Hulse and S. Sharma (ed.), Netherlands: Elsevier, pp. 111-124.

Hutton, D. and C.E. Haque. 2003. Patterns of coping and adaptation among erosion-induced displaces in Bangladesh: implications for hazard analysis and mitigation. *Natural Hazards* **29**: 405-421.

IASC and EC. 2022. Inform Report 2022. Luxembourg: European Union. JRC129343

Islam, M. M., M. Shahin, M. Miraj, S. Ghosh, M.N. Islam and A.I. Islam, 2021. Climate Change Impacts and Mitigation Approach: Coastal Landscape, Transport, and Health Aspects. In: 'Bangladesh II: Climate Change Impacts, Mitigation and Adaptation in Developing Countries', M. N. Islam, A. v. Amstel and J. Dodson (ed.), Gewerbestrasse, Cham, Switzerland: Springer Nature Switzerland AG, pp. 41-102.

Khongsatjaviwat, D. and J.K. Routray. 2015. Assessment of capacities of TAOs and CBOs for local development in Thailand. In: Spatial Diversity and Dynamics in Resources and Urban Development, A. K. Dutt, A.G. Noble, F.J. Costa, S.K. Thakur, R. Thakur and H.S. Sharma (ed.), Vol. 1, Regional Resources, Dordrecht: Springer, pp. 501-527.

Mamun, M.Z. 1996. Awareness, preparedness and adjustment measures of riverbank erosion prone people: a case study for settlement planning for disaster mitigation in Bangladesh. *Disasters*. **20**(1): 68-74.

Mojid, M. A. 2020. Climate change-induced challenges to sustainable development in Bangladesh. IOP Conf. Series: *Earth Environ. Sci*. **423**: 1-13.

Nooriafshar, M., R. Williams and T. Maraseni. 2004. *The use of virtual reality in education*. Paper presented at the American Society of Business and Behavioural Sciences, 2004 Seventh Annual International Conference, Cairns, Australia.

Pakzad, P., P. Osmond, and L. Corkery. 2016. *Developing key sustainability indicators for assessing green infrastructure performance.* Paper presented at the International High-Performance Built Environment Conference - A Sustainable Built Environment Conference, Sydney, 17-18 December 2016, Series SBE16.

Pati, J.K, J. Lal, K. Prakash and R Bhusan. 2008. Spatio-temporal shift of western bank of the Ganga River at Allahabad city and its implications. *J. Indian Soc. Remote Sens*. **36**(3): 289-297.

ACAPS and Start Network. 2019. Disaster summary sheet: Bangladesh riverbank erosion. https://reliefweb.int/report/bangladesh/disaster-summary-sheet-bangladesh-riverbank-erosion-21-march-2019.

Shahriar, S. 2021. Impacts of Floods and Riverbank Erosions on the Rural Lives and Livelihoods Strategies in Bangladesh: Evidence from Kurigram. In: Handbook of Climate Change Management: Research, Leadership, Transformation, W. L. Filho, J. L. Ayal, W. L. Filho, J. M. Luetz and D. Ayal. (eds.), Springer Nature Switzerland AG, pp. 797-822.

Yamane, T. 1967. *Statistics: An introductory analysis.* New York: Harper & Row.

(Revised copy revised on 10.09.2023)

J. Asiat. Soc. Bangladesh, Sci. **49**(2): 193-201, December 2023 DOI: https://doi.org/10.3329/jasbs.v49i2.70768

A NEW SPECIES OF CRAB-SPIDER UNDER THE GENUS *THOMISUS* WALCKENAER, 1805 (ARANEAE: THOMISINAE: THOMISIDAE) FROM BANGLADESH

V. BISWAS[1*] AND D. RAYCHAUDHURI[2]
[1]*Department of Zoology, Khulna Government Womens' College, Khulna, Bangladesh*
[2]*Entomology Laboratory, Department of Zoology, University of Calcutta, India*

Abstract

Taxonomic description of a new species of crab-spider genus *Thomisus* Walckenaer, 1805 is provided herewith. The species *Thomisus aruni* n. sp. was identified as new to science. The paper contains an illustrated description of the species together with the generic diagnosis and distribution of the species.

Keywords: Taxonomy, Crab-spider, Araneae, Thomisinae, Thomisidae, *Thomisus*, Bangladesh.

Introduction

Crab-spiders are the members of the moderately largest family Thomisidae which are world wide in distribution. These spiders are one of the common, attractive and fascinating groups in the garden and forests. Their body is short, strong and slightly flattened and the legs are laterigrades. They are small to medium in size (about 2 mm to 23 mm in length).

Thomisids do not build any web to trap preys though all of them produce silk for drop lines and sundry reproductive purpose. Some are wandering hunters and are known as 'ambush predators'. Thomisids are usually wandering spiders inhabiting mainly on leaf litter, grasses, foliages of plants and a few live under loose barks and on the ground. Some species sit on or besides flower so that sometimes they are called 'flower spiders'. These spiders are able to change colour showing mimicry over a period of several days. The spiders of the family Thomisidae are not known to be harmful to humans, but majority are helpful predators and consume small pest insects of crop-fields, gardens and forests.

Thomisidae is one of the largest families with 2,155 species belonging to 177 genera and its members are distributed world wide (World Spider Catalog, 2022; Buchar and Ruzicka, 2002). The members of the genus *Thomisus* Walckenaer, 1805 are commonly found in the garden and forests of Bangladesh and all of them are small, but robust and

* Corresponding author: vivekarach@gmail.com

colourful. The genus was first established by Walckenaer in 1805 with the type-species *T. onustus* Walckenaer, 1805. At present, it is represented by 145 species in the world fauna (World Spider Catalog, 2022) and 45 species in the Indian Sub-continent (Tikader, 1980; Majumder, 2005, 2007; Keswani *et al*., 2012). In Bangladesh, only 7 (seven) species are recorded (Okuma *et al.,* 1993; Biswas *et al*., 1993; Chowdhury and Nagari, 1981; Chowdhury and Pal, 1984; Begum and Biswas, 1997; Biswas, 2009, 2019), but a good number of species is described in other Asian countries like – China (Chen and Zhang, 1991; Zhao, 1993; Song *et al*., 1999; Song and Zhu, 1997), Japan (Yaginuma, 1986; Ono, 1988; Shinkai and Takano, 1984), Singapore (Koh, 1989), Korea (Paik, 1978; Kim and Lee, 2012) etc. In the present paper an illustrated description of a new species of the genus *Thomisus* together with its generic diagnosis and distribution of the species has been given.

Materials and Methods

Collection: The specimens of new species was collected from the gardens and crop-fields of southern coastal areas of districts Faridpur and Pirojpur of Bangladesh. The collection was made by jarking the branches of Jaba plants (*Hibiscus rosa-sinensis*) from Agricultual Diploma Institute (ADI), Faridpur on an inverted umbrella placed underneath the plants and from the rice-plants (*Oryza sativa*) of district Pirojpur by hand sweeping net. The specimens thus collected were then placed to a large glass jar containing a wade of cotton with chloroform for anesthesizing specimens. These are transferred to a petridish filled with 70% ethyl alcohol for sorting. After sorting, the specimens were then placed in glass vials with 70% ethyl alcohol for identification and future study.

Preservation: The collected specimens were preserved temporarily in 70% ethyl alcohol and after identification, these were preserved permanently (separate specimen in separate vial) in Audman's Preservatives (90 parts 70% ethyl alcohol + 5 parts glycerine + 5 parts glacial acetic acid) following Lincoln and Sheals (1985).

Identification

The specimens thus preserved, were identified by the study of different important taxonomic characters viz.- shape, size, colour, dorsal decoration, structure of legs, male pedipalp, female epigynum, cheliceral structure and dentition, eye patterns etc. These were done following the keys and description made by Tikader (1971, 1980, 1987), Ono (1988, 2009), Barrion and Litsinger (1995), Song and Zhu (1997), Dondale and Redner

(1978), Okuma *et al.* (1993), Koh (1989), Chen and Zhang (1991), Zhao (1993), Levy (1973, 1985), Yaginuma (1986), Biswas (2009) and Kim and Lee (2012).

After identification, the species was later confirmed from the Arachnida section, Zoological Survey of India, Kolkata. At present, the preserved specimens are placed in the Department of Zoology, Khulna Government Womens' College, Khulna and will be deposited to the Museum of the Department of Zoology, University of Dhaka, in due course of time.

Illustration and Photograph

The whole body of spider and its different body-parts were illustrated under a Stereozoom Binocular Microscope fitted with Camera Lucida. Leg measurements were taken under the same condition in the following sequences: femur, patella, tibia, metatarsus, tarsus and total length, and all measurements were taken in millimeters (mm).

The photographs of the identified specimens were taken both in natural condition (in the field) by DSLR Camera fitted with 90 mm macrozoom lens and in the laboratory by Camera fitted with microscope (model SV8, Zeiss).

Results and Discussion

Systematics

Family: THOMISIDAE Sundevall, 1833
Subfamily: Thomisinae Sundevall, 1833
Genus: *Thomisus* Walckenaer, 1805
Type-species: *T. onustus* Walckenaer, 1805

Diagnosis

Spiders (under the genus *Thomisus*) with short, compact and robust bodies. Body bright in colour. Cephalothorax truncated in front, with the upper fore corners strongly and conically protruberant and divergent. Eyes very small, arranged in two rows, with lateral eyes on distinct eye tubercles; anterior row strongly recurved with medians nearer to laterals than the others. Legs long, relatively much longer in males; leg I and II much longer than III and IV.

Abdomen narrow and truncated in front, enlarging to a considerable width behind, where at either corner with a short, blunt, conical protruberance.

Females small to medium in size (usually 2 mm - 11 mm). Carapace usually as wide as long, high and convex but posterior margin concave. Males are much smaller (1.9 mm –

3.6 mm) and most species darker in colour, with strong erect setae both on the carapace and abdomen. Eye tubercles in all species distinct and sharply pointed.

Biological note

Spiders of the genus *Thomisus* usually live in vegetation, mainly inside flower corollas. They can not make any web and can consume small insects in the crop-fields and gardens. Some can change their colours to match the substratum (Levy 1985). They catch their prey lurking on the flowers with their legs spread widely.

Distribution: Africa, America, Asia, Australia and Europe.

Description of the new species

***Thomisus aruni* n. sp.**

(Figs. 2a-f & 1a-b)

Material examined: Holotype: 1 female, ADI, Faridpur, 12. VIII. 1993 & 08. V. 1995, Coll. V. Biswas; Allotype: 1 male, Pirojpur, 18.IX. 1991, Coll. V. Biswas; Paratype: Nil.

Designation of the type

Holotype: This is a single female specimen preserved permanently in Audman's preservatives. It was collected from a shrub (*Hibiscus rosa-sinensis*) of Agricultural Diploma Institute (ADI) campus, Faridpur and the whole illustrated description is made on the basis its taxonomic characters.

Allotype: This is a single male specimen collected from Pirojpur. Its single pedipalp is drawn showing the male identifying character of the new species.

General: Body small and robust but bright in colour (Fig. 2). Cephalothorax brown, legs and abdomen pale brown. Total body length (holotype) 6.20 mm. Carapace 2.40 mm long, 2.00 mm wide; abdomen 3.80 mm long and 2.60 mm wide. Total body length (allotype) 5.20 mm long; Carapace 1.90 mm long, 1.50 mm wide; abdomen 3.30 mm long and 2.00 mm wide.

Cephalothorax: Nearly rounded, slightly longer than wide, medially wide, anteriorly convex; cephalic region raised with 2 distinct, anteriorly wide cervical furrows. Eyes

situated on an elevated, laterally concave, pointed, chalk-white tubercle; anterior row recurved, anterolaterals slightly larger than the anteromedians; posterior row longer, posterolaterals situated on the lateral margin. Chelicerae brown, broad, both inner and outer margins with 1 tooth (Fig. 2b). Maxillae longer than wide, anteriorly wide and scopulate (Fig. 2c). Labium broad, posteriorly flat, anteriorly rounded and scopulate (Fig. 2c). Sternum brown, longer than wide, posteromedially wide, posteriorly pointed, clothed with fine hairs (Fig. 2d). Legs long and slender, clothed with hairs and spines; leg formula 1243 and the measurements (in mm) of different leg segments are shown in Table 1.

Abdomen: Broad, posteriorly wide, narrowing anteriorly; posterior margin with 2 deep constrictions forming a median rounded concave area; each of antero and posterolateral margins pointed forming a tetrangular shape; dorsum with few spots; epigyne as in Fig. 1e.

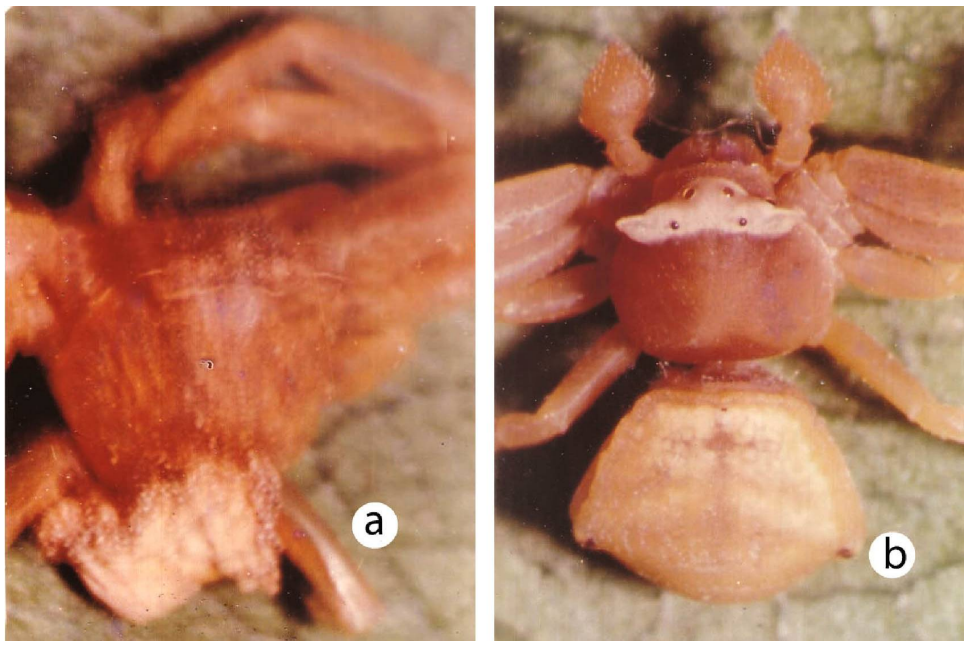

Figure 1. *Thomisus aruni* n. sp. a. Female; b. Male

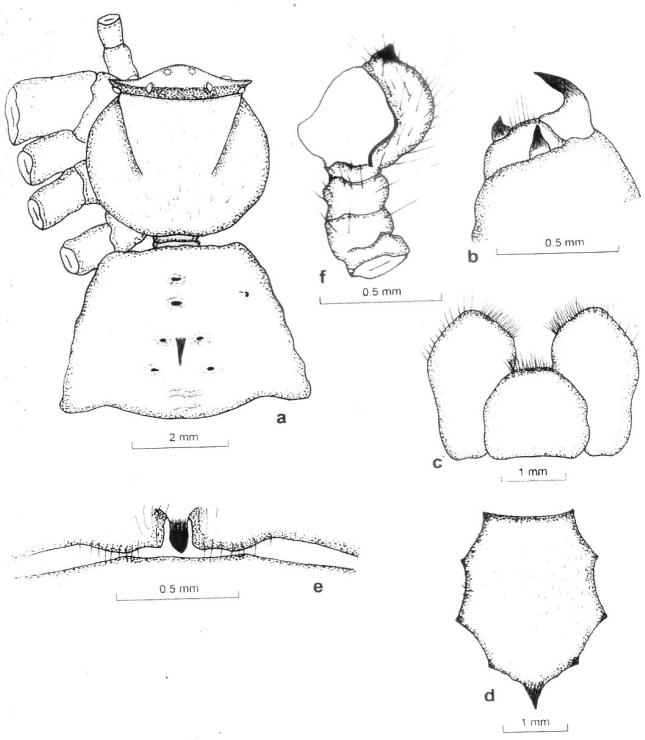

Figure 2. *Thomisus aruni* n. sp. a. Whole body of female (dorsal view); b. Chelicerae; c. Maxillae & Labium; d. Sternum; e. Epigynum; f. Male palp

Table 1. Measurements (in mm) of the leg segments of *Thomisus aruni* n. sp.

Leg	Femur	Patella	Tibia	Metatarsus	Tarsus	Total
I	4.00/4.00	1.80/1.80	2.50/2.50	2.50/2.50	0.90/0.90	11.70/11.70
II	3.90/3.90	1.80/1.80	2.30/2.30	2.00/2.00	0.80/0.80	10.80/10.80
III	1.50/1.50	0.90/0.90	1.00/1.00	1.00/1.00	0.80/0.80	5.20/5.20
IV	2.20/2.20	1.00/1.00	1.20/1.20	1.50/1.50	0.80/0.80	6.70/6.70

Male little smaller than female and comparatively darker in colour. Male palp as in Fig. 1f.

Etymology: The species is named after Professor Arun Kumar Das, Department of Botany, Government Profulla Chandra College, Bagerhat, Bangladesh, who helped in the collection of specimens.

Distribution: Bangladesh: Gardens of Agricultural Diploma Institute (ADI), Faridpur and the rice-fields of district Pirojpur (type- localities).

Remarks: The species *T. aruni* n. sp. shows the following diagnostic characters:

1. Cervical furrows deep and distinct.
2. abdomen not overhanging the cephalothorax.
3. anterior margin of abdomen straight posteriorly, weakly convex.
4. transverse band on the ocular area of cephalothorax white and
5. much different epigynum.

Discussion

The new species *Thomisus aruni* n. sp. is a small, unique and brightly coloured crab-spider. These are found in the gardens and crop-fields of Bangladesh. It shows some special diagnostic features on the basis of those it is established as a species new to science. From this study, we can expect that there are some considerable numbers of endemic species present in the country.

Reports on the study of thomisid spiders in Bangladesh is scarce, except Okuma *et al.* (1993), Biswas (2009) and Biswas and Raychaudhuri (2003, 2017). Therefore, a detailed taxonomic study on these spiders may discover some new species in future.

Moreover, as the new species *Thomisus aruni* n. sp. is distributed in the gardens and crop-fields, so, it may be assumed that they must have a predatory role in controlling insect pests of both these ecosystems (as crab-spiders are good predators of insect pests).

Acknowledgements

The authors are grateful to Dr. S. C. Majumder, Scientist– SD, Arachnida Section, Zoological Survey of India, Kolkata, India, for the confirmation of species identification and also to the Head, Department of Zoology, University of Calcutta, India, for kind permission to allow his laboratory during the study.

References

Barrion, A.T. and J.A. Litsinger, 1995. *Riceland spiders of South and Southeast Asia.* CAB International; International Rice Research Institute, Wallingford, UK. 700 p. + 16 plates.

Begum, A. and V. Biswas, 1997. A list of spider fauna of Barisal division, Bangladesh (Araneae: Arachnida). *Bangladesh J. Zool.*, **25** (2): 207-210.

Biswas, V. 2009. *Encyclopedia of flora and fauna of Bangladesh.* Vol. 18, Part 1, *Archopoda: Crustacea*, (Ahmed Z., ed.), Asiatic Society of Bangladesh, pp. 437.

Biswas, V. 2019. Checklist of the spider fauna of Bangladesh (Araneae: Arachnida). *Bangladesh J. Zool.* **47**(2): 185-227.

Biswas, V. and D. Raychaudhuri, 2003. A new species of the genus *Tibellus* Simon (Araneae: Thomisidae) from Jhenidah, Bangladesh. *J. Bombay Nat. Hist. Soc.*, **100** (1): 84-86.

Biswas, V. and D. Raychaudhuri, 2017. New species of the genus *Camaricus* Thorell, 1887 (Araneae: Thomisidae) from Bangladesh. *Bangladesh J. Zool.*, **44** (2): 255-265.

Biswas, V., H.R. Khan, N.Q. Kamal and A. Begum, 1993. A preliminary study of the rice-field spiders of Jhenidah, Bangladesh. *Bangladesh J. Zool.*, **21** (2): 85-92.

Buchar J. and V. Ruzicka, 2002. *Catalogue of Spiders of the Czech Republic*. (Peter Merrett ed.), Praha, Peres, pp. 351.

Chen, Z.F. and Z.H. Zhang, 1991. *Fauna of Zhejiang, Araneida.* Zhejiang Science and Technology Publishing House, pp. 356.

Chowdhury, S.H. and S. Nagari, 1981. Rice-field spiders from Chittagong. *Proc. Zool. Soc. Bangladesh*: 53-72.

Chowdhury, S.H. and S.K. Pal, 1984. Further report on rice-field spiders from Bangladesh. *Chittagong Univ. Stud.* **II**(8): 25-39.

Dondale, C.D. and J.H. Redner, 1978. *The Crab-spiders of Canada and Alaska* (Araneae: Philodromidae: Thomisidae). Biosystematic Research Institute, Agriculture, Canada, pp. 255.

Keswani, S., P. Hadole and A. Rajoria, 2012. Checklist of spiders (Arachnida: Araneae) from India –2012. *Indian J. Arachnol.*, **1** (1): 1-129.

Kim, S.T. and S. Y. Lee, 2012. *Invertebrate fauna of Korea. Araneid spiders*. National Institute of Biological Resource, Ministry of Education, Republic of Korea. **21**(16): 1-127..

Koh, J.K.H. 1989. *A Guide to Singapore Spiders.* Singapore Science Centre, 160pp.

Levy, G. 1973. Crab-spiders of six genera from Israel (Araneae: Thomisidae). *Israel J. Zool.*, **22:** 107-141.

Levy, G. 1985. *Fauna Palaestina, Arachnida - II, Araneae: Thomisidae.* Israel Academy of Sciences and Humanities, Jerusalem, pp. 114.

Lincoln, R.J. and J.G. Sheals. 1985. *Invertebrate Animals: collection and preservation.* British Museum (Natural History), London, pp. 150.

Majumder, S.C. 2005. Studies on some spiders from eastern coastal region of India. *Mem. Zool. Surv.* India, **20**(3): 1-57.

Majumder, S.C. 2007. *Pictorial Handbook on spiders of Sunderbans, West Bengal, India.* Zoological Survey of India, Kolkata, pp. 138.

Okuma, C., N.Q. Kamal, Y. Hirashima, M.Z. Alam and K. Ogata, 1993. *Illustrated Monograph of the Rice-field spiders of Bangladesh.* IPSA – JICA, Salna, Gazipur, Bangladesh. pp. 93.

Ono, H. 1988. A revisional study of the spider family Thomisidae (Arachnida: Araneae) of Japan. National Science Museum Monographs Vol. 5, Tokyo, pp. 252.

Paik, K.Y. 1978. *Araneae : Illustrated flora and fauna of Korea.*, **21**: 1-548.

Shinkai, E. and H. Takano, 1984. *A field-guide to the spiders of Japan.* Tokai University Press, Kanagwa, 204pp.

Song, D.X. and M.S. Zhu, 1997. *Fauna Sinica, Arachnida: Araneae (Thomisidae: Philodromidae).* Science Press, Beijing, pp. 259.

Song, D.X., M.S. Zhu and J. Che, 1999. *The Spiders of China*. Hebei Science and Technology Publishing House, Shijiazhuang, pp. 640.

Tikader, B.K. 1971. Revision of Indian crab spiders (Araneae: Thomisidae). *Mem. Zool. Surv. India*, **15**(8): 1-90.

Tikader, B.K. 1980. *Fauna of India, Araneae* (Thomisidae), **1**(1), Zoological Survey of India, Kolkata, pp. 247.

Tikader, B.K. 1987. Handbook Indian Spiders: A Manual for the Study of the Spiders and Their Relatives, pp. 251.

World Spider Catalog, 2022. *World Spider Catalog*, Version 22.5, Natural History Museum of Bern, Bern., Online at – http : // www.wsc.nmbe.ch (accessed on 21st December, 2023).

Yaginuma, T. 1986. *Spiders of Japan in colour*. 2nd edition, Hoikusha Publishing Co., Ltd., Osaka, pp. 305.

Zhao, J.Z. 1993. *Spiders in the cotton fields in China*. Wuhan Publishing House, Wuhan, China, pp. 552.

(Revised copy received on 01.09.2023)

J. Asiat. Soc. Bangladesh, Sci. **49**(2): 203-224, December 2023 DOI: https://doi.org/10.3329/jasbs.v49i2.70769

VEGETATION DYNAMICS OF COASTAL MANGROVE FOREST

MD. ABDUL QUDDUS MIAH*
Research Officer, Plantation Trial Unit Division, Bangladesh Forest Research Institute, Rupatali, Barishal, Bangladesh

Abstract

In the man-made coastal forest, the vegetation dynamics of protected and unprotected coastal forests have been identified. This study examined and quantified the impacts of grazing on coastal vegetation. The investigation was conducted between January 2013 and December 2020. In a transect line, fifty-two distinct tree, herb, and shrub species were found in unprotected coastal areas, and 36 were found in protected areas. After eight years, the number of saplings (p=0.031), poles (p=0.030), and total (p=0.026) (seedling, sapling, and pole) regeneration were substantially different between protected and unprotected areas. The current study found no significant differences in regeneration and tree density after one and five years of establishing the protected zones. The greatest number of natural poles were found in protected and unprotected areas from 2017 to 2020. The changes in tree density were considerable (p=0.03) after eight years. From 2014 to 2017, the highest rate of seedling recruitment was 36622 to 43439 individuals observed in protected and unprotected areas. In protected areas, *Excoecaria agallocha* L. and *Avicinnia officinalis* L. had the most extensive regeneration coverage, and nine species of seedlings, saplings, and poles were seen in 2013 protected areas. After 8 years, *E. agallocha* had a 47.01% while *Phoenix paludosa* Roxb. had a 30.81% success rate. In 2020, seedlings of *Pongamia pinnata* L. (6.6%), *Herietiera fomes* Buch.-Ham. (5.5%), *A. officnalis* (5.30%) and the remaining six species were also seen. The species *E. agallocha* comprised 69.11% of the trees at Soner Char tree density, followed by *Sonneratia apetala* Buch.-Ham. (23.30%), *P. paludosa* (8.82%), *H. fomes* (3.43%), and the remaining two species in 2020. After eight years, the species *S. apetala* declined by 43.64% and 23.90% in protected and unprotected areas, respectively. The species *Phoenix paludosa*, *H. fomes*, *A. officinalis*, and *Dolichandrone spathacea* (L.F) Baill. Ex K. Schum. was found to replace *S. apetala* in protected areas. Grazing affects the natural recruitment stage of saplings and poles and tree stem density in unprotected areas. The observations assume that *S. apetala* will diminish due to climatic conditions, and *E. agallocha* will become the main dominating species in coastal areas.

Keywords: Vegetation, Soner Char, Char Kashem, Protected area, Tree density, Natural regeneration, Man-made coastal forest.

Introduction

The coastline of Bangladesh is 710 km long and is associated with various environmental and production activities (Ahsan, 2013). Bangladesh is a world leader in mangrove and coastal afforestation. An afforestation program was started in newly accreted *char*lands

*Corresponding author: maqmiah2009@yahoo.com

along the coastal belt in 1966 (Rahman and Pramanik, 2015). Mangrove plantation areas have increased in Bangladesh daily (Hasan, 2013). The Bangladesh Forest Department has established approximately 209,140 hectares of coastal plantation in coastal regions, with mangrove species accounting for more than 93% (DoE, 2015). The actual area under the coastal plantation now stands at 61,574 hectares due to the plantation's failure and extermination from natural adversity (BFD and UNDP 2018). Plantations along the coast are seen as a successful adaptation strategy against the extreme weather events that climate change is projected to bring about more frequently (Ahammad and Nandy, 2012). It performs a wide range of beneficial ecological and biophysical tasks, such as expanding the nation's forest cover, acting as a highly effective carbon sink, trapping sediment, preventing erosion, stabilizing the land, providing habitat and a breeding ground for wildlife and fisheries, and enhancing the recreational value of coastal areas (Uddin *et al.*, 2014; Iftekhar and Islam, 2004; Alongi, 2012; Saintilan *et al*., 2014; Krauss *et al*., 2014; Lee *et al*., 2014). The coastal man-made forests are a source of various economic products, including fish, mollusks, crabs, honey, fuelwood, timber, and thatching materials (Islam and Wahab, 2005). Also, coastal forests are used as pasture land for buffalo and cattle in Bangladesh. Approximately 0.5 million buffalo and many cows have been grazing in Bangladesh's artificial coastal forest. (Faruque *et al*., 1990; Huque and Borghese, 2013).

Forest protection practiced in Bangladesh was introduced by both *in situ* and *ex-situ* conservation methods to maintain the country’s biological diversity (Mukul, 2007). The Char Kukri-Mukri wildlife sanctuaries in the Bhola district, the Nijhum Dweep National Park in the Noakhali district, the Kua-Kata eco-park (Fatrar Char), and the Soner Char wildlife sanctuaries in the Patuakhali district are the coastal forest's protected areas (Chowdhury and Koike, 2010; Mukul *et al*., 2017). Forest protection zones are a powerful and effective tool for preserving the environment and the world's natural resources for the long term (Mukul, 2007).

In Bangladesh, mangrove afforestation has been ongoing for about 55 years (Hasan, 2013). The forest floors of plantations and surrounding areas contain enormous amounts of seeds. Any forest ecosystem's natural regeneration is a biological process of reproduction. The assessment of regeneration is a fundamental tool for detecting the overall condition of a forest (Wang *et al*., 2008; Rahman *et al*., 2019). To assess the regeneration, vegetation, and tree density of the artificial coastal forest, Islam *et al*., 2015, undertook a partial assessment of various islands or char in the coastal regions of Patuakhali, Bhola, Hatiya, and Chattgram. Before now, no information was available

regarding long-term observation of protected and unprotected vegetation in coastal forests.

Additionally, recent grazing is seriously hampering the growth of the artificial coastal forest (Islam *et al.*, 2013; Miah *et al*., 2014). For baseline comparisons and to assess the vegetation dynamics and regeneration condition of these forests, we included unprotected forests. Our study aims to define tree vegetation change in both protected and unprotected coastal forest areas. The impact of grazing on coastal forests was also considered. The current study's findings will likely improve our knowledge of the status of protected forest vegetation, including how it relates to artificial grazing as common land use.

Materials and Methods

Study sites: The two study sites were under the Rangabali Upazilla. The Rangabali Upazilla is located in the Patuakhali coastline district of Bangladesh. Both protected and unprotected man-made coastal forests were chosen as the study areas. Soner Char Wild Life Sanctuary was the protected coastal forest, and Char Kashem was the unprotected coastal forest. These two islands had mangrove plantations developed in 1973-1974 and 1975, approximately the same periods, with similar tree diversity. There have been 2377 mm of rain, and the weather is humid (District Statistics, 2011). The soil is non-calcareous alluvium. The combined actions of the rivers Meghna, Brahmaputra, and Ganges have influenced the landforms (FAO, 1988; SRDI, 2010). During the monsoon season, the experiment sites almost experienced ebb and tide. Soner Char and Char Kashem sites were submerged for nine to twelve months and three to five months.

Soner Char: The Soner Char Wildlife Sanctuary is situated in Bangladesh's Patuakhali District, near Rangabali Upazila. It is located in the Patuakhali district's most southern region. Soner Char Wildlife Sanctuary was established in December 2011 and had a 2026.5-hectare forest (Mukul *et al*., 2016). The IUCN classifies these areas as protected areas. According to the Vulture Safe Zone-2 Schedule issued by the government of Bangladesh in 2012, it is one of the safe zones for vultures (BFD, 2020). The Soner Char Wildlife Sanctuary's soil was non-saline for most of the year in the northern regions, but it became saline to variable degrees during the dry season. During the rainy season, some moderately deep flooding occurred in the northeast (IPAC, 2012). It is the floodplain of the Ganges. The little river and canal that ran through this island group split it into smaller islands. Soner char inhabits coastal plantation-type forests. The Soner Char wildlife reserve is located at latitude $21^{0}50'$-$26^{0}30'$ N and longitude $88^{0}47'$-$90^{0}10'$ E (IPAC 2012).

The mangrove plantation began at Soner Char in 1974-1975, covering 7270 hectares (Char Development and Settlement Project-4 2012). These locations support a considerable number of weed species. Initial plantings in the Soner char included *Sonneratia apetala* and *Avicennia officinalis.* Later, in 1995, the Bangladesh Forest Research Institute introduced several significant mangrove species as experimental bases, including *Heritiera fomes*, *Excoecaria agallocha*, *Xylocarpus molucencis* (Lam) M. Roem., *Xylocarpus granatum* J. Koenig., *Bruguira sexangula* (Lour.) Poir., *Aegiceras corniculatum*, *Ceriops decandra* (Griffith) Ding Hou., and *Phoenix paludosa*, *Lumnitzera racemosa* willd. (Islam *et al*., 2013). Additionally, certain mainland plants were introduced on an experimental basis on the raised ground of Soner Char Island, including *Thespesia populnea* (L.) Sol. Ex Correa. on small mounds, *Pithocellobium dulce* (Roxb.) Benth., *Samania Saman* (Jacq.) Merr., *Casuarina equisetifolia* L. *Acacia nilotica* (L.) Delile and *Albizia lebbeck* (L.) Benth. (Islam *et al.,* 2014). Most experiments were successful, and the current plantations' growth performance is impressive (Islam *et al*., 2013). Islam *et al*., (2015), conducted a partial investigation of this island and discovered the regeneration of *A. officinalis*, *H. fomes* (Sundri), *E.agallocha* (Gewa), *X. mekongensis* (Passur), *A. corniculatum* (Khalshi), *P. paludosa* (Hantal), *Tamarix indica* (Nona Jhao). There are restrictions on this island because it is a wildlife sanctuary, and grazing has not been allowed after December 2011. This one is safer from anthropogenic disruptions than other nearby or coastal islands. Generally speaking, this island is home to various wildlife species, including deer, monkeys, feral buffalo, wild boar, pigs, rats, snakes, and other creatures. Among the notable bird species are spines, cranes, wild geese, ducks, and jungle fowl.

Char Kashem: An adjoining island of Rangabali called Char Kashem is divided from the main island by the Buragauranga River. It is located at latitude $21^{0}52'$-$21^{0}54'18''$N and $90^{0}25'$-$90^{0}27'48''$E. The mangrove plantation at Char Kashem was created over roughly 10,000 hectares during the fiscal years 1973-1974. However, due to soil degradation, the current mangrove forest is only 4459.5 acres (Ahmed, 2019). This coastal habitat is not protected. Grazing is permitted for cattle, buffalo, and other animals. Grazing and soil erosion have seriously disrupted the Char Kashem coastal forest. Eighty-seven homesteads and 600 people live in Char Kashem, adjacent to a forest (BBS, 2011). These people rely entirely on the forest to supply their fuelwood needs. They depend on fishing, a small quantity of agriculture, and collecting fuel wood to survive. Initially, pioneer mangrove species were tried in these chars and other recently accreted chars in the coastal areas. In the 1990s, the Bangladesh Forest Research Institute planted some experimental plantations with notable mangrove and non-mangrove species like Soner

Char under the *S. apetala* forest. The cultivated species demonstrated Impressive growth rates (Islam *et al*., 2013; Islam *et al.*, 2014). *A. officinalis*, *H. fomes*, *E. agallocha*, *X. molucensis*, *P. paludosa*, *T. indica*, *D. spathacea* (pani kapila/gorshingra/vaterkathi), *P. pinnata*, and other kinds of herbs were identified to regenerate (Islam *et al.*, 2015). A few weeds flourish on each of these islands. As well as certain mammal species, including wild boar, monkey, and deer, this area is home to notable bird species like wild geese, wild ducks, jungle fowl, cranes, and spines.

Data collection: In the chosen Permanent Sample Plots (PSP) regions, the transect approach was used to determine the tree species currently serving as seed suppliers. When measured parallel to the water channel, the transect width was 3 meters, and its length was 200 meters. In each location, there were five transects. Data on only the tree species used as seed sources were collected from these transect lines to understand the diversity of mature tree species in the research sites. The Random Simple Selection Method was used to choose the Permanent Sample Plots (PSPs). Under artificial *S. apetala* plantations, PSPs were developed in both protected and unprotected areas. There were no other types of artificial plantations in the PSP areas. Each island had 12 PSPs created for 24 PSPs in protected and unprotected areas. The Permanent Sample Plots (PSPs) size was 10 meter×10 meter (100 m^2). The sample plots were chosen randomly from different age groups in both locations. The naturally existing information, such as seedlings noted (up to 0.5 height), saplings reported (0.51 m - 1.0 m height), poles noted (1.1 m - 3 m height), and trees documented (3 m above), was gathered for various tree species. Between January 2013 and December 2020, the survey was conducted in various PSP areas on the Soner Char and Char Kashem. From January 2013 through December 2020, data has been gathered once a year. Data on other types of plants, such as herbs and shrubs, was noted annually.

Data analysis: Data on various growth parameters and regeneration states were computed and examined using Excel and Minitab statistical software. T-tests were used to compare the protected and unprotected coastal forests regarding seedling, sapling, pole, new seedling recruitment, tree density, herb and shrub abundance, etc. The threshold for statistical significance was fixed at 0.05, and p-values below this threshold were regarded as significant.

Results and Discussion

Table 1 shows the presence of various plant species along the transect line. Thirty-six plant species were identified in January 2013 along the five transect lines of the Soner

Char protected forest, the sanctuary for wild animals. Thirty-six herb, shrub, and climber species and tree, palm, and rattan species were found in 2013 at Soner Char. Most of this island's tree and palm species were planted at various times. *D. spathacea*, *T. indica*, *S. caseolaris*, and other herbaceous, shrubby, climber, and rattan species were observed to be grown in natural conditions (Table 1).

Fifty-two species at Char Kashem's unprotected flora were documented simultaneously along the five transect lines. Most of the tree and palm species were planted, and the Char Kashem homesteads contained 15 cultivated species. Only three tree species—*Dolichandrone spathacea*, *Tamarix indica*, *Sonneratia caseolaris*, and all herbaceous shrub and climber species—were found in their natural habitat (Table 1).

Natural regeneration (seedling, sapling, pole) was recorded in the Soner Char protected areas in 2013, and these were 8 tree species, 2 palm species, and 8 species of herb and shrub. In the Char Kashem area, 9 tree species, 2 palm, and 7 herb and shrub species were identified at PSPs in 2013. In the PSP areas of Soner Char, 8 tree species, 2 palm species, 1 climber, and 7 species of herb shrub were found in 2020. In the case of Char Kashem, 9 trees, 1 palm, and 9 herbs and shrub regenerated species (seedling, sapling, and pole) were found in 2020 after eight years. Seven and nine species of herbs and shrubs were counted in PSP areas of Soner Char and Char Kashem in 2020 (Table 2). The naturally regenerating *Cynmetra ramiflora* and *Buruguiera sexangula* species were recorded in Char Kashem but not present on Soner Char in 2020. The natural regeneration of *Amoora cuculata* and *Calamus tenuis* was not present in Char Kashem in 2020, but they were found at Soner Char. On Soner Char island and Char Kashem, the largest total number of natural regeneration (seedlings, saplings, and poles) per hectare area was observed in 2013. Soner Char protected forest had higher seedlings (10644), saplings (4311), and poles (589) than that of Char Kashem unprotected forest (seedlings 7455, saplings 2778, and poles 522) in 2013. (Fig. 1).

However, there were no significant differences between Soner Char (protected area) and Char Kashem, 2013 (unprotected region) in terms of seedling ($p=0.92$), sapling ($p=0.91$), pole ($p=0.75$), or total regeneration number ($p=0.91$) (Fig. 1).

In 2016, after five years of declaration as a wildlife sanctuary, Soner Char registered more natural regeneration than Char Kashem (46722 nos, 33633 nos), seedlings (34067 nos, 26589 nos), and saplings (12144 nos, 6300 nos), respectively. In 2016, after four years, the establishment of PSP at Char Kashem (811) surpassed Soner Char (522) as the pole with the greatest number. However, there were no significant differences between

Table 1 The tree species, herbs, and shrubs that were present at Soner Char (a protected coastal forest) and Char Kashem (unprotected coastal forest) in 2013.

Sl. No	Name of Species	Vernacular Name	Family	Type of Plant	Forest type	Soner Char*	Char Kashem^{O}
1.	*Sonneratia apetala* Buch.-Ham.	Keora	Sonneratiaceae	Tree	Planted	+	+
2.	*Excoecaria agallocha* L.	Gewa	Euphorbiaceae	Tree	Planted	+	+
3.	*Avicennia officinalis* L.	Baen	Avicenniaceae	Tree	Planted	+	+
4.	*Heritiera fomes* Buch.-Ham.	Sundri	Sterculiaceae	Tree	Planted	+	+
5.	*Xylocarpus molucences* (Lam) M. Roem.,	Passur	Meliaceae	Tree	Planted	+	+
6.	*Aegiceras corniculatum* (L.) Blanco	Khalshi	Myrsinaceae	Tree	Planted	+	+
7.	*Phoenix paludosa* Roxb.	Hantal	Arecaceae	Palm	Planted	+	+
8.	*Cynometra ramiflora* L.	Shingra	Leguminosae	Tree	Planted	+	+
9.	*Xylocarpus granatum* J. Koenig.	Dhandul	Meliaceae	Tree	Planted	+	+
10.	*Cerops decandra* (Griffith) Ding. Hou.	Goran	Rhizophoraceae	Tree	Planted	+	+
11.	*Lumnitzera racemosa* willd	Kirpa	Combretaceae	Tree	Planted	+	+
12.	*Nypa fruticans* Van Wurmb.	Golpata	Arecaceae	Palm	Planted	+	+
13.	*Casuarina equisetifolia* L	Jhao	Casuarinaceae	Tree	Planted	+	+
14.	*Albizia lebbeck* (L.) Benth.	Kala koroi	Fabaceae	Tree	Planted	+	+
15.	*Albizia procera*(Roxb.) Benth.	Sada koroi	Fabaceae	Tree	Planted	+	+
16.	*Samanea saman Jacq.) Merr.*	Raintree	Fabaceae	Tree	Planted	+	+
17.	*Thespesia populnea* (L.) Sol. Ex Correa.	Sonboloi	Malvaceae	Tree	Planted	+	+
18.	*Calamus tenuis* Roxb.	Jalibet	Arecaceae	Climber	Natural	+	-
19.	*Dolichandrone spathacea* (L.F) Baill. Ex K. Schum	Panikapila/ Gorshinga	Bignoniaceae	Tree	Natural	+	+

*Protected, ^{O}Unprotected.

Contd.

Sl. No.	Name of Species	Vernacular name	Family	Type of plant	Forest type	Soner char	Char Kashem
20.	*Tamarix indica* Willd.	Nona Jhao	Tamaricaceae	Small tree	Natural	+	+
21.	*Sonneratia caseolaris* (L.) Engl.	Soyla	Sonneratiaceae	Tree	Natural	+	+
22.	*Pongamia pinnata* L.	Karanja	Leguminosae	Tree	Planted	+	+
23.	*Anodendron paniculatum* (Roxb.) A.Dc.	Bonjhul	Asclepiadaceae	Woody climber	Natural	+	+
24.	*Derris trifoliate* Lour	Kalialata	Fabaceae	Climber	Natural	+	+
25.	*Finlaysonia obovata* Wall.	Mamakola	Apocynaceae	Herb	Natural	+	+
26.	*Dalbergia spinosa* Roxb.	Tambulkata	Fabaceae	Armed shrub	Natural	+	+
27.	*Acanthus ilicifolius* L.	Hargoza	Acanthaceae	Thorny herbs ,woody	Natural	+	+
28.	*Sapium indicum* Willd.	Hurmuri	Euphorbiaceae	Herb	Natural	+	+
29.	*Ipomoea fistulosa* L.	DholKolmi	Convolvulaceae	Herb, woody	Natural	+	+
30.	*Mikania cordata*. (Burm.F.) B.L.Rob.	Germanlata	Asteraceae	Climber herb	Natural	+	+
31.	*Alternanthera philoxeroides* (Mart.) Griseb.	Helencha	Amaranthaceae	Herb	Natural	+	+
32.	*Crinum amoenum* Ker Gawl. Ex Roxb.	Bonroshun	Apocynaceae	Herb	Natural	+	+
33.	*Cynodon dactylon* (L.) Pers.	Durbaghash	Poaceae	Herb	Natural	+	+
34.	*Mucana monosperma* Roxb.ex Wigh.	Natai	Fabaceae	Woody climber	Natural	+	+
35.	*Vitis trifolia* L.	Amallata	Vitaceae	Climber	Natural	+	+
36.	*Salacia prinoides* L	Modhu phal	Celastraceae	Herb	Natural	+	+

Contd.

Sl No	Name of Species	Vernacular name	Family	Type of plant	Forest type	Soner Char*	Char Kashem^{O}
37.	*Bruguiera saxangula (Lour.) Poir*	Kankra	Rhizophoraceae	Tree	Planted	-	+
38.	*Phoenix sylvestris* (L.) Roxb.	Khejur	Arecaceae	Palm	Homesteads	-	+
39.	*Cocos nucifera* L.	Narikel	Arecaceae	Palm	Homesteads	-	+
40.	*Areca catechu* L.	Supari	Arecaceae	Palm	Homesteads	-	+
41.	*Borassus flabellifer* L.	Tal	Arecaceae	Palm	Homesteads	-	+
42.	*Mangifera indica* L.	Aam	Anacardiaceae	Tree	Homesteads	-	+
43.	*Diospyros blancoi* A.Dc.	Gab	Ebenaceae	Tree	Homesteads	-	+
44.	*Artocarpus heterophyllus* Lam.	Kanthal	Moraceae	Tree	Homesteads	-	+
45.	*Psidium guajava* L.	Payara	Myrtaceae	Tree	Homesteads	-	+
46.	*Citrus maxima* (Burm.) Merr.	Jambura	Rutaceae	Tree	Homesteads	-	+
47.	*Tamarindus indica*	Tentul	Fabaceae	Tree	Homesteads	-	+
48.	*Citrus limon* (L.) Burm	Lebu	Rutaceae	Tree	Homesteads	-	+
49.	*Zizypus mauritania* Lam.	Boroi	Rhamnaceae	Tree	Homesteads	-	+
50.	*Cryptocoryne retrospiralis* (Roxb.) Kunth.	Antispiral water Trumpet	Araceae	Herb	Natural	-	+
51.	*Colocasia esculenta* (L.) Schott.	Kala kochu	Araceae	Herb	Natural	-	+
52.	*Cyperus rotundus* L.	Muthagash	Cyperaceae	Herb	Natural	-	+
53.	*Eichhornia crassipes*(Mart.) Solms	Kochoripana	Pontederiaceae	Herb	Natural	-	+

*Protected, ^{O}Unprotected.

Table 2. Regeneration of several species (seedling, sapling, and pole) identified at Soner Char and Char Kashem at PSPs between 2013 and 2020.

Sl. No	Name of Species	Location and Data Collection Year			
		Soner Char		Char Kashem	
		January 2013	December 2020	January 2013	December 2020
1.	*Excoecaria agalocha*	+	+	+	+
2.	*Avicinnea officinalis*	+	+	+	+
3.	*Nypa fruticans*	+	+	+	-
4.	*Hibiscus teliacea*	+	+	+	+
5.	*Phoenix paludosa*	+	+	+	+
6.	*Herietiera fomes*	+	+	+	-
7.	*Aegeras corniculatum*	+	+	+	-
8.	*Xylocarpus molucensis*	+	-	+	+
9.	*Tamarix indica*	+	-	+	+
10.	*Buruguiera sexangula*	+	-	+	+
11.	*Dolichandrone spathacea*	+	+	+	+
12.	*Anodendron paniculatum*	+	+	+	+
13.	*Derris trifoliate*	+	+	+	+
14.	*Dalbergia spinosa*	+	+	+	+
15.	*Acanthus ilicifolius*	+	+	+	+
16.	*Ipomoea fistulosa*	+	+	+	+
17.	*Mikania cordata*	+	+	+	+
18.	*Mucana monosperma*	+	+	+	+
19.	*Aglaia cuculata*	-	+	-	-
20.	*Pongamia pinnata*	-	+	-	+
21.	*Calamus tenuis*	-	+	-	-
22.	*Cynometra ramiflora*	-	-	-	+
23.	*Salacia prinoides*	-	-	-	+
24.	*Colocasia esculenta*	-	-	-	+

(+ present, - absent)

Soner Char and Char Kashem in terms of recruitment of seedlings (p=0.35), saplings (p=0.25), poles (p=0.87), and overall numbers of regeneration (p=0.31) (Fig. 2). The total number of regeneration (seedling, sapling, and pole) per hectare area was highest after eight years in 2020, with a value of 24233 stems in the Soner Char protected area and 11558 in the Char Kashem unprotected regions (p=0.026). After eight years, Soner Char and Char Kashem had the highest number of seedlings per hectare (15283 and 6500, respectively; p=0.084). After eight years, Soner Char Wild Life Sanctuary discovered 5767 and 2833 stems of the sapling and pole value, respectively (Fig. 3).

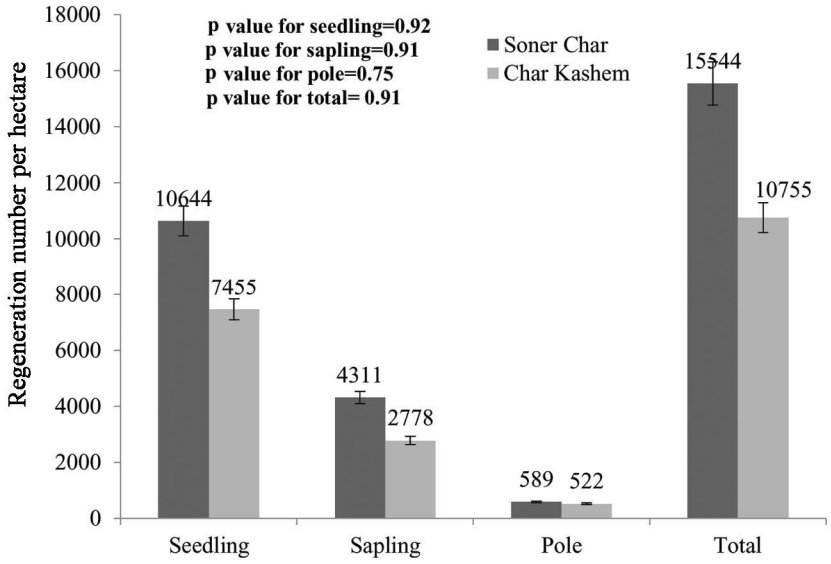

Fig. 1. Regeneration status of vegetation at protected forest (Soner Char) and unprotected forest (Char Kashem) in 2013 (at the initial stage of the wildlife sanctuary).

In Char Kashem's unprotected areas, after eight years, the numbers of sapling and pole stems were 3425 and 1633 per hectare, respectively. After eight years, the p values for the seedling, sapling, and pole were determined as (0.084), (0.030), and (0.030), respectively. After eight years, there was a noticeable difference between protected and unprotected forests in the overall number of regeneration, saplings, and pole stems. Conversely, there were no appreciable changes regarding seedling recruitment between protected and unprotected forests (Fig. 3).

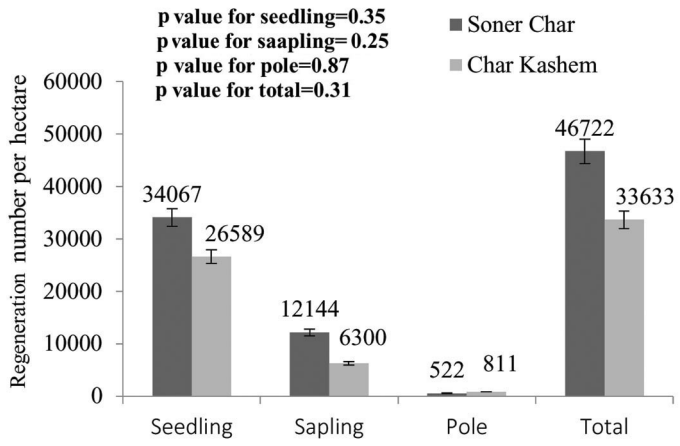

Fig. 2. Regeneration status of vegetation at wildlife sanctuary (Soner Char) and open forest (Char Kashem) in 2016 (after four years).

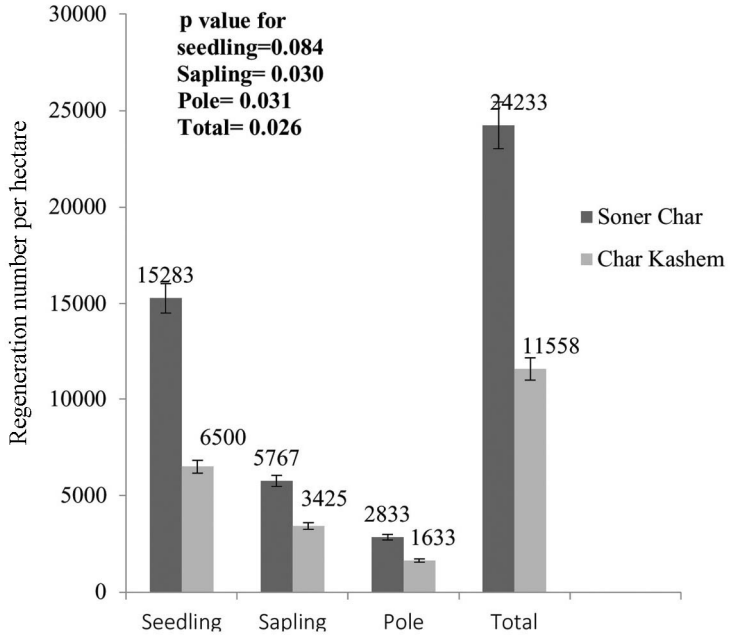

Fig. 3. Regeneration status of the vegetation at protected area (Soner Char) and unprotected area (Char Kashem) in 2020 (after eight years).

Between 2014 and 2017, the highest naturally occurring seedling recruitments were observed at Soner Char (a protected area) and Char Kahsem (an unprotected area) PSPs (36622 to 43439 seedlings per hectare) (Fig. 4).

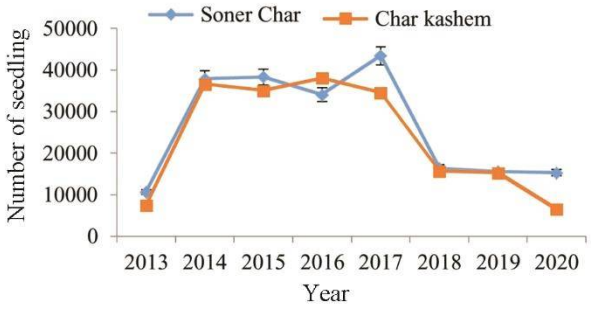

Fig. 4. Variations in recruitment of seedlings at Protected Forest (Soner Char) and Unprotected Forest (Char Kashem) in Selected PSP Areas from January 2013 to December 2020.

In protected regions, the greatest natural pole stems were seen between 2017 and 2020 with a value of 1132 to 2833/hectare, respectively, and in unprotected areas, the values were 930 to 1633/hectare, respectively (Fig. 5).

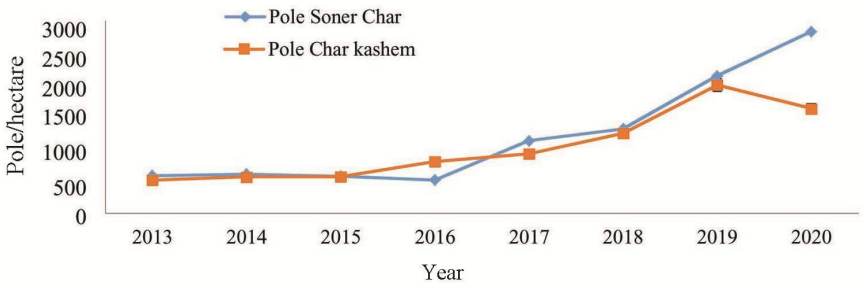

Fig. 5. Variations in the recruitment of pole stem at Protected Forest (Soner Char) and Unprotected Forest (Char Kashem) in Selected PSP Areas from January 2013 to December 2020.

After eight years of the proclamation of a wildlife sanctuary, Soner Char had the largest number of trees per hectare (2250). At the same time, Char Kashem had the lowest number of trees per hectare (1567). In the initial stages of the wildlife sanctuary, 355 trees per hectare at Soner Char and 811 trees per hectare at Char Kashem were observed in the PSPs area in January 2013. After four years, the protected and unprotected sites

had tree densities of 833 trees per hectare and 711 trees per hectare, respectively (Fig. 6). Calculated were the p values for tree density in 2013 (0.068), 2016 (0.44), and 2020 (0.013). After eight years, the forest cover per hectare (2250) in protected locations varies markedly from unprotected forests (1567). However, there were no apparent variations in the tree density between these two locations between 2013 and 2016 (Fig. 6).

In PSP areas in Soner Char, 27411, 12878, and 7677 herb, shrub, and climber stems per hectare were counted in 2016, 2020, and 2013, respectively. Conversely, Char Kahsem was the site where the greatest variety of herb, shrub, and climber species was identified, with 8678 stems in 2016, 8577 stems in 2020, and 5233 stems in 2013, respectively.

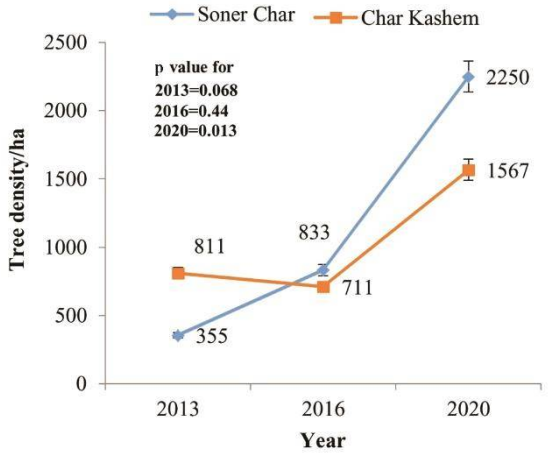

Fig. 6. Variations in tree density per hectare stems of Soner Char and Char Kashem between 2013 and 2020 of the PSP areas.

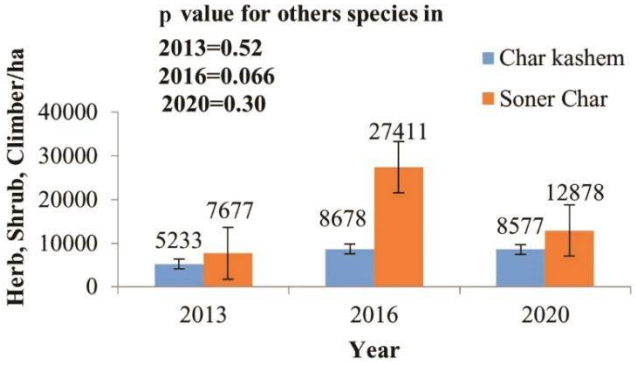

Fig. 7. State of the vegetation for various herb, shrub, and climber species in protected and unprotected PSP regions in 2013, 2016, and 2020.

The number of herb, shrub, and climber species between Soner Char and Char Kashem PSPs regions stayed the same in 2013, 2016, and 2020. (Fig. 7). *E. agallocha* made up 80.43% of the total number of seedling recruitments, followed by *A.officinalis* (10.45 %), *T.x indica* (2.48%), and eight other species, including *N. fruticans*, *H. teliacea*, *P. paludosa*, *H. fomes*, *A. corniculatum*, *X. molucensis*, *D. spathacea*, and *B. sexangula* (6.59%) were found in 2013 at Soner Char wildlife protected areas (Fig. 8).

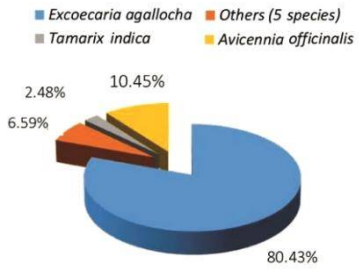

Fig. 8. Seedling recruitment of different species at the protected area (Soner Char) in 2013.

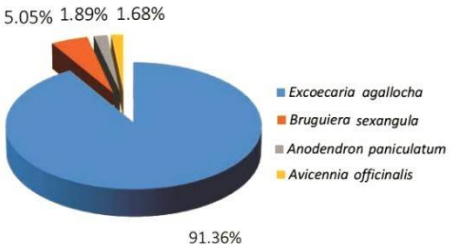

Fig. 9. Seedling recruitment of different species at the unprotected area (Char Kashem) in 2013.

Excoecaria agallocha made up 91.36% of the Char Kashem (unprotected forest) in 2013, followed by *Bruguiera sexangula* (5.05%), *Dolichandrone spathacea* (1.89%), and *Avicennia officinalis* (1.68%) (Fig. 9).

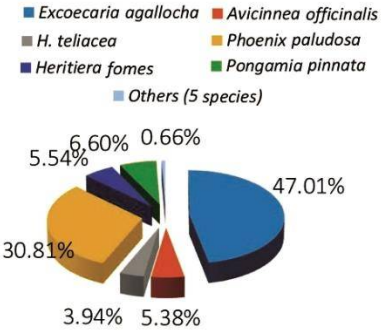

Fig. 10. Seedling recruitment of different tree species in 2020 at Soner Char.

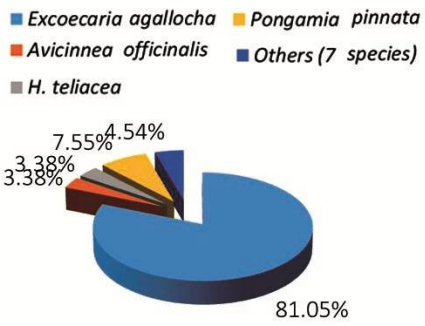

Fig. 11. Seedling recruitment of different tree species in 2020 at Char Kashem.

E. agallocha makes up 47.01% of all seedling recruitment at Soner Char Wild Life Sanctuary in 2020 PSPs, followed by *P. paludosa* (30.81%), *P. pinnata* (6.6%), *H. fomes* (5.5%), *A. officinalis* (5.3%), *H. teliacea* (3.94 %), and other 5 species (0.6%) (Fig. 10).

In 2020, *E. agallocha* accounts for 81.05% of seedling recruitment in Char Kashem unprotected areas, followed by *P. pinnata* (7.55%), *A. officinalis* (3.38%), *H. teliacea* (3.38%), and other 7 species (4.54%) (Fig. 11).

When Soner Char was first declared a wildlife sanctuary, *S. apetala* comprised 66.67% of the trees there, while *E. agallocha* made up 33.33%. At the same time, Char Kashem had 62.50% *E. agallocha* species and 37.50% *S. apetala* species (Fig. 12 and Fig. 13).

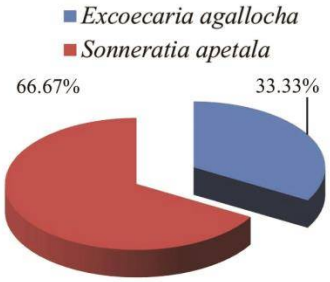

Fig. 12. Tree density of different species at Soner Char in 2013.

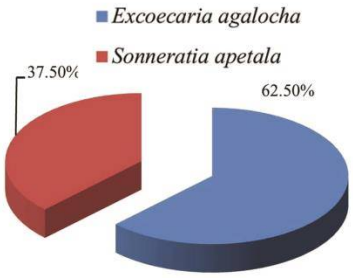

Fig. 13. Tree density of different species at Char Kashem in 2013.

Fig. 14. Tree density of different species at Soner Char in 2020.

Fig. 15. Tree density of different species at Char Kashem in 2020.

In 2020 at the PSP areas, *E. agallocha* made up 69.11% of the total tree vegetation of Soner Char Wild Life Sanctuary (a protected area), followed by *Sonneratia apetala* (23.03%), *Phoenix paludosa* (8.82%), *Heritiera fomes* (3.43%), *Dolichandrone spathacea* (0.98%), and *Avicennia officinalis* (0.49%). *E. agallocha* comprised 85.79% of the species documented at Char Kashem in the unprotected region, followed by

Sonneratia apetala (13.60%) and *Dolichandrone spathacea* (0.61%) in 2020. (Fig. 14 and Fig. 15).

The current study examined the human-developed forests in Bangladesh's coastal regions and changes in species composition over 8 years. Individual tree seedling, sapling, pole, naturally regenerated tree, herb, and shrub species distributions were described in coastal areas and contrasted with protected and unprotected forests. In this study, we observed that 10 different mangrove species could naturally regenerate in the Soner Char Wildlife Sanctuary and Char Kashem in 2020, respectively. In the coastal regions of Chattogram, Bhola, and Patuakhali Coastal Afforestation Division, Siddiqi *et al*. (1995) undertook a visual observation between 1985 and 1994, but they did not find any naturally occurring regeneration. Islam *et al*. (2014) found six natural regeneration species on Rangabali Island in seven separate islands. Additionally, the locations where the current study showed 46722 stems/ha of natural regeneration (seedling, sapling, and pole) in the Soner Char protected PSP area and 33633 stems/ha at Char Kashem in 2016, and each had the greatest seedling density of 36,000 stems per hectare. After eight years, Soner Char Wild Life Sanctuary PSPs and Char Kashem Unprotected Forest PSPs were found to have distinct total natural regeneration (stems, saplings, and poles) per hectare ($p=0.026$, Fig. 3). The graph of natural seedling recruitment from 2013 to 2020 showed that Soner Char Wild Life Sanctuary had the maximum number of seedlings from 2014 to 2017; that number substantially decreased in 2018 and was found there again in 2019 and 2020. Like Soner Char island, unprotected sites in Char Kashem displayed the largest seedling recruitment between 2014 and 2017. However, seedling recruitment in Char Kashem significantly fell in 2018 and declined through the end of 2020. This can result from grazing activity and human involvement (Fig. 4). In Char Kashem, the eye observation revealed that numerous significant tree species were illegal between 2018 and 2020. From 2013 to 2016, the pole stems regeneration recruitment pattern remained unchanged; from 2016 to 2020, it grew. The graph showed that protected regions had more pole stems per hectare. Between 2013 and 2019, pole recruitment increased at the unprotected Char Kashem site, but it decreased significantly in 2020 (Fig. 5). At the Char Kukri-Mukri islands, Siddiqi and Khan (2004) noted spontaneously growing seedlings of *S. apetala* and *S. caseolaris*. Additionally, they claimed that these species' seedlings, particularly *S. apetala*, rarely mature into saplings. Grazing was recognized as one factor contributing to this species extinction. The Char Kashem unprotected PSP area and the Soner Char wildlife sanctuary could increase the number of trees per hectare from 2013 to 2020.

When investigations began at Soner Char protected areas, *E. agallocha* seedlings were found in the greatest numbers, followed by *A. officinalis* in tenths of a percentage. According to the most recent findings, *E. agallocha*, *P. paludosa*, *P. pinnata*, *H. fomes*, and the other seven species had higher seedling recruitment rates in 2020 than the other species combined. The Soner Char Wildlife Sanctuary exhibited the recruitment of multiple species of seedlings. At Soner Char Wild Life Sanctuary, more *E. agallocha* seedlings are being recruited than in the first half of 2013. This pattern suggests that the Soner Char Wildlife Sanctuary will be converted into a forest with diverse species. Because of the established seed sources and untouched environment in the PSPs area of Soner Char, certain key species were found to regenerate there (Fig. 8 and Fig. 10). In the current research, due to observed tree vegetation and seedling recruitment during the most recent observation in Soner Char Wild Life Sanctuary, the species *E. agallocha* has been classified as a climax species and next *P. paludosa.* Only four distinct seedling recruitment patterns were observed in the Char Kashem PSP zones in 2013. Of these species, *Excoecaria agallocha* exhibited the highest recruitment (91.36%), followed by the other three species (Fig. 9 and Fig. 11). *Excoecaria agallocha* seedlings made up the majority (81.05%) of the PSPs in 2020, eight years after they were created, with the remaining *A. officinalis*, *Hibiscus teliacea*, *Phoenix paludosa*, *Herietiera fomes*, *Aegeras corniculatum*, *Aglaia cuculata*, *Pongamia pinnata*, *Dolichandrone spathacea* and *Calamus tenuis* species. In the seven chars of Rangabali, 95.41% of *E. agallocha* seedlings were documented by Islam *et al.* (2014), confirmed by the study's 2013 findings (Fig. 9 and Fig. 11). Buffalo and cattle commonly graze in the vast plains of Char Kashem. Grazing has recently reached an alarming level at Char Kashem. In the 2020 trial, *S. apetala* was found to be replaced by *E. agallocha* in both protected and unprotected regions. The current study found that between 2013 and 2020, the tree stems density of *S. apetala* decreased by 43.64% at Soner Char Wild Life Sanctuary and 23.90% at Char Kashem Unprotected PSPs, respectively. Whereas the tree stems density of *E. agallocha* increased by 35.78% and 23.29% between 2013 and 2020 in Soner Char and Char Kashem (Figs. 12, 13, 14, 15). After eight years, *E. agallocha* was shown to be the most abundant tree species in both research areas.

Additionally, under the current ecological conditions at these two trial locations, *S. apetala* will decline and may become a minor species. According to Das and Siddiqi (1985), *S. apetala* comes after *E. agallocha* in the ecological succession. Our investigation showed that *E. agallocha* had replaced *S. apetala* in both places. However, we also noticed that *P. paludosa, H. fomes,* and *D. spathacea* had done so at Soner Char Wild Life Sanctuary. The tree stems of *E. agallocha*, *P. paludoa*, *H. fomes*, *A. officinalis*,

and *D. spathacea* were spontaneously grown in the PSPs of Soner Char Wild Life Sanctuary rather than planted. Unfortunately, at Char Kashem, only two species of stems were identified as growing naturally simultaneously as Soner Char. In the current investigation of 2020, the principal tree stems of *E. agallocha*, *P. paludosa*, and *H. fomes* were recorded at Soner Char. After eight years, Soner Char Wild Life Sanctuary had greater tree stem counts per hectare than the Char Kashem PSPs area. According to the current research, Soner Char Wild Life Sanctuary will be converted into a mixed-species forest owing to natural disturbances. Grazing for the relocated mixed forest also impacted the Char Kashem areas.

Figs 16-19: (16). Transect line established in January 2013 at Soner Char. (17). Permanent sample plot no. 1 at Soner Char established in January 2013. (18). Regeneration plot at Char Kashem PSP areas (Photo: 2017). (19). Regenerated tree species of *D. sparthacea* and *P. paludosa* at Soner Char protected areas (December 2020).

Because seedling recruitment was essentially the same in forests with and without protection, after eight years, however, Soner Char Wild Life Sanctuary had more saplings and pole stems than Char Kashem. This finding shows that interference from humans,

livestock, and buffalo in Char Kashem areas affected the results. The current study states that Char Kashem will find it more difficult to convert from a mono-specific to a mixed-species forest due to human engagement and grazing influence. It should be mentioned that the Bangladesh Forest Research Institute (BFRI) underplanted trials in the two research regions. This has led to the seed sources of many mangrove species in this region.

The *S. apetala* plantations had been growing for around 46 years, and the trees in both study sites were already mature. The *S. apetala* species over-matured, and successional alterations occurred due to the geomorphological changes and absence of inundation in the planted regions. It is now important to develop various species of seed sources in the many chars beneath the *S. apetala* forest to retain the natural regeneration inside the coastal man-made forest. According to the current observation, grazing impacts natural regeneration in unprotected places. Eight years later, protected areas are densely covered in plants and have a diverse forest floor. Plans for the protected area include creating a mixed-species forest. To improve a dense, long-lasting mangrove forest, conserving more coastal forests that are not already protected is especially important. The main environmental governing aspects of these two locations are climate (rainfall, temperature, humidity, evaporation, wind, and cyclones), hydrological (tidal activities), edaphic (soil salinity, nutrient status, and accretion), and biotic. These components engage in mutual interaction and have an impact on ecosystem development. This study only focused on the vegetation's condition and the species' dynamics affected by grazing, leaving out the soil salinity, organic carbon levels, and other edaphic parameters in these two locations.

References

Ahmed, H. 2019. Bangladesh coastal zone management status and future trends. *J. Coast Zone Manag*. **22**(1): 466.

Ahammad, R. and P. Nandy, 2012. Navigating mangrove resilience through the ecosystem-based adaptation approach: lessons from Bangladesh. In: Sharing Lessons on Mangrove Restoration, D.J. Macintosh, R. Mahindapala, M. Markopoulos (eds.), Bangkok, Thailand: Mangroves for the Future and Gland, Switzerland: IUCN. pp. 243-254.

Ahsan, M.E. 2013. Coastal zone of Bangladesh. fisheries resources and potentials. Lap Lambert Academic Publishing, Germany. pp 1-70.

Alongi, D.M. 2012. Carbon sequestration in mangrove forests, a review. *Carbon Manag*. **3**(3): 313-322.

BBS (Bangladesh Bureau of Statistics), 2011. Bangladesh Population and Housing Census (Community Report), Patuakhali, July 2013. Ministry of Planning, Government of the People's Republic of Bangladesh.

BFD. 2020. *"Vulture Safe Zone"*, bforest.gov.bd., retrieved: 10 June 2020.

BFD and UNDP. 2018. Co-management and benefit-sharing from coastal afforestation. Integrating Community-based Adaptation into Afforestation and Reforestation (ICBA-AR) Programme in Bangladesh. Dhaka: Bangladesh Forest Department, Ministry of Environment, Forest and Climate Change and UNDP Bangladesh. pp.1-43.

Char Development and Settlement Project-4. 2012 Char development and Settlement Project Phase IV Bangladesh. Short listing of Char Areas for Feasibility Studies under CDSP IV, Technical Report no-4, pp.1-80.

Chowdhury, M. S. H. and M. Koike. 2010. An overview of the protected area system for forest conservation in Bangladesh. *J. For. Res.* **21**(1): 111-118.

Das, S. and N.A. Siddiqi. 1985. The mangroves and mangrove forests of Bangladesh. Mangrove Silviculculture Division. Bulletin No. 2. Bangladesh Forest Research Institute. pp.142.

District Statistics, Patuakhali. 2011. (Published in December, 2013) Bangladesh Bureau of Statistics (BBS), Statistics and Informatics Division, Ministry of Planning, Government of the People's Republic of Bangladesh. pp. 115.

DoE. 2015. Fifth National Report of Bangladesh to the Convention on Biological Diversity. Dhaka: Department of Environment (DoE), Ministry of Environment and Forests, Government of the People's Republic of Bangladesh.pp.1-147.

Faruque, M.O., M.A. Hasnath and N.N. Siddique. 1990. Present status of buffalos and their productivity in Bangladesh. *Asian-Austr. J. Anim. Sci.* **3**(4): 287-292.

FAO. 1988. Land Resource Appraisal of Bangladesh for Agricultural Development UNDP/FAO Project BGD/81/035. Technical Report -2. UNDP/FAO, Rome. pp. 582.

Hasan D.Z 2013. Plants in mangroves and coastal afforestation in Bangladesh. Dewan House, Ukilpara, Naogaon-6500, Bangladesh. p. 164.

Huque, Q.M.E. and A. Borghese. 2013. Status and perspectives of Buffalo in Bangladesh. *Buffalo Bull.* **32**(2): 1179-1183.

Iftekhar, M. S. and M. R. Islam. 2004. Managing mangroves in Bangladesh: A strategy analysis. *J. Coast. Conser*. **10**(1): 139-146.

IPAC, 2012. Integrated protected area co-management (IPAC). State of Bangladesh Forest Protected Areas, 2010. USAID contract N^0 EPP-1-00-06-00007-00, Task order no: EPP-1-01-06-00007-00, February 28, 2012, pp 1-90.

Islam, S. A., M. A. Q. Miah, M. A. Habib, M. G. Moula and M. G. Rasul, 2013. Growth performance of underplanted mangrove species in *Sonneratia apetala* (Keora) plantations along the western coastal belt of Bangladesh. *Bangladesh J. For. Sci.* **32**(2): 26-35.

Islam, S.A., M.A.Q. Miah, M.A. Habib and M.G. Moula, 2014. Performance of some mainland trees and palm species planted in the coastal islands of Bangladesh. *J. Asiat. Soc. Bangladesh, Sci*. **40**(1): 9-15.

Islam, S. A., M. A. Q. Miah, M. A. Habib and M.G. Rasul, 2015. Regeneration diversity of mangrove species inside *Sonneratia apetala* plantations along the coastal belt of Bangladesh. *J. Biosci. Agricul. Res.* **5**(02): 80-87.

Islam, M.S. and M.A. Wahab, 2005. A review on the present status and management of mangrove wetland habitat resources in Bangladesh with emphasis on mangrove fisheries and aquaculture. *Hydrobiol*. **542**: 165-190.

Krauss, K. W., K. L. McKee, C. E. Lovelock, D. R. Cahoon, N. Saintilan, R. Reef and L. Chen, 2014. How mangrove forests adjust to rising sea level. *New Phytol*. **202**: 19-34.

Lee, S. Y., J. H. Primavera, F. Dahdouh-Guebas, K. McKee, J. O. Bosire, S. Cannicci and S. Record, 2014. Ecological role and services of tropical mangrove ecosystems: A reassessment. *Global Ecol. Biogeogr.* **23**: 726-743.

Miah, M.A.Q., S.A. Islam, M.A. Habib and M.G. Moula, 2014. Growth performance of *Avicennia officinalis* L. and the effect of spacing on growth and yield of trees planted in the western coastal belt of Bangladesh. *J. For. Res.* **25**(4): 835-838.

Mukul, S.A. 2007. Biodiversity conservation strategies in Bangladesh: The state of protected areas. *Tigerpaper*. **34**(3): 28-32.

Mukul, S.A., A. Z. M. M. Rashid and N. A. Khan. 2016. Forest protected area systems and biodiversity conservation in Bangladesh. Preprints (www.preprints.org), pp. 1-16.

Rahman, M.M. and A.T. Pramanik. 2015. Monitoring mangrove plantation along the coastal belts of Bangladesh (1989-2010). *J. For. Environ. Sci.* **31**(3): 225-234.

Rahman, M.A, M.A. Alim, M.K. Hossain and M.A. Hossain. 2019. Prospect of natural regeneration of tree species in Hazarikhil Wildlife Sanctuary of Chittogram, Bangladesh. *J. Biodivers. Conserv. Bioresour. Manag.* **5**(2): 1-12.

Saintilan, N., N. Wilson, K. Rogers, A. Rajkaran and K.W. Krauss. 2014. Mangrove expansion and salt marsh decline at mangrove poleward limits. *Glob. Chan. Biol.* **20**: 147-157.

Siddiqi, N.A., M.J. Alam and M.A. Habib. 1995. Natural Regeneration of Mangroves in the Coastal areas of Bangladesh with particular reference to Noakhali. *Bangladesh J. For. Sci.* **24**(1): 62-69.

Siddiqi, N.A. and M.A.S. Khan. 2004. Human –induced succession of vegetation on new accretions in the coastal areas of Bangladesh. *J. Trop. For. Sci.* **16**(2): 187-198.

SRDI. 2010. Saline soils of Bangladesh. Soil Resource Development Institute (SRDI), Government of the People's Republic of Bangladesh. pp. 43-60.

Uddin, M.M, M.S. Rahman, M.K. Hossain and S. Akhter. 2014. Growth density and regeneration of afforested mangroves of Mireresarai forest range in Bangladesh. *For. Sci. Technol.* **10**(3): 120-124.

Wang, H., G. Li, D. Yu, and Y. Chan. 2008. Barrier effect of litter layer on natural regeneration of forests: A review. *Chinese J. Ecol*. **27**: 83-88.

(Revised copy received on 26.09.2023)

J. Asiat. Soc. Bangladesh, Sci. **49**(2): 225-235, December 2023 DOI: https://doi.org/10.3329/jasbs.v49i2.70770

EFFECTIVENESS OF DIFFERENT TREATMENTS ON THE INCIDENCE AND DAMAGE OF FLEA BEETLE (*PHYLLOTRETA NIGRIPES*) AND THRIPS (*MEGALUROTHRIPS USITATUS*) ON MUNGBEAN

MOHAMMAD HABIB ULLAH[1] AND MD. MOHASIN HUSSAIN KHAN[2*]
[1]Research Officer (Agriculture), Bangladesh Water Development Board, Dhaka, Bangladesh.
[2]Department of Entomology, Patuakhali Science and Technology University, Patuakhali, Bangladesh.

Abstract

An experiment was conducted to evaluate the effectiveness of different treatments for the management of flea beetles and thrips of mungbean using BARI Mung-6 as experimental material. Nine treatments, viz., T_1 = Use of White sticky trap, T_2= Bioneem plus (Azadirachtin) 1%EC @ 1 ml/L of water at 40 DAS, T_3 = Virtako (Chlorantraniliprole + Thiamethoxam) 40 WG @ 0.15g/L of water at 40 DAS, T_4 = Amithrin plus 3% WDG @ 1 ml/L of water at 40 DAS, T_5 = Ecomec (Abamectin) 1.8 EC @ 1 ml/L of water at 40 DAS, T_6 = Nitro (Chlorpyriphos + Cypermethrin) 505 EC @ 1 ml/l of water at 40 DAS, T_7 = Raise (Chlorantraniliprole) 20 SL @ 3 ml/L of water at 40 DAS and T_8 = control were applied. Data were recorded on the number of flea beetles per plant, leaf area damaged by flea beetles, number of thrips-infested flowers per plant, and number of thrips per 20 opened flowers. Results revealed that the lowest number of flea beetles (3.00/m^2 plants) and the highest percent reduction (64.71%) of flea beetle population over control were recorded in Virtako 80 WG at 0.15 g/L of water-treated plots. The lowest percent damage (3.75%) of leaf area and the highest percent reduction (79.73%) of leaf area damage over control were observed in Virtako-treated plots. The lowest number of thrips population (1.50/20 flowers), the highest percent of thrips population reduction (85.37%) over control, the lowest number of infested flowers (0.88/20 flowers) by thrips, and the highest percent reduction (88.65%) of flower infestation over control were found in mungbean plants treated with Raise 20 SL @ 3 ml/L of water. A strong negative correlation between the number of flea beetles and total yield was observed. There were negative relationships between the number of thrips, percent flower infestation, and total yield. Therefore, the application of Virtako 80 WG at 0.15 g/L and Raise (Chlorantraniliprole) 20 SL at 3 ml/L were found to be the best treatments for controlling flea beetles and thrips on mungbean.

Keywords: Insecticide, Pulse, Control, Yield.

Introduction

Mungbean (*Vigna radiata* L.) is also known as "Greengram," which belongs to the family Leguminosae. India, China, Philippines, Burma, Bangladesh, and Pakistan are the major

* Corresponding author: mohasin1965@pstu.ac.bd

mungbean-growing countries in the world. In Bangladesh, mungbeans occupy an area of 46,117.06 hectares and produce 41,548.48 tons (BBS, 2023). Despite having a very low yield (900.93 kg/ha) per unit area, it is recognized as a quality pulse in the country compared to many other countries around the globe (BBS, 2023). It also plays a significant role in supplementing protein for the Bangladeshi people who consume cereal-based low protein.

Mungbean is infested by whiteflies (*Bemisia tabaci*), thrips (*Megalurothrips usitatus*), jassids (*Amrasca biguttula*), stem fly (*Ophiomyia* sp.), epilachna beetle (*Epilachna dodecastigma*), galerucid beetle (*Madurasia obscurella* Jacoby), blister beetle (*Mylabris pustulata* Thunberg), pod sucking bug (*Riptortus dentipes*), tobacco caterpillar (*Spodoptera litura*), and spotted pod borer (*Maruca vitrata*) throughout the year and have significant effects on yield (Kooner *et al.*, 2006; Lal, 1985). The incidence of insect pests considerably reduces the yield and quality of mungbean (Malik, 1994; Elias *et al.*, 1986). The prevailing weather conditions, such as temperature, relative humidity, and precipitation, affect the incidence and development of all insect pests (Aheer *et al.*, 1994; Yadav and Singh, 2013; Yadav *et al*., 2015).

Among different insect pests, flea beetles and thrips are the most damaging insects of mungbean. Flea beetles (*Phyllotreta nigripes*) attack cotyledons and leaves of seedlings and young plants and feed on them by making innumerable round holes. The percentage of leaf area damaged by flea beetle on BARI Mung-6 is 11.33% (Islam *et al.*, 2021). Older infested leaves dry up, hampering the plant's growth having reduced number of pods (Hossain, 2015). On the other hand, thrips (*Megalurothrips distalis* Karny, *Megalurothrips usitatus* Bangall, and *Caliothrips indicus* Bangall) cause damage mainly on young buds and flowers of mungbean (Lal, 1985). Extensive flower damage of mungbean by thrips resulted in flower shedding, causing significant yield loss (Lal 1985; Chhabra and Kooner, 1985). *Megalurothrips usitatus* causes mung bean production losses ranging from 13% to 64% (Farajallah, 2013).

Several investigators (Litsinger *et al.*, 1988; Singh and Singh, 1977; Hossain, 2015; Alam *et al.*, 2021) studied insect control by chemical insecticides against mungbean pests. Ahmad *et al.* (1998) found that the application of dimethoate (0.03%) or monocrotophos (0.04%) at 45 and 60 days after sowing effectively reduced the insect pest complex of mungbean. Amongst management practices, Admire 200SL (Imidacloprid) @ 0.25 ml/L of water was more effective for the management of whiteflies and thrips in mungbean, followed by Voliam Flexi (Thiamethoxam + Chlorantraniliprole) @ 0.25 ml/L of water

(Alam *et al.*, 2021). Considering the above facts, the experiment was carried out to determine the most effective treatment against flea beetles and thrips on mungbean.

Material and Methods

An experiment was carried out in the farmers' field at Sonakhali village, Barguna Sadar, Barguna district of Bangladesh, from January to April 2017. The experiment was laid out in a randomized, complete design with 3 replications. The entire field was divided into 3 blocks representing replications, and each block was divided into 9 plots. This experiment used 27 plots, and the individual plot size was 3.0 m × 2.0 m. The spacing between plots was 0.75 m, and between blocks was 1 m. Treatments were randomly assigned to each plot within a block. Variety BARI Mung-6 was utilized in this experiment. Seeds were sown continuously in the line at a depth of 4-5 cm on the 1st of February, 2017, at the rate of 20 kg/ha, and covered by loose soil with the help of hand. The row-to-row distance was 15 cm, and the plant-to-plant was 10 cm. Nine treatments viz., T_1 = Use of White sticky trap, T_2= Bioneem plus (Azadirachtin) 1% EC @ 1ml/L of water at 40 DAS, T_3 = Virtako (Chlorantraniliprole + Thiamethoxam) 40 WG @ 0.15g/L of water at 40 DAS, T_4 = Amithrin plus 3% WDG @ 1 ml/l of water at 40 DAS, T_5 = Ecomec (Abamectin) 1.8 EC @ 1 ml/L of water at 40 DAS, T_6 = Nitro (Chlorpyriphos + Cypermethrin) 505 EC @ 1 ml/L of water at 40 DAS, T_7 = Raise (Chlorantraniliprole) 20 SL @ 3 ml/L of water at 40 DAS and T_8 = control were applied. Insecticides were purchased from the Biotech division of Ispahani Agro Limited and the local market. Spray solutions were prepared in the Knapsack sprayer by mixing insecticides with water as recommended, with a pre-fixed concentration of the respective treatments, as required, just before spraying. The spray solution prepared in such a way was sprayed in the assigned plot designed for each treatment. Spraying was done in the afternoon to avoid bright sunlight and to escape pollinators. The precaution was taken to prevent the drift of spray solution to adjacent plots at the time of spray. All sorts of intercultural activities were performed as and when required to ensure the growth and development of the plant.

Data were collected and recorded at ten-day intervals and different growth stages by direct counting early in the afternoon (4.0 - 6.0 pm). Meter square (1 m × 1 m) plants were selected randomly from each plot. The number of flea beetle data was counted by visual eye from each plot's infested and healthy leaves/plants per square meter plants. The flea beetle population was once recorded at the vegetative stage (36 DAS). The leaf area of 5 representative leaves from 5 randomly selected plants of each unit plot was recorded on a leaf area meter (Model LI-3100C), and the mean leaf area was computed.

The percentage of damaged leaves area/plants by flea beetles was determined by eye estimation.

Data on thrips were collected once (at 100% flowering stage) from the flowering stage of mungbean. For assessing the thrips population, twenty opened flowers were randomly collected from two rows on each side of the plot, avoiding border rows and the selected 1 m^2 area of the center of each unit plot. The collected flowers were opened immediately on the white paper and counted thrips. The area of one square meter in the center of each unit plot was kept undisturbed for recording yield data.

Data on total flowers and number of damaged flowers were recorded from 10 randomly selected infested inflorescences of each plot. Then, the percentage of flower infestation by thrips was calculated using the following formula:

$$\% \text{ Flower infestation} = \frac{\text{Total number of infested flowers}}{\text{Total number of flowers}}$$

Statistical Analysis: Data were analyzed using WASP 1.0 (Web-based Agricultural Statistical Package) software following RCB design. Graphical presentation and correlation studies were performed through the Excel program.

Results and Discussion

Effectiveness of different treatments on the population of flea beetles: The effects of different treatments on the incidence of flea beetles and their damage are presented in Table 1. The flea beetle population varied significantly, ranging from 3.0 to 8.50. The square meter of plants with the lowest mean number of flea beetles (3.00/plot) was observed in Virtako 40 WG treated plots followed by Nitro 505 EC (3.75/plot), Raise 20 SL (4.25/plot), Ecomec (5.0/plot), White sticky trap (5.25/plot), Bioneem plus (5.75/plot) and Amithrin plus 3% WDG (6.0/plot). The average flea beetle was recorded maximum in control plots (8.50/plot), which differed statistically from the remaining treatments. The highest percent reduction (64.71%) of flea beetle population was found in Virtako 40 WG treated plots over control, followed by Nitro 505 EC (55.88%) and Raise 20 SL (50.0%), Ecomec (41.18%). The lowest percentage was found in Amithrin plus 3% WDG (29.41%), followed by Bioneem plus (32.25%) and White sticky trap (38.25%).

Again, the damaged leaf area by flea beetles varied significantly, ranging from 3.75 to 18.50%. The lowest percent damaged leaf area (3.75%) was observed in Virtako 40 WG treated plots, followed by Nitro 505 EC (6.0%), Raise 20 SL (7.25%), Amithrin plus 3% WDG (9.50%), Ecomec (10.75%), Bioneem plus (11.50%) and White sticky trap (13.0). The significantly highest mean leaf area damage was recorded in control plots (18.50%), statistically different from other treatments. The highest percent reduction (79.73%) of damaged leaf area was found in Virtako 40 WG treated plots over control, followed by Nitro 505 EC (67.57%), Raise 20 SL (60.81%), Amithrin plus 3% WDG (48.65%). Bioneem plus (41.91%), Ecomec (37.83%). The lowest leaf area damage reduction was found in the White sticky trap (29.72%).

Table 1. Effectiveness of treatments on the incidence of flea beetle on mungbean

Treatments	Mean number of flea beetle/plot	Reduction of flea beetle over control (%)	Leaf area damaged by flea beetle (%)	Reduction of leaf area damaged over control (%)
White sticky trap	5.25 cd	38.25	13.00 c	29.72
Bioneem plus 1% EC @ 1 ml/L of water	5.75 bc	32.35	10.75 d	41.91
Virtako 40 WG @ 0.15 g/L of water	3.00 h	64.71	3.75 h	79.73
Amithrin plus 3% WDG @ 1 ml/L of water	6.00 b	29.41	9.50 bc	48.65
Ecomec @1 ml/L of water	5.00 de	41.18	11.50 cd	37.83
Nitro 505 EC @ 1 ml/ L of water	3.75 g	55.88	6.00 g	67.57
Raise 20 SL @ 3 ml/L of water	4.25 fg	38.24	7.25 ef	60.81
Untreated control	8.50 a	-	18.50 a	-
Level of significance	**	-	**	-
CV (%)	8.43	-	14.81	-

**Significant at 1% level

Means that a column followed by the same letter does not differ significantly from one another by CD values. Values are an average of 3 replications.

Effectiveness of different treatments on the incidence of thrips population and flower infestation: The effect of different treatments on the flower infestation and thrips population reduction over control are presented in Table 2. The significantly lowest

average number of thrips damaged flowers (0.88/20 flowers) was found in Raise 20 SL treated plots followed by Virtako 40 WG (1.25/20 flower), White sticky trap (1.75/20 flowers), Nitro 505 EC (1.75/20 flowers), Bioneem plus (2.25/20 flower), Ecomec (2.50/20 flowers) and Amithrin plus 3% WDG (3.25/20 flowers). The highest mean number of thrips-infested flowers was observed in untreated control plots (7.75/20 flowers), which differed statistically from other treated plots. Likewise, the highest percent reduction (88.65%) of flower infestation was recorded in Raise 20 SL applied plots over control which was followed by Virtako 40 WG (83.86%), White sticky trap (77.42%), Nitro 505 EC (77.42%), Bioneem plus (70.97), Ecomec (76.74%) and Amithrin plus 3% WDG (58.06%). These findings are supported by Bhede *et al.* (2008), who found that Imidacloprid was the best for controlling chili thrips. Hossain *et al.* (2013) showed the best performance of Regent 50 SC (Fipronil) for managing onion thrips with maximum benefit. Imitaf 20 SL (Imidacloprid) was also found effective in reducing thrips population and flower infestation of mungbean (Hossain, 2014)

Table 2. Effectiveness of different treatments on the number of thrips population and flower infestation of mungbean.

Treatments	No. of infested flower by thrips /plant	Percent reduction of infested flowers over control	Mean no. thrips/20 opened flower	Percent reduction of thrips over control
White sticky trap	1.75 de	77.42	2.00 bcd	80.48
Bioneem plus 1% EC @ 1 ml/L of water	2.25 cd	70.97	7.25 bcd	78.05
Virtako 40 WG @ 0.15 g/L of water	1.25 ef	83.87	1.75cd	82.93
Amithrin plus 3% WDG @ 1 ml/L of water	3.25 b	58.06	3.00bc	70.73
Ecomec1ml/liter of water	2.50 c	67.74	6.50bcd	75.61
Nitro 505 EC @ 1 ml/L of water	1.75 de	77.42	1.75cd	82.93
Raise 20 SL@ 3 ml/L of water	0.88 f	88.65	1.50d	85.37
Untreated control	7.75 a	-	10.25a	-
Level of significance	**	-	**	-
CV (%)	17.21	-	18.45	-

**Significant at 1% level. Means that a column followed by the same letter does not differ significantly by CD values. Values are the mean of 3 replications.

In case of thrips population, the lowest mean number of thrips population (1.50/20 flowers) was observed in Raise 20 SL treated plots followed by Virtako 40 WG (1.75/20 flowers), Nitro 505 EC (1.75/20 flowers), White sticky trap (2.0/20 flowers), Bioneem plus (2.25/20 flowers), Ecomec (2.50/20 flowers) and Amithrin plus 3% WDG (3.00/20 flowers). The maximum mean number of thrips population was found in control plots (7.75/20 flowers), which differed statistically from other treatments. The highest percent reduction of thrips population (85.37%) was found in Raise 20 SL treated plots over control followed by Virtako 40 WG (82.93%), Nitro 505 EC (82.93%), White sticky trap (80.48%), Bioneem plus (78.05). The lowest percent reduction was found in Amithrin plus 3% WDG (70.71%), followed by Ecomec (75.61%).

Relationship between flea beetle population and yield: Yield is influenced by the incidence of flea beetle per square meter plant. A strong negative correlation between the number of flea beetles and yield was observed, indicating a progressive decline in the yield with the increasing flea beetle population. A linear regression was fitted between flea beetle abundance and yield (Fig. 1). The correlation coefficient (r) was 0.79, and the contribution of the regression (R^2 = 0.6302, when Y = -24.861x + 674.23) was 63.02%.

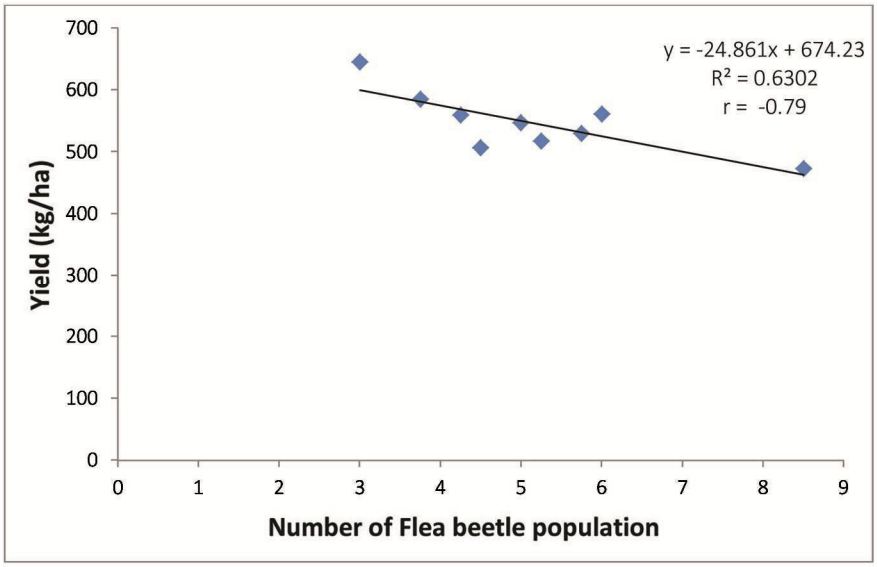

Fig. 1. Relationship between flea beetle incidence and yield of mungbean obtained from different treatments.

Relationship between thrips population and yield: Yield was moderately influenced by the incidence of thrips per square meter area of plant. There was a negative correlation between number of thrips and yield. It was evident that there was a gradual decrease in the yield with the increase of thrips. A linear regression was fitted between thrips abundance and yield (Fig. 2). The correlation coefficient (r) was 0.64, and the contribution of the regression (R^2 = 0.4142, when Y= -11.686x + 583.85) was 41.24%.

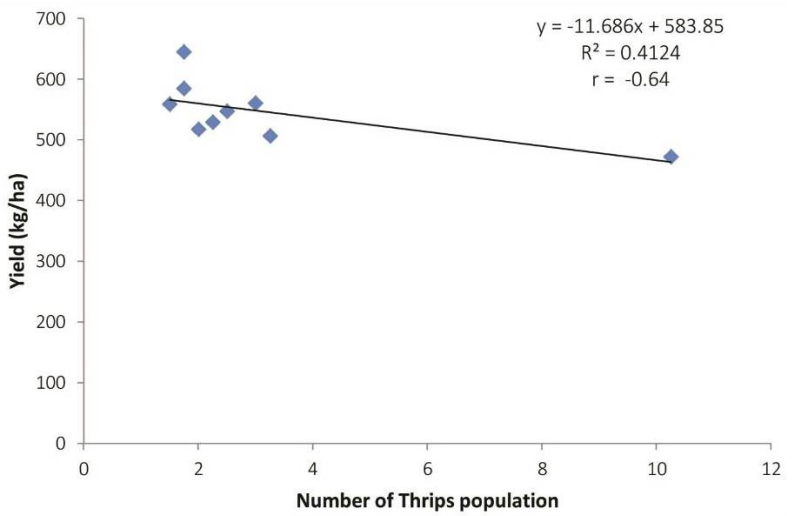

Fig. 2. Relationship between thrips incidence and yield of mungbean obtained from different treatments.

Relationship between flower infestation and yield: A negative relationship between percent flower infestation and yield was found in different treatments, revealing that the yield gradually decreased with increasing flower infestation by thrips. A linear regression existed between thrips infestation and yield (Fig. 3). The correlation coefficient (r) was 0.66, and the contribution of the regression (R^2 = 0.4371, when Y = - 16.108x + 590.35) was 43.71%.

The results of the present study are supported by Ullah *et al.* (2022), who found that the application of Virtako 80WG @ 0.15 g/L water + white sticky trap was the best package for managing flea beetle and thrips in mungbean. Alam *et al.* (2021) also found that the application of Admire 200SL @ 0.25 ml/l of water and Voliam Flexi (Thiamethoxam+ Chlorantraniliprole) @ 0.25 ml/L of water at 10-day intervals were more effective for suppressing whitefly and thrips in mungbean. Yasmin *et al.* (2019) found that Stargate.

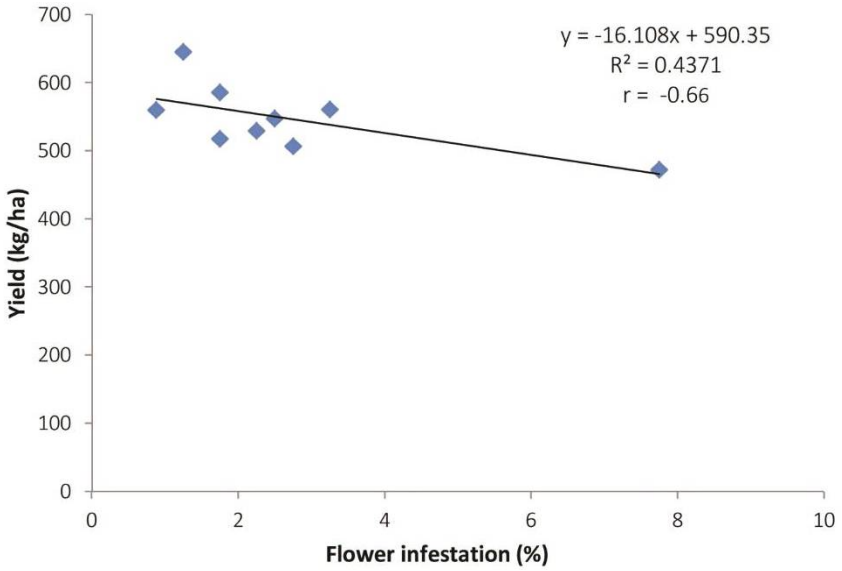

Fig. 3. Relationship between thrips infestation and yield of mungbean obtained from different treatments.

48SC (clothianidin) was the most effective insecticide against the thrips species Megalurothripsusitatus and Thrips palmi, with the highest reduction of the population on top trifoliate leaves and terminal shoots (100.00 and 89.40%, respectively) at vegetative stage and reduction on flower buds and flowers (86.04 and 85.95%, respectively) at reproductive stage of mung bean. Sachan (1986) has reported widespread thrips damage to mungbean flowers. They stated that flowers, petioles, and stigmas were eaten by thrips, which resulted in deformed inflorescences and immature flowers dropped. Spraying of Fenitrothion 0.1% at the flowering stage and a second spray either at an interval of 15 days or at the pod-forming stage provided the highest cost-benefit ratio (Rahman, 1989).

Conclusion

The treatment compositions Virtako (Chlorantraniliprole + Thiamethoxam) 80 WG @ 0.15 g/L of water and Raise (Chlorantraniliprole) 20 SL @ 3 ml/L of water were found effective for the management of flea beetles and thrips, respectively. Hence, these two insecticides could be suggested for their management.

References

Aheer, G.M., K.J. Ahmed and A. Ali. 1994. Role of weather in fluctuating aphid density in wheat crop. *J. Agril. Res.* **32**(3): 295-301.

Ahmad, M.A., C.P. Yadav and S.S. Lal. 1998. Evaluation of spray schedule for the control of insect pests of mungbean. *Indian J. Pulses Res.* **11**(2): 146-148.

Alam, M.S., M. Ali, M.M. Hossain, M.S. Hossain, M.A. Islam and M.H.R. Hera. 2021. Management practices for whitefly and thrips in mungbean. *Malaysian J. Halal Res. J.* **4**(2): 42-51.

Bhede B.V., D.S. Sunyawanshi and D. G. More. 2008. Population dynamics and bioefficacy of newer insecticide against chilli thrips, Scirtothrips Dorsalis. *Indian J. Entomol.* **70**(3): 223-226.

BBS (Bangladesh Bureau of Statistics) 2023. "Statistical Yearbook of Bangladesh. Bangladesh Bureau of Statistics (2021-2022), Statistics Division", Ministry of Planning, Govt. of Peoples Republic of Bangladesh.

Chhabra, K.S. and B.S. Kooner. 1985. Problem of flower shedding caused by thrips, *Megalurothrips distalis* (Karny), on summer mungbean, *Vigna radiata* (L) Wilczek, and its control. *Trop. Pest Manage.* **31**(3): 186-188.

Elias, S.M., M.S. Hussain, F.S. Sikder, A. Juber and M.R. Karim. 1986. Identification of constraints to pulse production with special reference to present farming systems. Annual report of Agricultural Economic Division. BARI, Joydebpur. p 1.

Farajallah, A., 2013. Effect of chemical and botanical insecticides on thripsand yield of mungbean. *Indonesian J. Agril*. **6** (2): 87-92.

Hossain M.A. 2014. Development of IPM practices for the control of flower thrips and pod borers in mungbean (*Vigna radiata* L.). *Bull. Inst. Trop. Agr. Kyushu. Univ.* **37**: 85-92.

Hossain, M.A. 2015. Efficacy of some insecticides against insect pests of mungbean (*Vigna radiata* L.) *Bangladesh J. Agril. Res.* **40**(4): 657-667.

Islam, K.N., M.M.H. Khan, M.M. Islam, M.M. Uddin and M.A. Latif. 2021. Prevalence of the infestation of flea beetle (*Phyllotreta nigripes*) against different varieties of mungbean. *Acta Scientifica Malaysia*. **5**(2): 56-61.

Kooner, B. S., H. K. Cheema and R. Kaur. 2006. Insect pests and their management. In: Advances in mungbean and urdbean (Eds. M. Ali and Shivkumar), Indian Institute of Pulses Research, Kanpur. pp. 335-401.

Lal, S.S. 1985. A review of insect pests of mungbean and their control in India. *Trop. Pest Manage.* **31**(2): 105-114.

Litsinger, J A., A.T. Barrion, J.P. Bangdog, C.G. dela Cruz, B.L. Canapi and R.F. Apostol. 1988. Food web, yield loss and chemical control of insect pests of wetland rice-based mungbean in the Philippines. Mungbean: Proceedings of the second International Symposium. Asian Vegetable Research and Development Center, Shanhua, Taiwan.

Malik, B.A. 1994. Grain legumes: Crop production. *Melanagromyza sojae* (Zehntner) on soybean. *Indian J. Plant Protect.* **18**: 271-275.

Rahman, M.M. 1989. Efficacy of some promising insecticides on pest incidence, plant growth and grain yield of cowpea. *Trop. Grain Legume Bull.* **35**: 19-22.

Sachan, J.N. 1986. Consolidated reports on Kharif pulses for the year 1985-86. Entomology AICPIP (ICAR) Directorate of Pulses Research, Kanpur. pp. 113.

Singh, K.M. and R.N. Singh. 1977. Succession of insect pests in green gram and black gram under dry land conditions at Delhi. *Indian J. Plant Protect.* **18**: 271-275.

Ullah, M.H., M.M.H. Khan, M.A. Latif, G.P. Das and M.O. Faruq. 2022. Integrated management of flea beetle and thrips on mungbean in coastal habitat. *Jahangirnagar University J. Biol. Sci*. **11**(1 & 2): 81-91.

Yadav, N.K. and P.S. Singh. 2013. Seasonal abundance of insect pests on mungbean and its correlation. *J. Entomol. Res*. **37**(4): 297-299.

Yadav, S.K., M. Agnihotri and R.S. Bisht. 2015. Seasonal incidence of insect-pests of blackgram, *Vigna mungo* (L.) and its correlation with abiotic factors. *Agril. Sci. Digest*. **35**(2): 146-148.

Yasmin, S., M.A. Latif, M. Ali and M.M. Rahman. 2019. Management of thrips infesting mungbean using pesticides. *SAARC J. Agric*. **17**(2): 43-52.

(Revised copy received on 20.11.2023)

J. Asiat. Soc. Bangladesh, Sci. **49**(2): 237-263, December 2023 DOI: https://doi.org/10.3329/jasbs.v49i2.70771

- Review Article

A COMPREHENSIVE REVIEW ON BLACK NIGHTSHADE (*SOLANUM NIGRUM*): CHEMICAL CONSTITUENTS, PHARMACOLOGICAL ACTIVITIES AND ITS ROLE IN COVID-19 TREATMENT

SIFAT ANZOOM[1], MD. RAFAT TAHSIN[3], SHAILA KABIR[2] AND MD. SHAH AMRAN[2*]

[1]*Department of Pharmacy, Faculty of Pharmacy, University of Dhaka, Bangladesh*
[2]*Molecular Pharmacology and Herbal Drug Research Laboratory, Department of Pharmaceutical Chemistry, Faculty of Pharmacy, University of Dhaka, Bangladesh*
[3]*Department of Pharmaceutical Sciences, North South University, Bangladesh*

Abstract

Three-fourths of the world's population uses 30% of all plant species as a safe source of disease control and treatment. Similarly, *Solanum nigrum* (Black nightshade), a therapeutic herb with small, spherical berry fruits, is used as an herbal remedy to treat many different diseases, including respiratory diseases. According to recent research, this plant can aid in the management of COVID-19. Alkaloids, flavonoids, steroids, glycoproteins, tannins, polysaccharides, polyphenolic compounds etc. are found in this plant. Among them, polyphenolic compounds are mostly responsible for showing various pharmacological activity. Anti-tumor, antioxidant, anti-diabetic, anti-inflammatory, anti-seizure, immunostimulant, hepatoprotective, antimicrobial activities are shown by *S. nigrum* according to multiple studies. The aim of this article is to compile different aspect of this plant like plant description, uses, chemical constituents, pharmacological activities and especially its role in the management of COVID-19 and probable mechanism behind this role.

Keywords: Solanum nigrum, Black nightshade, Phytochemical analysis, Pharmacological activities, COVID-19, Pathogenesis.

Introduction

Pharmaceutical lead compounds have been obtained from medicinal plants since the early days. They are considered rich sources of traditional remedies, and also many modern medicines are derived from them. Dating back to the prehistoric period, plants are utilized for medical purposes. Early human beings, depending only on their instinct, taste and experience, used plants to treat their illnesses. Herbs were described in ancient Egyptian papyrus, Unani texts, and Chinese writings. There is evidence that people have

* Corresponding author: amrans@du.ac.bd

used plants as medicine for more than 4000 years, including Indian Vaids, Unani Hakims, and people from European and Mediterranean cultures (Khan, 2016; Khan *et al.,* 2009; Dar, 2017). According to published data, plants and plant extracts are the basic source of health care for almost 75% of the global population. And more than 30% of all plant species have been used for medical reasons at one time or another. The usage of medicinal plants is seen to be relatively safe, as there is no or very few side effects. The fact that these medicines are in touch with nature is the best thing. In addition, herbal medicines are used by people of all ages and genders (Khan, 2016; Silori and Badola, 2000). There is a bright future for medicinal plants, as there are over half a million plants on the planet, the majority of which have not yet been investigated for their medicinal properties, and their hidden medicinal potential could play significant role in present and future studies (Dar, 2017).

S. nigrum, generally known as black nightshade in English, Makoi in Hindi and Bengali local name is Kakmachi, is a dicot weed which belongs to the Solanaceae family. This medicinal plant has long been utilized for a range of diseases such as liver disorder, inflammation, chronic skin problems, painful periods, diarrhea, fever, eye infections, hydrophobia, and so forth. And for these medicinal purposes leaves, whole plant and roots are used whereas black colored fruits of *S. nigrum* cannot be used as they possess toxicity (mainly because of high concentration of solanine). This plant is mostly seen in the Europe, Africa and Indian continent. Only few countries semi-cultivate this plant, but generally it grows spontaneously on waste lands, beside fences and roads and as weeds in cultivated lands (Jain *et al.,* 2011; Saleem *et al.,* 2009; Chauhan *et al.,* 2012; Zhou *et al.,* 2006).

S. nigrum is an annual herb, which is 25 to 100 cm long, erect, bifurcately branched, suffrutescent and pubescent. It has ovate or oblong or lanceolate, toothless or sinuate-toothed, glabrous and dull dark green color leaves. The plant contains 3-8 small white flowers with a little petiole and five petals in extra-axillary umbels. Generally, black and reddish brown berries are the two types of fruit found in two varieties of *S. nigrum*. They are small, globose and only 8-10 mm in diameter. They turn black when ripe and these black colored ones are toxic (Saleem *et al.,* 2009; Chauhan *et al.,* 2012; Zhou *et al.,* 2006).

A large amount of chemical compounds is present in *S. nigrum* and they show various pharmacological activities. The main chemical constituents are alkaloids, flavonoids, steroids, glycoproteins, tannins, polysaccharides, and polyphenolics such as caffeic acid, catechin, gallic acid, protocatechuic acid, rutin, epicatechin, etc. The major acid

constituents of *S. nigrum* are citric acid, malic acid, acetic acid, and tartaric acid. This plant also contains some important minerals like Mg, K, Ca, Fe, Na, Mn, Zn etc. Also, some researchers discovered that the fruit and root of this plant contains ascorbic acid and the fruit contains the highest concentration. Whereas, the seeds are rich of lipid content and have moderate amount of protein (17.63%). The phytochemical analysis of the plant gives us some important qualitative value such as, ash values for leaf, fruit and stem are 3.928%, 6.723% and 11.90%, respectively, whereas crude fibre values are 8.42%, 15.19% and 14.73%, respectively. Solanine, a deadly glycoalkaloid present throughout most of the plant as a natural defense system, accounts for 95% of the total alkaloid content of *S. nigrum*. Although, the raw fruit has the highest quantity of solanine, the concentration decreases eventually with fruit maturation (Jain *et al.,* 2011; Saleem *et al.,* 2009; Chauhan *et al.*, 2012; Zhou *et al.,* 2006; An *et al.*, 2006). Researchers identified six novel steroidal saponins, which are collectively known as solanigrosides, and one known saponin, degalactotigonin. Again two new disaccharides and steroidal saponins, called nigrumnins I and II have been isolated from *S. nigrum* (Saleem *et al.,* 2009; Chauhan *et al.,* 2012; Akubugwo *et al.,* 2007). Like other *Solanum* species, *S. nigrum* possesses diverse pharmacological activities like anti-tumorigenic, antioxidant, anti-inflammatory, anti-diabetic (in Sprague Dawley rats and albino rats), anti-HCV, anti-cancer (on HeLa cell line), anti- diarrheal, immunostimulant, hepatoprotective (against CCl4 induced liver damage in rats), cardioprotective, analgesic, diuretic, antipyretic agent, antimicrobial, anti-convulsant, antiulcerogenic etc (Lin *et al.,* 2008; Jainu and Devi, 2006; Parez *et al.*, 1998). Also, studies revealed that *S. nigrum*'s fruits have neuropharmacological activities. It showed a potent CNS-depressive effect in animal studies (Parez *et al.,* 1998).

As this plant possesses various pharmacological activities *S. nigrum* has been broadly used in the oriental medicine. For example, leaves are used for the cure of skin problems, rheumatic gout, dropsy and nervous disorders. Flowers and berries extracts are used for the treatment of cough, erysipelas, diarrhea, opthalmopathy and rabies. Even roots are employed in opthalmopathy, otopathy, hepatitis and rhinopathy. Mostly, people from different parts of Africa and India follow these traditional ways to treat diseases (Jain *et al.,* 2011; Saleem *et al.,* 2009; Chauhan *et al.,* 2012; Atanu *et al.,* 2011). A lot of studies have already proved that various illnesses, particularly respiratory conditions, can be treated using *Solanum* species (including *S. nigrum*). Recent studies revealed that some polyphenolic compounds specifically glycoalkaloids such as quercetin, kaempferol and apigenin, which are present in *S. nigrum*, had shown interaction with SARS-CoV-2 protease. Here stated quercetin is a strong natural antioxidant and two quercetin

glycosides are present in *S. nigrum*. Moreover, the immunostimulant activity of this plant can help in the regulation of Covid-19 (Mbadiko *et al.*, 2020; Nallusamy *et al.*, 2020).

Methods and Materials

Several procedures were followed to ensure a high quality review of the literature on the medicinal plant, *S. nigrum*. At first, an extensive literature searches of peer-reviewed journals, but not conference paper or reports, was conducted based on a wide range of key words like, medicinal plant, *S. nigrum*, phytochemical analysis and therapeutic functionality of *S. nigrum* in COVID-19 treatment etc. The search engines and journal websites used in this step are Google Scholar, PubMed, Researchgate, ScienceDirect, International Journal of Pharmacy and Pharmaceutical Sciences, World Journal of Pharmacy and Pharmaceutical sciences, and others. Second, the reference section for each article found was also searched to find additional articles. And the pictures of the plant were taken from website. Word 2016 installed in HP Probook 450 G5 device was used to write this review and to prepare the tables. PowerPoint 2016 has been used to prepare the figure. And ChemDraw pro 12.0 was used to draw the phytochemical constituents. All the valuable information, most importantly the pharmacological activity, therapeutic role and medicinal uses of the plant are mentioned in this paper.

Findings and Discussion

S. nigrum is one of the mostly utilized medicinal plants in Indian continent. Numerous chemical constituents are responsible for a number of pharmacological activities. It is popular for its use in respiratory diseases.

Taxonomical Classification

Kingdom: Plantae, **Subkingdom:** Tracheophyta, **Superdivision:** Spermatophyta, **Division:** Angiospermae, **Class:** Dicotyledonae, **Subclass:** Asteridae, **Order:** Solanales, **Family:** Solanaceae, **Genus:** *Solanum*, **Species:** *Solanum nigrum L* (Saleem *et al.* 2009; Rani *et al.*, 2017).

Chemical Constituents

Different chemicals have been extracted from various areas of the plant and researchers reported about the variability of concentration of these compounds depending upon maturation time and place. The phytochemical analysis of *S. nigrum* extracts shown that there were tannins, flavonoid, phytosterols, and fixed oils and fats in benzene and hexane

extracts. While the *S. nigrum* berries' aqueous and ethanolic extracts included alkaloids, coumarins, tannins, saponins, phenols, phytosterols, and carbohydrates (Atanu *et al.*, 2011; Ravi *et al.*, 2009). Many steroidal alkaloids, steroidal glycosides, steroidal oligoglycosides (such as solasonine, solamargine, solasdamine, solavilline, and solanine), flavonoids, glycoprotein and steroidal saponins, and many polyphenolic compounds are found in *S. nigrum*, which can be clearly seen from the phytochemical screening shown in Table-1. There have also been claims of proteins, carbohydrates and coumarins, polyphenols, crude polysaccharides, luteolin, gentisic acid, kaempferol, apigenin, and anthocyanidin. The anti-tumor activity of steroidal alkaloids and glycoproteins has been discovered (Jain *et al.*, 2011).

S. nigrum whole plant Berries of *S. nigrum*

Fig. 1. Berries and whole plant of *S. nigrum*
(Pictures are taken from https://www.indiamart.com/proddetail/solanum-nigrum-extract-makoi-extract-16684056088.html)

Glycoalkaloids

The glycoalkaloids present in *S. nigrum* include solasonine, solamargine, solanigrine, solasodine and solanine (Table 2) from the tropane group of compounds. Solanidine with MW=397.62 and formula: $CH_{43}NO$, can be obtained by hydrolysing solanine and solasonine, is less toxic in nature. These glycoalkaloids have anticancer activity across an array of tumor cell lines. According to studies, the alkaloidal concentration of plant sections changes as it develops. Over the period of leaf development, the quantity of alkaloid per leaf rises, but the concentration decreases. Small green *S. nigrum* fruits

contained a high amount of solasodine, but as the fruit matures, both the concentration and absolute amount of solasodine per fruit decrease (Atanu *et al.,* 2011).

Table 1. Phytochemical screening of crude extract of *S. nigrum* (Ewais *et al.,* 2015).

Name of chemical groups	Test conducted	Result	Inference
Alkaloids	Wagner's test	+ve	Present
	Dragndorrf test	+ve	Present
Glycosides	Glycosides test	+ve	Present
	Modified borntrager's test	+ve	Present
Phenolic compound	Ferric chloride test	+ve	Present
Saponins	Foam test	+ve	Present
Sterol	Salkawskis test	-ve	Absent
	Libermannburchard's test	-ve	Absent
Flavonoids	NaOH test	+ve	Present
Tannins	Gelatin test	+ve	Present
	Lead acetate test	+ve	Present

Phenolics

Caffeic acid, gallic acid, catechin, quercetin (Table 2), protocatechuic acid (PCA), epicatechin, rutin, naringenin and flavonoids are the polyphenolic compounds found in *S. nigrum.* Phenolics are the most significant antioxidants found in plant materials. Among the largest groups of molecules that operate as principal antioxidants or free radical scavengers is contributed by them. Flavonoids are a class of natural chemicals that are diverse in their chemical and biological properties, including the ability to scavenge free radicals. Total phenolic and flavonoid concentrations were determined to be 3222.66 mg/g gallic acid equivalents and 2262.81 mg/g quercetin equivalents, respectively (Jain *et al.,* 2011; Atanu *et al.,* 2011; Jasim *et al*., 2015; Prasath 2016).

Table 2. Most abundant chemical constituent found in *S. nigrum* (Jain *et al.*, 2011; Jasim *et al.*, 2015; Atanu *et al.*, 2011; Prasath, 2016; Saleem *et al.*, 2008; Chauhan *et al.*, 2006)

Constituent Name	Description	Structure
Solanine	Solanine makes up 95% of the overall amount of alkaloid in the plant and can be found in any part but unripe berries contain the highest portion. Because it is toxic even in minute amounts, it is among the most essential defense mechanisms of the plant. It is made up of an aglycone, solanidine, and three sugar molecules linked to the third position of the aglycone (glucose, galactose, and rhamnose, together known as solatriose). Its chemical formula is C45H73NO15, and its molecular weight is 868.04 g/mol. Although it is most frequently found as α-solanine, it can also be hydrolyzed into β- and γ-solanine.	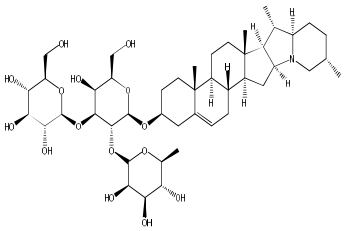
Quercetin	Quercetin is one of the most powerful antioxidants present in nature. Quercetin 3-O-(2Gal-α- rhamnosyl)-β-glucosyl(1→6)-β-galactoside and quercetin 3-O-α-rhamnosyl(l→2)-β-galactoside are two quercetin glycosides found in Sn. Quercetin 3-glucosyl(l→6)galactoside, 3-gentiobioside, 3-galactoside and 3-glucoside are also present in this plant.	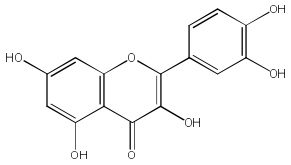
(+)-Catechin	Catechin is one of the phenolic compounds found in *S. nigrum.*	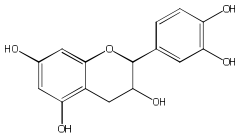
Degalactotigonin	It is a saponin identified in *S. nigrum* by spectroscopic analysis, chemical degradation	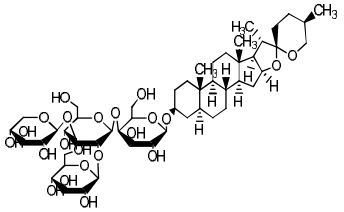
Vitamin C	Vitamins are present in *S. nigrum* in sufficient amount. Both the leaves and seeds of the plant contain vitamins in the following order: vit C > vit B > vit E > vit A. Ascorbic acid is mostly present in fruits of *S. nigrum.*	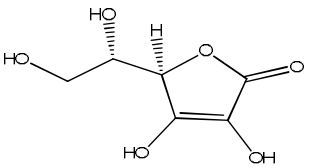

Glycoprotien

S. nigrum glycoproteins are extracted by precipitating them with 80 percent ammonium sulphate. Fruits, stems, and leaves contain SNL glycoprotein II of 210 kDa and SNL glycoproteins I of 150 kDa and 100 kDa. Glycoproteins are composed of carbohydrate (69.74%) and protein (30.26%), with the majority of the amino acids being hydrophobic, such as glycine and proline. In HCT-116 cells, it has been found that a 150 kDa phytoglycoprotein that was found in seeds using affinity chromatography and ammonium sulphate precipitation exhibits anticancer, diuretic, and antipyretic properties (Jain *et al.*, 2011).

Saponins

Spectroscopic analysis, chemical degradation, and derivatization of *S. nigrum* instigated the discovery of six new steroidal saponins known as solanigrosides, as well as one known saponin degalactotigonin. Sn was used to characterize a pair of steroidal saponins known as nigrumins I and II. Nigrumnin I, also known as (25R)-5alpha-spirostan-3beta-ol 3-O-betaD-xylopyranosyl- (1-->3)-[alpha-L-arabinopyranosyl-(1–>2)]-beta-D-glucopyranosyl-(1—>4)-[alpha-L-rhamnopyranosyl(1-->2)] -beta-D-galactopyranoside and nigrumnin II was identified as (25R)-3beta, 17alpha-dihydroxy-5alpha- spirostan-1 2-one 3-O-beta-D- xylopyranosyl-(1-->3)-[alpha-L-arabinopyranosyl-(1-->2)] -beta-D-glucopyranosyl-(1—>4)-[alpha-L-rhamnopyra-nosyl-(1-->2)]- beta-D-galactopyranoside. In addition, five non-saponins were discovered: 6-methoxycoumarin, syringaresinol-4-O-beta-D-glucopyranoside, pinoresinol-4-O-beta-D-glucopyranoside, 3, 4-dihydroxh-benzoic acid (IV), p-hydroxybenzoic acid, and 3-methoxy-4-hydroxyienzoic acid (Atanu *et al.*, 2011).

Other Pharmacological Activities

S. nigrum has also shown several other pharmacological actions that are not displayed in Table 3, such as, antimicrobial, immunomodulatory, anti-ulcer, anti-HCV, cardio-protective, analgesic activity etc.

Antimicrobial activity

Antimicrobial activity of *S. nigrum* is evaluated against various types of gram-positive and gram-negative bacteria, along with fungus by using different extractions of the plant and disc diffusion method. Potential of the extract as antimicrobial agent is assessed on the basis of zone of inhibition. It is clear form Table 4 that different bacteria had different levels of susceptibility to crude extracts according to the microorganism and extracting solvent. The active components that are responsible for this antimicrobial activity of *S.*

nigrum have been identified as saponins (Chauhan *et al.*, 2012; Atanu *et al.*, 2011; Zubair *et al.*, 2011).

Table 3. Therapeutic Activities of *S. nigrum* on different models (Jain *et al.*, 2011; Son *et al.*, 2003; Zhao *et al.*, 2018; Dong *et al.*, 2021; Patel *et al.*, 2009; Atanu *et al.*, 2011; Loganayaki *et al.*, 2010; Muthuvel *et al.*, 2020; Alam *et al.*, 2012; Chauhan *et al.*, 2006; Lin *et al.*, 2008; Prasath 2016; Cai *et al.*, 2010; Parez *et al.*, 1998; Aali *et al.*, 2010; Sugunabai *et al.*, 2014)

Therapeutic activity	Preparation types	Constituent name	Dose	Mechanism of action	Model
Anticancer Activity	Methanolic extracts	Diosgenin	0.0196-10 mg/mL	By interfering with the tumor cell membrane's constitution and function, disturbing DNA and RNA synthesis, and obstructing the NF-kappaB anti-apoptotic pathway.	*In vitro*
Antioxidant Activity	Methanolic Extract	Polyphenols	IC_{50}: 120.22 µg/mL; IC_{50}: 301.99 µg/mL; IC_{50}: 194.98 µg/mL	1, 1-diphenyl-2- picrylhydrazyl (DPPH) radicals, hydroxyl radical (OH), and superoxide anion (O^{2-}) scavenging activity	*In vitro*
Hepatoprotective Activity	Methanolic Extract	Polyphenols, alkaloids and saponins	0.2, 0.5, and 1.0 g /kg bw	By modulating detoxification enzymes (GSTs) and antioxidant enzyme (SOD) and ultimately by blocking the oxidative stress	Sprague-Dawley (SD) rats
Anti-inflammatory Activity	Ethanolic extract	(E)-ethyl caffeate; 150 kDa glycoprotein	100, 250 & 500 mg/kg bw	By lowering nitric oxide synthesis, lactate dehydrogenase release, and thiobarbituric acid reactive substances concentrations; Also, through controlling the expression of the iNOS and COX-2 enzymes.	Rats; A/J mouse
Anti-convulsant Activity	Aqueous extract	Flavonoid	30-60 mg/kg bw; 10-40 mg/kg bw	The mode of action of the extract is yet unknown.	Rats and mice; Chicks
Antidiabetic activity	Aqueous and hydro-alcoholic extracts	Alkaloids and solanines	200,250 and 400 mg/kg bw	Most likely by increasing Insulin secretion from pancreatic beta cells.	Albino rat

Mechanism of Action /Clinical Indication

Diverse therapeutic activities of *S. n5igrum* with their mechanism of actions are demonstrated in Table 3.

Immunostimulant activity

It was observed *in vivo* that treatment with crude polysaccharide extracted from *S. nigrum* enhanced the ratio of CD4/Cd8 and T-lymphocyte subpopulations in peripheral blood. Additionally, SNL-P therapy led to a notable decline in IL-α ($p < 0.05$, 360 mg/kg bw.) and a considerable increase in IFN-α ($p < 0.01$, 90, 180, and 360 mg/kg bw.), both of which were evaluated using the ELISA method. From these data, we can say that SNL-P is a potential immunostimulant which can help to fight infection and tumor (Atanu *et al.*, 2011).

Cardioprotective activity

A worldwide *in vitro* ischemia-reperfusion injury model was used to assess the cardioprotective activity of methanolic extract of *S nigrum* berries. The experiment was conducted using dosages of 2.5 and 5.0 mg/kg six days a week for 30 days. This experiment's findings imply that the extract has considerable cardioprotective properties (Chauhan *et al.*, 2012).

Table 4. Antimicrobial activity of different extracts of fruits of *S. nigrum* (dose level = 20mg/ml) (Abbas *et al.*, 2014).

No	Microorganisms	Zones of inhibition (mm) ± SE(Standard error)				
		Chloroform	Ethyl acetate	Acetone	Methanol	Water
1	**Gram positive organisms**					
	Micrococcus luteus	9.2±1.25	6.5±3.2	7.6±1.3	3.4±2.1	13.5±3.4
	Staphylococcus aureus	8.5±2.12	7.2±2.0	8.3±2.0	15.2±3.5	14.7±2.4
2	**Gram negative organisms**					
	Escherichia coli	6.7±1.4	7.5 ± 2.3	7.9 ± 2.1	14.3 ± 2.6	16.4±3.0
	Salmonella typhi	7.6±1.8	6.7±2.5	6.5±2.0	15.2±3.3	15.3±3.2
3	**Fungal species**					
	Candida albicans	5.8±2.6	6.7±1.3	5.3±1.0	7.6±1.0	4.8±2.10

Analgesic activity

Using Eddy's hot plate and acetic acid-induced writhing method, the analgesic activity of ethanolic extracts of *Solanum nigrum* was assessed. 100, 250, and 500 mg/kg orally administered dosages were employed in the trial. The result is that noteworthy pain-relieving effect was observed at the dose of 500 mg/kg ($P<0.01$) (Chauhan *et al.*, 2012).

Traditional Uses

For its various important pharmacological activity *S. nigrum* has been taken as folk remedy all across the world. Some of its uses are shown in Table-5.

Table 5. Overview of traditional uses of *S. nigrum* in different parts of the world (Jain *et al.*, 2011; Saleem *et al.*, 2008; Rani *et al.*, 2017; Atanu *et al.*, 2011; Khan, 2016).

Country	Plant Part	Preparation	Condition
Tamil Nadu, India	Leaf paste	Applied directly	Rabies; wound healing; rheumatic and gouty joints
	Complete plant	As food item	Cold
Himalayan region, India	Leaf	-	Indigestion; liver excitant
Assam, India	Roots	Extraction of root juice	Whooping cough and Asthma
Thar Desert, India	Roots	Boiling roots with a little sugar	Boost female fertility
Tanzania, Africa	Leaf	Pounded leaves are applied topically	Treatment of infection with ringworm
	Leaf	The crushed and broiled leaves	Used as a wart dressing
	Fruit	Ripe fruits	Provided to children in order to prevent bedwetting
United Republic of Congo, Africa	Whole plant	Maceration	Snake bite or poisonous animal's sting
Tunisia, Africa	Sap	-	Erysipelas (acute Streptococcus bacterial infection)
Algeria, Africa	Fruit	Diluted infusion of berries	Blindness; glaucoma; conjunctivitis; trachoma; cataract
	Whole plant	Decoction	Burns and skin problems

Toxicity of *S. nigrum*

Despite of the fact that *S. nigrum* is famous for its use in the traditional medicine it can be very toxic. In fact, the majority of species in the Solanaceae family are toxic to both people and animals. Tropane alkaloids are found, for example, in deadly nightshade. The classic anticholinergic poisoning is the symptom of tropane alkaloids-containing plant toxicity. The glycoalkaloid solanine, which causes varying levels of toxicity with dose-dependent effects, is primarily responsible for *S. nigrum*'s toxicity. Solanine poisoning can cause a variety of symptoms in humans, including diarrhea nausea, vomiting, headaches, vertigo, chills, speaking impediment, perspiration, blindness, arrhythmia, mental confusion, seizures, coma, and death. Consuming nightshade plants including tomato, potato, and eggplant is known to aggravate joint pain. According to reports, the solanine found in these plants' green parts is probably to blame. However, ripe fruits and cooked plants of this family are safe to eat as the toxic compound is reduced or destroyed (Jain *et al.,* 2011).

***S. nigrum* in management of COVID-19**

COVID-19 is one of the most lethal pandemics the world has seen. The world has been startled by the rapid spread of this lethal virus, which presents a challenge to worldwide medical and scientific communities (Sikander *et al.* 2020) Natural plant chemicals are being studied for their ability to suppress the SARS-CoV-2, the source of COVID-19, in order to combat the current pandemic. Natural products, such as antiviral chemicals of very little toxicity, are employed by the pharmaceutical industry because of their pharmacological activities, could be a useful resource in the formulation of COVID-19 treatments. They are taken into consideration since they have already made contributions to the research and development of medications that treat viruses like HIV, influenza, and MERS-CoV (da Silva Antonio *et al.,* 2020; Teli *et al.,* 2021). The potential of flavonols, flavanols, and flavanones as anti-SARS-CoV-2 agents, moreover the reason that angiosperm plants contain a lot of these substances, have given hope to the people of the world. However, critical problems regarding their absorption and real efficacy in vivo remain unresolved (da Silva Antonio *et al.,* 2020). The plant *S. nigrum* containing some of these compounds like solanine, quercetin, kaempferol, apigenin etc can also be an option for the treatment. The main reason for choosing this plant as an option is been previous record of antiviral and immunomodulatory activity. With limited but systematic clinical studies, some formulations can be developed using this plant, it is intended to establish a presence on the global market and offer up new avenues for the study of COVID-19 and related illnesses (Goyal *et al.,* 2021).

Pathogenesis of COVID-19

For a better knowledge of how natural compounds or phytomolecules might successfully combat new coronavirus, it is crucial to identify the structural characteristics, pertinent targets, and receptors associated with these viruses. To build a COVID-19 therapeutic natural-sources-based regimen, it may also be helpful to comprehend the action mechanism of classical antiviral medications and possible drug development targets (Patel *et al.*, 2021). Coronaviruses are members of the Coronaviridae family. The average size of coronaviruses, which range from 60 nm to 140 nm in diameter and under electron microscopy display a crown-like appearance, varies considerably depending on their genotype and phenotype. They have single-stranded RNA and are positive sense enveloped viruses. Although it is thought to have been transmitted by bats, the exact origins of SARS-CoV-2, enzootic transmission patterns, and animal reservoir are unknown. SARS-CoV-2 is made up of four basic structural proteins: membrane protein (M), spike protein (S), envelop protein (E), and helically symmetrical nucleocapsid protein (N), as well as non-structural proteins like nsp12-RNA-dependent RNA polymerase (RdRp), Nsp5- 3C-like main protease, Nsp3-Papain-like proteinases, and nsP13 SARS-CoV helicase (Patel *et al.*, 2021; Mirzaie *et al.*, 2020, Khan and Al-Balushi 2021).

Inoculation and Replication

The SARS-CoV-2 virus infects healthy cells by attaching to the ACE2 receptor on the host cells, which is widely present in the heart, kidney, lungs, intestine, and blood vessels. This process is carried out by the viral spike (S) protein. After adherence of the S protein to the ACE2, the virus employs infected cell receptors (TMPRSS2) to reach the cytoplasm of the host cell. And after being uncoated, the cytoplasm is where the viral gRNA is discharged. Viral proteins are created by the protein synthesis mechanism of the host cell, and they are subsequently broken down by viral proteases and then transported to the replicase complex. Using its RdRP, the virus produces viral RNA. Additionally, viral assembly and structural proteins are produced, allowing for the finalization of the assemblage and the exocytosis-mediated discharge of viral progeny. β-CoVs generate pp1a and pp1ab through the translation of genomic RNA. Main protease (Mpro) and papain-like protease break them into structural and non-structural proteins (PLpro). The virion assembly will be discharged from the host cell once it is complete (Khan and Al-

Balushi, 2021). The ACE converts angiotensin I to angiotensin II while converting angiotensin 1-9 to angiotensin 1-7. Vasoconstriction, fibrosis, inflammation, prothrombotic, and arrhythmogenic actions are brought on by angiotensin II's binding to AT1 receptors in the body. Also Angiotensin II protects tissues by acting on AT2 receptors. Angiotensin 1-7 binds to the MAS receptor and has anti-proliferative, anti-inflammatory, antifibrotic, and antithrombotic properties (Goyal *et al.*, 2020).

Inflammatory Response

Cellular reactions are triggered by viral replication. This resulting in invasion of many inflammatory cells, which include both innate and adaptive immune cells. The intrinsic immune cells chiefly responsible for lung damage are neutrophils. The majority of adaptive immune cells are T cells, specifically cytotoxic CD8+T cells, that not only destroy viruses but also harm the lungs. Overall result is the systemic inflammatory reaction, which causes a surge in cytokines such as TNF, IL1, IL6, IL10, and others, which is known as cytokine storm. It is one of the suggested mechanisms of SARS-CoV-2-induced lung damage. Increased levels of various cytokines cause Type-1 and Type-2 cells in the lungs to enlarge and die. This hinders oxygen delivery which causes cell death in the lungs' alveoli and producing Acute Respiratory Distress or syndrome (ARDS). Increased levels of circulating pro-inflammatory cytokines, including interferon, interleukin (IL-1, IL-6, and IL-12), and chemokines (CXCL10 and CCL2), are associated with pulmonary inflammation and the pathogenesis of ARDS. This is because inflammatory damage to the blood–air barrier causes an increase in lung permeation and the secretion of protein-rich respiratory edema fluid into the air passages. It eventually causes respiratory failure and the consequences that lead to multiple organ failure. When SARS-COV2 binds to open reading frames (ORFs), particularly the ORF8 proteins, iron dissociates from the 1-beta chain of hemoglobin, which subsequently binds to the membrane glycoprotein porphyrin, results in the internal respiration failure. Weak immune system along with cytokine storm is the major cause of reduced cellular oxygen at the alveolar level, which is thought to be the major factor in demise in COVD-19 (Patel *et al.*, 2021).

Strategy for developing treatment

The SARS-CoV-2 genome sequence was used to identify the crucial proteins and enzymes associated with the virus's inoculation and multiplication. Its genomic sequence has79.5% resemblance with SARS-CoV-1 and 96% similarity with a coronavirus strain that is only communicable in bats. According to genomic evidence, three proteins and enzymes are principally responsible for SARS-CoV-2 infection and viral proliferation in humans (Fig. 2). The papain-like protease (ACE2), 3 chymotrypsin-like proteases (3CLpro) and spike protein (TMPRSS2) are the proteins in concern (da Silva Antonio *et al.,* 2020).

The virus is a necessary intracellular parasite which depends on host metabolic components as well as the environment for reproduction and proliferation. So, the challenge in developing an antiviral medicine is to create one that is both effective and selective in its toxicity against viruses rather than the host. Since SARS-CoV-2 binds to ACE2, which is also implicated in the pathogenesis of cardiovascular, pulmonary, and gastrointestinal dysfunction, and is the site of virus proliferation, inhibiting ACE2 has been the main focus of anti-COVID-19 research, despite the fact that it is probably not the best choice of action to act on such a central control system. The virus's trimeric spike glycoprotein (TMPRSS2), which is a transmembrane protease serine type 2 (TMPRSS2), attaches to host cells and is a major objective for future treatments and diagnostics. In each spike monomer, the SARS-CoV-2 S2 subunit reportedly has a transmembrane domain, a fusion peptide, and a cellular domain that is very constrained and may be an antiviral drug target (anti-S2). Also, the virus polypeptide is proteolytically broken down by the 3CLpro into 11 non-structural proteins that are crucial in the virus' growth. The 3CLpro, which is unique to SARS-CoV-2 and absent from the host cell., attracted interest as a possible target for COVID-19 therapy development (Patel *et al.,* 2021; Goyal *et al.,* 2020).

Phytomolecules produced by many plants can be employed to approach these viral targets, as they have been for other viral infections such as SARS, HIV, HCV, and others. Antiviral plants with anti-inflammatory effects that protect the lungs from infections can also be examined as a synergetic therapy. Based on the above mentioned strategies, a search for possible plants with the following features may assist in the establishment of natural plant-derived antiviral medicines to combat the pandemic disease (Patel *et al.,* 2021; da Silva Antonio *et al.,* 2020).

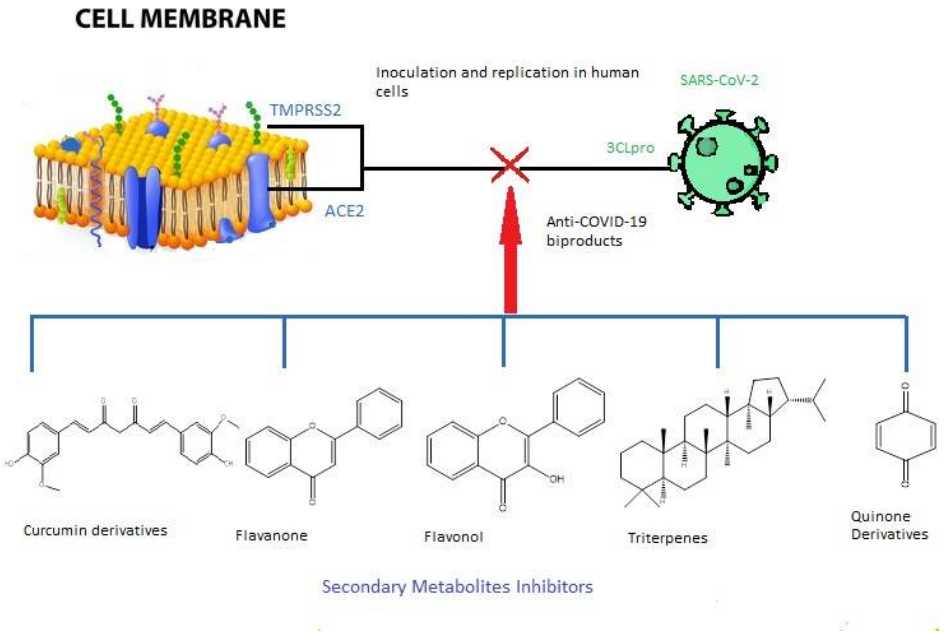

Fig. 2. Invasion of SARS-CoV-2 in human cell and action of some anti-COVID-19 compounds

Natural Therapeutic Options for COVID-19

Generally, developing bioactive natural cures for a particular ailment, such as COVID-19, should be faster than developing vaccines but it becomes a challenging process because of the variety of natural compounds, their extraction and chemical complexity. Fortunately, as an efficient method for comprehending and forecasting druggability in the early stages of drug development, in silico analysis by molecular docking technologies has expanded study fields and gained widespread acceptance. This is mainly used to predict how bioactive compounds bind with receptor proteins. Docking studies were conducted on flavonoids (flavones, flavonols, isoflavones, xanthones, flavanone, flavan 3-ols), tannins, phenolics, anthraquinones, alkaloids, lignans, and coumarins (simple, complex) targeting the papain-like protease (ACE2), 3 chymotrypsin-like proteases (3CLpro) and spike protein (TMPRSS2). The results demonstrate that flavonoids may attach to the S protein of the SARS-CoV-2 virus, a viral membrane glycoprotein necessary for early attachment and incorporation into host cells. Flavonoids such as luteolin, apigenin, quercetin, epigallocatechin (EGC), gallocatechin gallate (GCG),

amentoflavone, and kaempferol have been shown to suppress the proteolytic activity of SARS-CoV 3CLpro and 3a channel protein of the coronavirus. ACE2 inhibitory action was found in flavonoids such as luteolin, rutin, quercetin, apigenin and kaempferol. Furthermore, Mpro and spike glycoprotein inhibitors such as procyanidin A1, A3, A4, B2, acetoside, solanine, quercitrin, rutin, and theaflavin 3,3′-digallate can be subjected to future investigations in order to identify specific treatments to combat COVID-19 (da Silva Antonio *et al.*, 2020; Sulaiman *et al.*, 2021; Khan and Al-Balushi, 2021).

Natural ACE2 Inhibitors

The most effective method for COVID-19 therapy and prevention may involve limiting host cell entry by the virus. SARS-CoV-2 enters the cell via endocytosis after attaching to the ACE2 on the host cell membrane. Nucleoside analogs that inhibit viral replication and small compounds that target virus-host cell interaction, such as ACE2 in SARSCoV-2, are possible treatments for this viral illness. Similar to the mechanism seen with SARS-CoV-1 inhibitors, ACE and ACE2 inhibitors engage with the protein through amphiphilic molecule structures that typically have an aromatic component (Goyal *et al.*, 2020). As a component of the renin-angiotensin system, ACE2's primary job is to transform angiotensin II, a potent vasoconstrictor, into angiotensin (structural forms I, III, IV, V, VI, and VII), a vasodilator that helps to maintain and lower blood pressure by balancing ACE. Risks about coronavirus infections arise when ACE inhibitors (ACEIn) are used to treat diabetes and hypertension on a long-term basis. They make the patients more susceptible to COVID-19 by upregulating the activation of ACE2. Because of this, the vast bulk of COVID-19 identified patients had comorbid conditions, mainly diabetes or high blood pressure. As the level of angiotensin I increases as a function of ACE inhibition, ACE2 mRNA rises to balance. This is assumed to be caused by the reduced ability of ACE inhibitors to cleave angiotensin I. There are several compounds that function as both ACE2 inhibitors and Ace inhibitors, such as phenolics such as myricetin and glycosylated derivatives of quercetin. The molecular docking of several plant metabolites with the ACE2 against SARS-CoV-2 revealed 11 natural compounds that could block it. Baicalin (baicalein-7-O-glucuronide), hesperetin, scutellarin, glycyrrhizin, nicotianamine, naringin, neohesperidin, hesperidin, naringenin, and nobiletin are some of the naturally occurring metabolites reported as probable bioactive compounds against SARS-CoV-2. Natural ACE2 inhibitors, like ACE inhibitors, are classified as alkaloids, flavanones, flavonols, limonoids, terpenes, phenolic acids, lignans, tannins, terpenoids,

and fatty acids. Flavonoids, such as naringenin and naringin, were the main focus of the in silico studies of anti-COVID-19 natural compounds conducted at the primary stage. However, recent research indicates that glycosylated derivatives of quercetin have promising inhibitory activities with binding energies less than 8.3 kcal mol^{-1}. Quercetin 3-vicianoside and quercetin-3-glucuronide-7-glucoside and are two of these flavonoids (da Silva Antonio *et al.*, 2020).

Natural TMPRSS2 inhibitors

Flavonoids, terpenes, and peptides are all natural TMPRSS2 inhibitors. In in silico analyses against COVID-19, the flavonoids baicalin and baicalein were identified, which have earlier been described as expression-suppressing agents for TMPRSS-2. Molecular docking investigations have suggested that baicalein is also an ACE2 inhibitor. In fact, the proposed metabolite's bioactivity in vivo would be greatly increased if it could be employed to interact with a number of virus binding sites. Along with known human TMPRSS2 inhibitors, in silico investigations showed that iridoids, lignans and diterpenes, are possible anti-SARS-CoV-2 compounds that interact with TMPRSS2 (Khan and Al-Balushi, 2021). The researchers proposed 12 natural compounds such as silybin, geniposide, microcarpin, isogemichalcone B, withaferin A, excavatolide M, citocoline, (-)-epicatechin 3-o-(3'-o-methyl gallate) etc. with TPMRSS2 binding energies ranging from 11.06 to 14.69 kcal mol^{-1}. The geniposide was the natural metabolite with the highest inhibitory potential. Their inhibitory values are higher than previously mentioned ACE2 inhibition molecular docking (da Silva Antonio *et al.*, 2020).

Natural 3CLpro inhibitors

Researchers are focusing their attention more to 3CLpro's inhibition, which is the main protein of SARS-CoV-2, because it might restrict the virus from infecting the host. Procyanidin A3, acetoside, rutin, solanine, procyanidin A4, procyanidin B4, hypericin, quercetagetin, procyanidin, and astragalin were discovered to have highly excellent docking scores against 3CLpro of SARS CoV-2. An acetoside with α, β-unsaturated carbonyl group can attach covalently to the Cys145 residue of 3CLpro. These flavonoids' anti-SARS-CoV-2 action is beneficial due to the fact that they are easily found and abundant in angiosperm plant families. Apart from flavonoids, specialized metabolites called volatile terpenoids have some really promising early results that suggest their potential use. Geraniol, linalool, (E)-farnesene, and (E)-nerolidol, are themono and

sesquiterpenes, showed 3CLpro binding energy of 24.71, 24.05, 27.56, and 26.44 kcal mol^{-1}, respectively. These chemicals are present in a variety of plant species that have long been used as meals, medicines, and aromatics (da Silva Antonio *et al.*, 2020).

Inhibitory Phytoconstituents of Spike Glycoprotein

Acetoside binds to the spike glycoprotein RBD having a strong affinity (8.528 kcal/mol). Additionally, solanine has a great attraction for the spike glycoprotein RBD, which was similar to 3CLpro, and had a docking score of 9.501 kcal/mol. The H-bonding with Tyr449 (2.64Å) involved the oxygen atom of a glycosidic bond linked to a steroidal backbone. Rutin, quercitrin, epitheaflavin monogallate, procyanidin, procyanidin A1, procyanidin B2 also demonstrated considerable binding affinity with spike glycoprotein RBD (Khan and Al-Balushi, 2021).

RNA polymerase inhibitors

This process includes a very particular mechanism to inhibit virus proliferation using the RNA polymerase inhibitors. RNA-dependent RNA polymerase (RdRp), also called the nonstructural protein 12 (nsp12) has become a new target for therapeutic development against COVID-19. ACE2 or TMPRSS2 inhibitors, which attach to the host cell, are likely to be more harmful than metabolites having this feature. Though it's the safer option, its application in the treatment of coronavirus is still not very known. Hesperidin, naringin, apigenin-7-O-glucoside, hesperetin, quercetin, kaempferol, apigenin, solanine, solamargine, and other phytoconstituents are potential lead molecules for developing new RdRp inhibitors (da Silva Antonio *et al.*, 2020; Goyal *et al.*, 2020).

***Solanum nigrum* as a COVID-19 treatment option**

In consideration of COVID19's pathophysiology, medicinal plants with significant anti-inflammatory, antiviral and immunomodulatory properties are a promising candidate for developing COVID-19 treatments. As the plant *S. nigrum* has all these properties, it may become a natural solution for this deadly disease. Again, this plant has shown inhibitory HIV reverse transcriptase activity which also indicates its possible effectiveness against SARS-CoV-2. From the phytochemical investigation we already know that the plant contains flavonoids, steroidal glycoalkaloids, triterpenoids, flavonoid glycosides and other compounds of different classes. Different components of these classes has already

shown great inhibitory potential against SARS-CoV-2 (Table 6). Among them solanine, quercetin, quercitrin, apigenin, kaempferol, rutin, leteolin, naringenin and m coumarins showed great potency (Patel *et al.*, 2021).

Table 6. Phytoconstituents found through molecular docking against SARS-CoV-2 (da Silva Antonio *et al.*, 2020; Khan and Al-Balushi, 2021; Goyal *et al.*, 2020).

Phytoconstituent	Binding Energy (kcal mol^{-1})	Phytoconstituent	Binding Energy (kcal mol^{-1})
Binding with ACE2		**Binding with TMPRSS2**	
Quercetin 3-glucosyl-(1,4)-rhamnoside	−6.50	(−)-Epicatechin 3-*O*-(3′-*O*-methyl) gallate	−13.10
Quercetin	−8.664	Silybin	−11.928
Apigenin	−7.10	Geniposide	−14.69
Kaempferol	−7.20	Microcarpin	−13.31
Epicatechin-4-epigallocatechin	−7.20	5-Methoxyhydnocarpin	−13.92
Isoquercitrin	−7.80	Citocoline	−13.96
Silybin	−10.57	Withaferin A	−11.24
Solanine	−6.0	Excavatolide M	−14.38
Solasodine	−4.8	Dictyosphaeric acid A	−14.02
Solasonine	−2.6	Isogemichalcone B	−13.07
Quercetin 3-glucosyl-(1,4)-rhamnoside	−9.90	Solanine	−9.50
Apigenin	−7.80	Acetoside	−8.53
Kaempferol	−7.80	Rutin	−7.91
Isoquercitrin	−8.20	Quercitrin	−7.15
Quercetin	−8.47	Epitheaflavin monogallate	−7.52
Acetoside	−11.97	Procyanidin B2	−7.48
Rutin	−11.19	Theaflavin 3,3'-digallate	−7.02
Solanine	−10.30	Procyanidin A1	−6.84

Solanine is a glycoalkaloid found in European black nightshade (*S. nigrum*), tomato (*Solanum lycopersicum*), potato (*Solanum tuberosum*), and eggplant (*Solanum melongena*). Highest amount is found in *S. nigrum* berries. Fungicidal, antibacterial, and pesticidal activities are shown by this compound. At physiological pH, the nitrogen atom of solanine formed a salt bridge with Glu166 (4.87Å) and H-bonding with Glu166 (1.93Å). L-rhamnopyranose's hydroxyl group made an H-bond with Glu166 (2.64Å). The H-bonding with Tyr449 (2.64Å) involved the oxygen atom of a glycosidic bond linked to a steroidal backbone. Ser494 (1.92Å) demonstrated H-bonding with the methylene hydroxyl group of glucopyranose, which is connected to a steroidal backbone. Solanine had a strong binding affinity for the spike glycoprotein RBD, which was similar to 3CLpro, and had a docking score of 9.501 kcal/mol against PDB ID 6M0J (Khan and Al-Balushi, 2021).

Quercetin, a flavonoid containing five hydroxyl groups found in *S. nigrum*, has been shown antimicrobial, antitumour, anti-inflammatory, and antioxidant activities. Quercetin also possesses immunostimulatory properties, promoting the emergence of various important genes and the generation of Th-1-derived interleukin 1 (IFN-) while suppressing Th-2-derived interleukin 4. (IL-4). In addition, quercetin is thought to be a general inhibitor of immune cell buildup and activation, preventing chronic inflammation. It has evident antiviral effects on numerous respiratory and common cold viruses because of its capacity to decrease viral localization, proliferation, and load *in vitro*, as well as inflammatory responses and airway hyper-responsiveness in vivo. Quercetin-3-galactoside was found to block MERS-CoV 3CLpro's enzymatic activity *in vitro* and to inhibit a protease necessary for SARS-CoV viral multiplication. It has a stronger inhibitory effect on Angiotensin-Converting Enzyme than rutin, kaempferol, rhoifolin, and apigenin K flavonoids, as evidenced by their IC50 values (43 64 178 183 and 196 M, respectively). Furthermore, it has been demonstrated that the SARS-CoV 3CLpro's proteolytic activity is blocked (Khan and Al-Balushi, 2021, Khalil and Tazeddinova, 2020). Some other components having great inhibitory potential against SARS-CoV-2 are demonstrated in Table 7.

Table 7. Chemical constituents of *S. nigrum* that showed inhibitory potential against SARS-CoV-2 (Khalil and Tazeddinova 2020; Schwarz *et al.*, 2014).

Constituent Name	Description	Structure
Apigenin	*S. nigrum* contains a naturally occurring flavone molecule called apigenin (4′,5,7-trihydroxyflavone). It has a diverse array of biological actions, including powerful anti-inflammatory, antioxidant, antibacterial, and antiviral properties, as well as blood pressure lowering properties. Apigenin activates anti-inflammatory pathways such as p38/MAPK and PI3K/Akt, suppresses NF-B nuclear translocation, inhibits COX-2 activity, and significantly lowers IL-6, TNF-, and IFN- levels. It has demonstrated antiviral activity against adenoviruses (ADV) and the hepatitis B virus *in vitro*, blocking of the production of viral proteins by inhibiting viral IRES activity of picornaviruses, the African swine fever virus (ASFV) by inhibiting viral protein biosynthesis and reducing ASFV yield by 3 logs, and altering the viral RNA of enterovirus-71, and blocking of the production of viral proteins by inhibiting viral IRES (EV71). Apigenin, along with other flavonoids, has been demonstrated to reduce the enzymatic action of SARS-CoV 3CLpro, and the antiviral effect is assumed to be related to the suppression of SARS-CoV 3CLpro's activity.	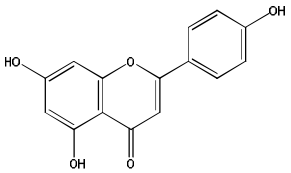
Kaempferol	Kaempferol, also known as 3,4′,5,7-tetrahydroxy-flavone, is a flavonoid seen in several medicinal plants, including *S. nigrum*. With its potent anti-inflammatory and antioxidant capabilities, kaempferol reduced LPS-induced TNF- and IL-1 production by raising the number of phagocytic cells and blocking NF-B moving inside the nucleus, so blocking the inflammatory cascade pathway. Kaempferol has been demonstrated to be a successful treatment for lung damage and inflammation brought on by the H9N2 influenza virus both *in vitro* and in vivo. Treatment with kaempferol reduced pulmonary edema, pulmonary capillary permeability, myeloperoxidase (MPO) activity, and inflammatory cell counts. Kaempferol glycosides and acylated kaempferol glucoside, two derivatives of kaempferol have already showed significant antiviral activity against the SARS coronavirus through inhibiting 3a channel protein. Kaempferol not only inhibits virus generation by blocking the 3a channel, but also affects the other stages of the viral life cycle, which indicates its potential as multi-target drugs.	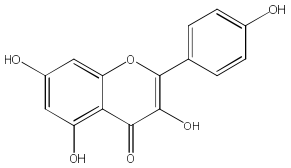

Naringenin	Naringenin, which is mainly 4′,5,7-trihydroxytlavanone, is a component of *S. nigrum*. Numerous pharmacological effects of naringenin include antidiabetic, anticancer, immunomodulatory, DNA protective, anti-inflammatory, hypolipidemic, antioxidant, antiasthmatic, antibacterial, antiviral, and PPAR activator. Through its antioxidant, anti-inflammatory, anti-nitrosative, and antitumor capabilities, it prevents the proliferation of various viruses in human cells, including dengue, chikungunya, and zika. It also offers significant protection against acute lung damage caused by LPS. Naringenin has the potential to be utilized to treat pneumonia linked with the spread of COVID-19 owing to its powerful anti-inflammatory and anti-oxidant properties.	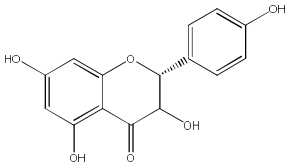
Luteolin	Luteolin, also known as 3′,4′,5,7-tetrahydroxyflavone, is a natural yellow dye found in a wide range of plants, notably *Solanum nigrum*. Like other flavonoid compounds, it has several pharmacological actions like immunostimulatory, anti-inflammatory, cytotoxic, antimicrobial, anti-oxidant, antiviral, anti-allergic, and neuroprotective activities. Using a wild-type SARS-CoV infection system, the anti-SARS-CoV effects of two small compounds, tetra-O-galloyl-d-glucose (TGG), and luteolin, were established. TGG and luteolin both efficiently inhibited the entry of HIV-luc/SARS pseudotyped virus into its host at the same potencies, suggesting that these two compounds could be used clinically as anti-SARS medicines. As it has significant antiviral and anti-inflammatory effects during infection, luteolin could be used as an alternate treatment as well as body immunity booster against COVID19 infection.	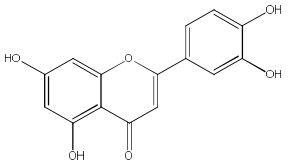

Conclusions

With the emergence of the COVID-19 pandemic, several scientists and physicians attempted to propose viable medications for treating the disease. Natural substances have been utilized to treat infectious diseases for decades. Natural medications and their active constituents may be advanced as a promising therapeutic candidate against SARS-CoV-2 according to past experiences with coronavirus outbreaks like SARS-CoV in 2002 and MERS-CoV in 2012, seasonal epidemics brought on by several viruses, and the therapeutic efficacy of natural ingredients in treating HCV, HIV, and influenza. So, they might be essential in overcoming the global crisis. In COVID-19 patients, medicinal herbs could be utilized to alleviate symptoms including fever and coughing, as well as enhance immunity. Among these medicinal plants *S. nigrum* was the point of interest for

this review. This review demonstrates that *S. nigrum* has a wide range of therapeutic characteristics. The plant could be utilized to make an oral medicine to treat respiratory infections, but further research is needed to isolate the bioactive components from the crude extract for optimal drug development. In addition to having effects on cardiovascular targets rather than the renin-angiotensin system, phytoconstituents must exhibit anti-inflammatory, antioxidant, and antiviral action to be beneficial for treating COVID-19, ACE-2 being the main target. From the review we can see that the plant possesses all of these properties. To summarize, *S. nigrum* may contain bio-active compounds that can be employed as an anti-SARS-CoV-2 drug to cure COVID-19 disorders with no adverse effects (Patel *et al.*, 2021; Khan and Al-Balushi 2021).

Authors' contribution

MSA has conceived the original idea. FAS, MRT and FA extensively consulted the literature and prepared the initial manuscript and arranged the reference section. JAC, AAC and SK critically reviewed the overall activities. MSA supervised the whole activity. All the authors read the review article meticulously and agreed to submit the article.

Funding statement

This work has been a self-finance activity.

Conflict of interest

There is no conflict of interest, according to the authors.

Acknowledgment

We would like to thank the authors of the articles we have cited. We also express our gratitude to the authority of the Department of Pharmaceutical Chemistry for using their computer of the Molecular and Herbal Drug Research Laboratory established under the HEQEP Project.

References

Aali, N.S., K. Singh, M.L. Khan and S. Rani. 2010. Protective effect of ethanolic extract of *Solanum nigrum* on the blood sugar of albino rats. *Int. J. Pharm. Sci. Res*. **1**(9): 97-9.

Abbas, K., U. Niaz, T. Hussain, M.A. Saeed, Z. Javaid, A. Idrees and S. Rasool. 2014. Antimicrobial activity of fruits of *Solanum nigrum* and *Solanum xanthocarpum*. *Acta Pol. Pharm*. **71**(3): 415-21.

Akubugwo, I.E., A.N. Obasi and S.C. Ginika. 2007. Nutritional potential of the leaves and seeds of black nightshade *Solanum nigrum* L. var *virginicum* from Afikpo-Nigeria. *Pakistan J. Nutr*. **6**(4): 323-326.

Alam, M.N., S. Roy, S.M. Anisuzzaman and M. Rafiquzzaman. 2012. Antioxidant activity of the ethanolic extracts of leaves, stems and fruits of *Solanum nigrum. Phcog Commn*. **2**: 67-71.

An, L., J.T. Tang, X.M. Liu and N.N. Gao. 2006. Review about mechanisms of anti-cancer of *Solanum nigrum. Zhongguo Zhong Yao Za Zhi* **31**(15): 1225-1226.

Atanu, F.O., U.G. Ebiloma and E.I. Ajayi. 2011. A review of the pharmacological aspects of *Solanum nigrum* Linn. *Biotech. Mol. Biol. Rev*. **6**(1): 1-8.

Cai, X.F., Y.W. Chin, S.R. Oh, O.K. Kwon, K.S. Ahn and H.K. Lee. 2010. Anti-inflammatory constituents from *Solanum nigrum. Bull. Korean Chem. Soc*. **31**(1): 199-201.

Chauhan, R., K.M. Ruby, A. Shori, and J. Dwivedi. 2012. *Solanum nigrum* with dynamic therapeutic role: A review. *Inter. J. Pharm. Sci. Rev. Res*. **15**(1): 65-71.

da Silva Antonio, A., L.S.M. Wiedemann and V.F. Veiga-Junior. 2020. Natural products' role against COVID-19. *Rsc. Adv*. **10**(39): 23379-23393.

Dar, R.A., M. Shahnawaz, and P.H. Qazi. 2017. General overview of medicinal plants: A review. *J. Phytopharm*. **6**(6): 349-351.

Dong, Y., L. Hao, K. Fang, X.X. Han, H. Yu, J.J. Zhang, L.J. Cai, T. Fan, W.D. Zhang, K. Pang and W.M. Ma. 2021. A network pharmacology perspective for deciphering potential mechanisms of action of *Solanum nigrum* L. in bladder cancer. *BMC Complement. Med. Ther*. **21**(1): 1-14.

Ewais, E.A., S.A. Desouky and E.H. Eshazly. 2015. Studies on callus induction, phytochemical constituents and antimicrobial activity of *Solanum nigrum* L. (Solanaceae). *Nat. Sci*. **3**: 133-138.

Goyal, R.K., J. Majeed, R. Tonk, M. Dhobi, B. Patel, K. Sharma and S. Apparsundaram. 2020. Current targets and drug candidates for prevention and treatment of SARS-CoV-2 (COVID-19) infection. *Rev. Cardiovas. Med*. **21**(3): 365-384.

Goyal, R.K., S. Apparsundaram, M. Dhobi and B.M. Patel. 2021. Herbal Formulations for the Treatment of COVID-19. In: *Delineating Health and Health System: Mechanistic Insights into Covid 19 Complications*. Springer, Singapore. pp. 431-447.

Jain, R., A. Sharma, S. Gupta, I.P. Sarethy, and R. Gabrani. 2011. *Solanum nigrum*: current perspectives on therapeutic properties. *Altern. Med. Rev*. **16**(1):78-85.

Jainu, M. and C.S.S. Devi. 2006. Antiulcerogenic and ulcer healing effects of Solanum nigrum (L.) on experimental ulcer models: possible mechanism for the inhibition of acid formation. *J. Ethnopharm*. **104**(1-2): 156-163.

Jasim, H., A.O. Hussein, I.H. Hameed and M.A. Kareem. 2015. Characterization of alkaloid constitution and evaluation of antimicrobial activity of Solanum nigrum using gas chromatography mass spectrometry (GC-MS). *J. Pharmaco. Phytoth*. **7**(4): 56-72.

Khalil, A. and D. Tazeddinova. 2020. The upshot of polyphenolic compounds on immunity amid COVID-19 pandemic and other emerging communicable diseases: An appraisal. *Nat. Prod. Bioprospec*. **10**(6): 411-429.

Khan, M.A. 2016. Introduction and importance of medicinal plants and herbs in Pharmacognnosy.

Khan, M.Y., S. Aliabbas, V. Kumar, and S. Rajkumar. 2009. Recent advances in medicinal plant biotechnology. *Indian J. Biotechnol*. **8**(1): 9-22.

Khan, S.A. and K. Al-Balushi. 2021. Combating COVID-19: The role of drug repurposing and medicinal plants. *J. Infect. Public Health*. **14**(4): 495-503.

Lin, H.M., H.C. Tseng, C.J. Wang, J.J. Lin, C.W. Lo and F.P. Chou. 2008. Hepatoprotective effects of *Solanum nigrum* Linn extract against CCl4-iduced oxidative damage in rats. *Chemico-Biol. Interac*. **171**(3): 283-293.

Loganayaki, N., P. Siddhuraju and S. Manian. 2010. Antioxidant activity of two traditional Indian vegetables: *Solanum nigrum* L. and *Solanum torvum* L. *Food Sci. Biotechnol*. **19**(1): 121-127.

Mbadiko, C.M., A. Matondo, G.N. Bongo, C.L. Inkoto, B.Z. Gbolo, E.M. Lengbiye, J.T. Kilembe, D.T. Mwanangombo, E.M. Ngoyi, C.M. Falanga and D.S. Tshibangu. 2020. Review on ethno-botany, virucidal activity, phytochemistry and toxicology of solanum genus: Potential bio-resources for the therapeutic management of COVID-19. *European J. Nutr. Food Saf*. 35-48.

Mirzaie, A., M. Halaji, F.S. Dehkordi, R. Ranjbar and H. Noorbazargan. 2020. A narrative literature review on traditional medicine options for treatment of corona virus disease 2019 (COVID-19). *Complement. Ther. Clin. Pract*. **40**: 101214.

Muthuvel, A., M. Jothibas and C. Manoharan. 2020. Effect of chemically synthesis compared to biosynthesized ZnO-NPs using Solanum nigrum leaf extract and their photocatalytic, antibacterial and in-vitro antioxidant activity. *J. Environ. Chem. Eng*. **8**(2): 103705.

Nallusamy, S., J. Mannu, C. Ravikumar, K. Angamuthu, B. Nathan, K. Nachimuthu, G. Ramasamy, R. Muthurajan, M. Subbarayalu and K. Neelakandan. 2020. Shortlisting phytochemicals exhibiting inhibitory activity against major proteins of SARS-CoV-2 through virtual screening. https://doi.org/10.21203/rs.3.rs-31834/v1

Patel, B., S. Sharma, N. Nair, J. Majeed, R.K. Goyal and M. Dhobi. 2021. Therapeutic opportunities of edible antiviral plants for COVID-19. *Mol. Cell. Biochem*. **476**(6): 2345-2364.

Patel, S., N. Gheewala, A. Suthar and A. Shah. 2009. In-vitro cytotoxicity activity of Solanum nigrum extract against Hela cell line and Vero cell line. *Int. J. Pharm. Pharm. Sci*. **1**(1): 38-46.

Perez G, R.M., J.A. Perez L, L.M. Garcia D and H. Sossa M. 1998. Neuropharmacological activity of Solanum nigrum fruit. *J. Ethnopharmacol*. **62**(1): 43-48.

Prasath, S. 2016. Studies on the phytochemical screening and free radical scavenging potentials of *Solanum nigrum* leaves extract.

Rani, Y.S., V.J. Reddy, S.J. Basha, M. Koshma, G. Hanumanthu and P. Swaroopa. 2017. A review on Solanum nigrum. *World J. Pharm. Pharm. Sci*. **6**: 293-303.

Ravi, V., T.S.M. Saleem, P.P. Maiti and J. Ramamurthy. 2009. Phytochemical and pharmacological evaluation of *Solanum nigrum* Linn. *African J. Pharm. Pharm.* **3**(9): 454-457.

Saleem, T.M., C. Chetty, S. Ramkanth, M. Alagusundaram, K. Gnanaprakash, V.T. Rajan, and S. Angalaparameswari. 2009. *Solanum nigrum* Linn.-A review. *Pharmaco. Rev.* **3**(6):342.

Schwarz, S., D. Sauter, K. Wang, R. Zhang, B. Sun, A. Karioti, A.R. Bilia, T. Efferth and W. Schwarz. 2014. Kaempferol derivatives as antiviral drugs against the 3a channel protein of coronavirus. *Planta Med*. **80**(02/03): 177-182.

Sikander, M., S. Malik, A. Rodriguez, M.M. Yallapu, A.S. Narula, S.K. Satapathy, V. Dhevan, S.C. Chauhan and M. Jaggi. 2020. Role of nutraceuticals in COVID-19 mediated liver dysfunction. *Molecules* **25**(24): 5905.

Silori, C.S. and R. Badola. 2000. Medicinal plant cultivation and sustainable development. *Mt. Res. Dev*. **20**(3): 272-279.

Son, Y.O., J. Kim, J.C. Lim, Y. Chung, G.H. Chung and J.C. Lee. 2003. Ripe fruits of Solanum nigrum L. inhibits cell growth and induces apoptosis in MCF-7 cells. *Food Chem. Toxicol*. **41**(10): 1421-1428.

Sugunabai, J., M. Jayaraj, T. Karpagam and B. Varalakshmi. 2014. Antidiabetic efficiency of Moringa oleifera and Solanum nigrum. *Inter. J. Pharm. Pharm. Sci*. **6**(Suppl 1): 40-42.

Sulaiman, C.T., M. Deepak, P.R. Ramesh, K. Mahesh, E.M. Anandan and I. Balachandran. 2021. Chemical profiling of selected Ayurveda formulations recommended for COVID-19. *Beni-Suef Univ. J. Basic Appl. Sci*. **10**(1): 1-5.

Teli, D.M., M.B. Shah and M.T. Chhabria. 2021. *In silico* screening of natural compounds as potential inhibitors of SARS-CoV-2 main protease and spike RBD: Targets for COVID-19. *Front. Mol. Biosci*.**7**: 429.

Zhao, Z., Q. Jia, M.S. Wu, X. Xie, Y. Wang, G. Song, C.Y. Zou, Q. Tang, J. Lu, G. Huang and J. Wang. 2018. Degalactotigonin, a natural compound from Solanum nigrum L., inhibits growth and metastasis of osteosarcoma through GSK3β inactivation–mediated repression of the Hedgehog/Gli1 pathway. *Clin. Cancer Res*. **24**(1): 130-144.

Zhou, X., X. He, G. Wang, H. Gao, G. Zhou, W. Ye and X. Yao. 2006. Steroidal saponins from *Solanum nigrum*. *J. Nat. Prod*. **69**(8): 1158-1163.

Zubair, M., K. Rizwan, N. Rasool, N. Afshan, M. Shahid and V.U. Ahmed. 2011. Antimicrobial potential of various extract and fractions of leaves of *Solanum nigrum*. *Inter. J. Phytomed*. **3**(1): 63.

(Revised copy received on 14.08.2023)